AD NUMBER

AD851052

NEW LIMITATION CHANGE

TO

Approved for public release, distribution unlimited

FROM

Distribution authorized to U.S. Gov't. agencies and their contractors; Administrative/Operational Use; Aug 1968. Other requests shall be referred to Naval Weapons Center, China Lake, CA.

AUTHORITY

USNWC ltr, 24 Mar 1972

NWC TP 4652

APPLICATION OF THE KALMAN FILTER TO AIDED INERTIAL SYSTEMS

by

Arthur A. Sutherland, Jr. and Arthur Gelb
The Analytic Sciences Corporation
for the
Weapons Development Department

ABSTRACT. The purpose of this tutorial report is to allow the reader with a limited background in optimum estimation techniques and/or inertial system theory to achieve a level of competence which will permit his participation in the design and evaluation of aided inertial guidance systems. To this end, the Kalman Filter is described in some detail, with full use of intuitive concepts. Next, the theory of inertial navigation is presented. Based on an understanding of inertial systems and the Kalman Filter, the reader is then shown how the two are combined to provide accurate, aided inertial systems. Problems arising in the application of the Kalman Filter to practical situations are discussed and common methods for solving them are illustrated. Examples in inertial navigation, gyrocompassing, and alignment transfer are provided in support of the theoretical development.

NAVAL WEAPONS CENTER
CHINA LAKE, CALIFORNIA • AUGUST 1968

157

NAVAL WEAPONS CENTER

AN ACTIVITY OF THE NAVAL MATERIAL COMMAND

M. R. Etheridge, Capt., USN — Commander
Thomas S. Amtic, Ph.D. — Technical Director

FOREWORD

In the analysis, synthesis, and design of strapped-down inertial guidance systems at the Naval Weapons Center, China Lake, Calif., it has become evident that the problem of alignment and initialization represents an area of great concern. Strapped-down alignment and initialization has been expected to engender problems different than gimballed, but not problems whose solutions are technically unfeasible.

As an aid to the research and development effort for strapped-down inertial guidance, some essential groundwork has been prepared with the procurement of this tutorial report for application of the Kalman filter techniques for aiding inertial systems.

This document was written for the Naval Weapons Center under Contract N60530-67-C-1052. The work was performed by Arthur A. Sutherland, Jr. and Arthur Gelb, of The Analytic Sciences Corporation. Professor Charles E. Hutchinson, University of Massachusetts, Department of Electrical Engineering, consulted during the program.

The work was performed under AirTask A36533205/216-1/F009-03-03.

Review for technical accuracy was given by Luke Crews and William F. Ball, Weapons Development Department, and by Professor Neville Rees, Department of Engineering, University of California, Los Angeles.

Released by
RICHARD V. BOYD, Head,
Guidance and Control Systems Division
22 August 1968

Under authority of
F. H. KNEMEYER, Head,
Weapons Development Department

NWC Technical Publication 4652

Published by ..... Weapons Development Department
Manuscript 40/MS 68-110
Collation ..... Cover, 77 leaves, DD Form 1473, abstract cards
First printing ..... 145 unnumbered copies
Security classification ..... UNCLASSIFIED

CONTENTS

Section 1. INTRODUCTION

HISTORICAL BACKGROUND

Inertial navigators are among the most precise of all electromechanical devices. The simple theoretical basis of inertial navigation is the measurement of linear and angular motion and employment of Newton's laws to compute changes in position, velocity, and attitude. Conceptually the inertial system is self-contained, but in practical use its performance deteriorates seriously with time unless external indications of the navigation quantities are used to remove self-generated errors. Thus, it can be said that the utility of the inertial system lies in its ability to provide information between external measurements.

Classically, external measurements were used to update the inertial system variables in a deterministic manner, i.e., system position indication was changed to agree with the results of a position fix, etc. And, by proper employment of external measurements, sensor errors were removed from the system calculations (assuming these errors to be constant). This approach ignored two important facts. First, external measurements themselves contain random errors which may be significant compared to the inertial system errors. Also, the system errors are primarily caused by random, time-varying inertial sensor errors. The optimum use of external measurements, properly accounting for measurement errors and sensor errors, has therefore become an important source of improvement in inertial navigation system accuracy.

Application of the Kalman Filter to inertial navigation systems began in the early 1960's, shortly after optimum recursive filter theory was developed and published. Because the errors in a useful inertial system propagate in essentially a linear manner and linear combinations of these errors can be detected from external measurements, the Kalman Filter is ideally suited for estimating them. Operationally, the filter relates to the inertial navigator and external measurements as illustrated in Fig. 1. It also provides useful estimates of all system error sources which have significant correlation times. Figure 2 demonstrates two common schemes for using the error estimates to correct system errors.

In addition, the Kalman Filter provides improved design and operational flexibility. As a time-varying filter, it can accommodate nonstationary error sources when their statistical behavior is known. Configuration changes in the inertial system are easily treated by simple programming changes. The Kalman Filter provides for optimum use of any number, combination, and sequence of external measurements. It is a technique for systematically employing all available external measurements, regardless of their errors, to improve the accuracy of inertial navigation systems.

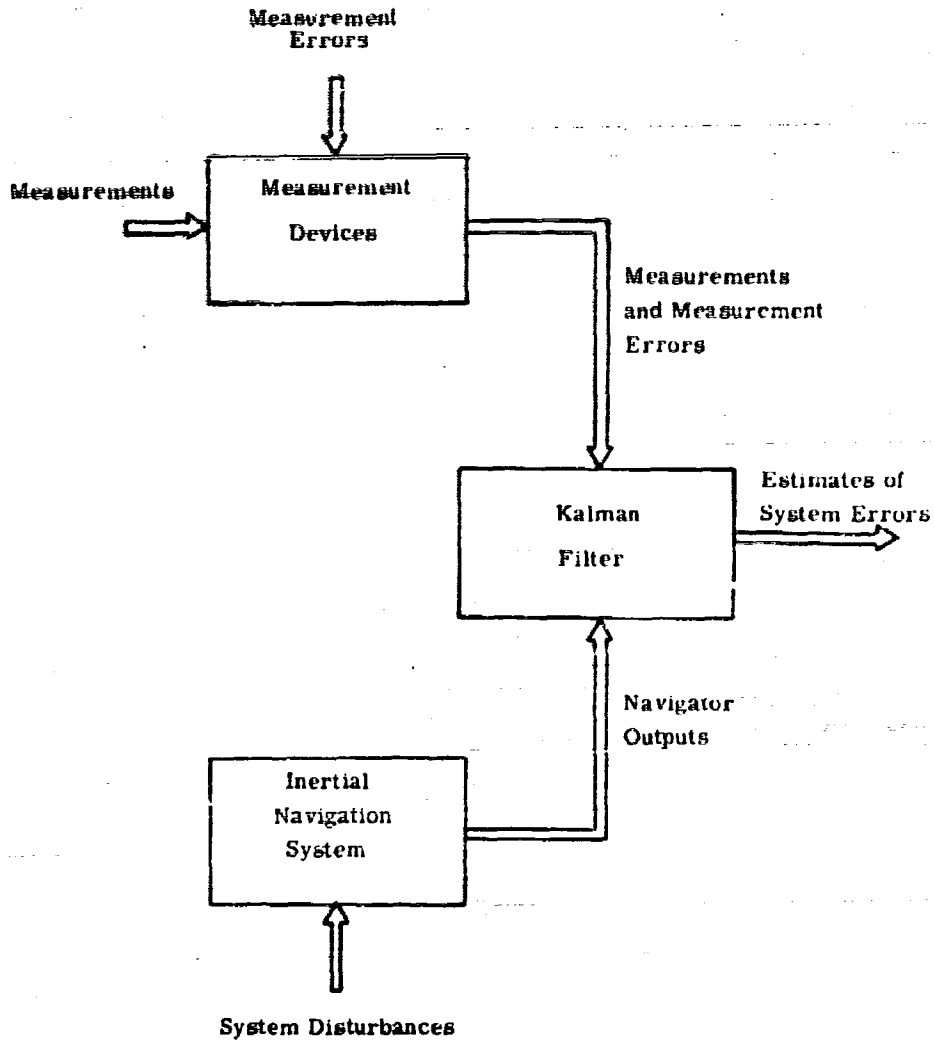

FIG. 1. Kalman Filter Operation in Inertial Navigators.

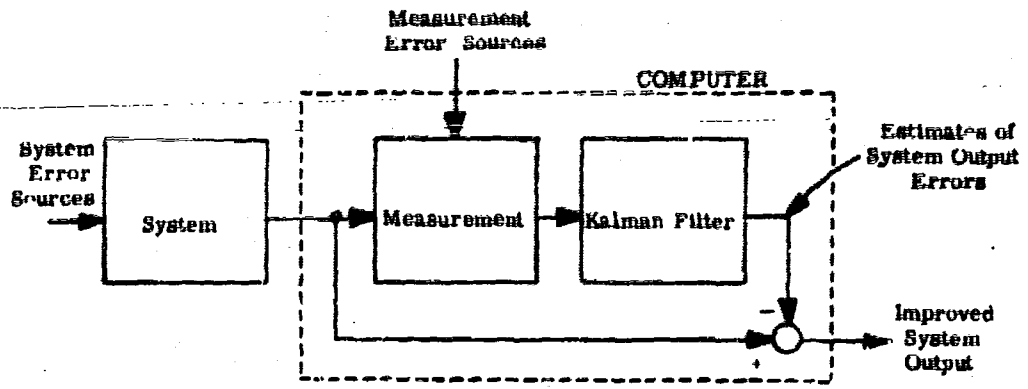

(a) Feedforward Configuration

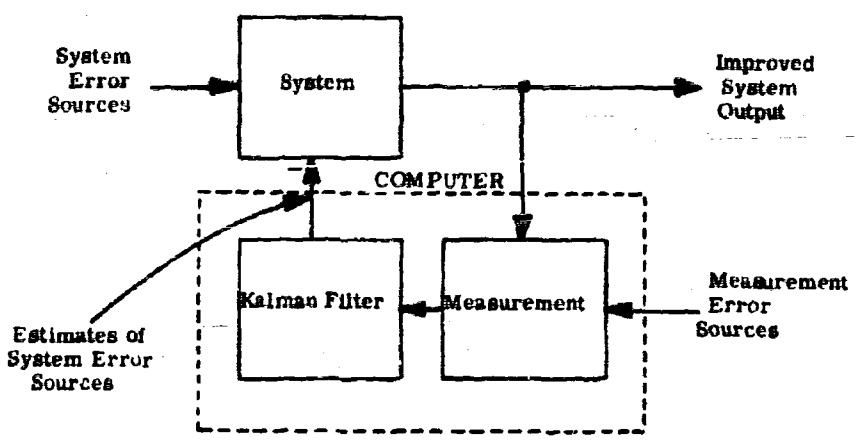

(b) Feedback Configuration

FIG. 2. Kalman Filter System Configurations.

The reader interested in further background information in the areas of matrix algebra and linear system theory is referred to Ref. 1.

ILLUSTRATION OF THE IMPROVEMENT POSSIBLE

A few figures serve to illustrate the ability of the Kalman Filter to provide superior performance in inertial systems. Figure 3 compares the RMS cruise mode azimuth error of an aircraft inertial navigation system when fixed-gain velocity damping is provided (constant gain feedback) and when the Kalman Filter (optimal feedback) is used. In both cases continuous external velocity measurements were provided and external position fixes were made every 15 minutes. The fixed-gain filter did not use position measurements to improve its knowledge of azimuth. However, the discontinuities in the trace indicate that the Kalman Filter was able to infer something about azimuth error each time a new position fix became available.

Figure 4 demonstrates the ability of the Kalman Filter to determine inertial sensor errors. It represents the RMS error in the knowledge of constant gyro drift rates in an aircraft inertial navigation system, starting with a 1 deg/hr uncertainty. For this example the Kalman Filter is operating on position fixes only. The dramatic improvement in calibration of gyro error suggests a considerable increase in navigation accuracy between position fixes.

An illustration of the Kalman Filter's ability to decrease alignment time of inertial navigators is provided by Fig. 5. It shows the RMS azimuth alignment error for fixed-gain and Kalman Filter airborne alignment modes of an inertial navigation system. Both schemes use an external indication of vehicle velocity, but the ability of the Kalman Filter to also utilize position fixes is demonstrated. It is evident that the optimal use of information provides a significant reduction in the time required to align to given accuracy or reduces errors at the end of a given alignment period.

OUTLINE OF SECTIONS

Section 2 continues with a discussion of the basic concepts which characterize the Kalman Filter. These include state space notation, uncorrelated random processes, the Kalman Filter equations, and the estimation error covariance matrix. Section 3 follows with a discussion of inertial navigation systems. Beginning with a brief description of inertial sensors, it progresses through gimballed and strapdown inertial measurement units to the equations of inertial navigation and the linearized expressions for inertial navigation errors.

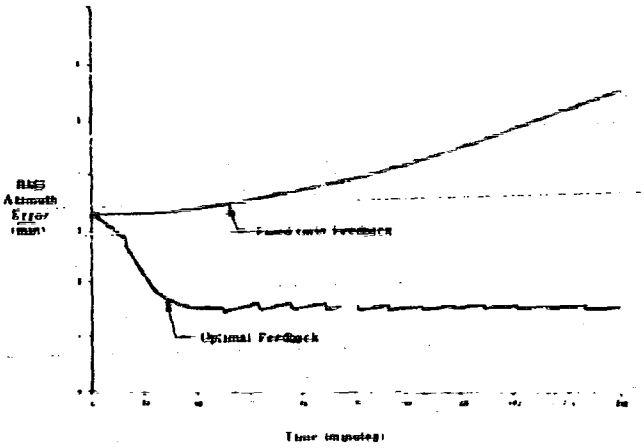

FIG. 3. Optimal Versus Conventional Filter Cruise Mode Azimuth Error (Ref. 2).

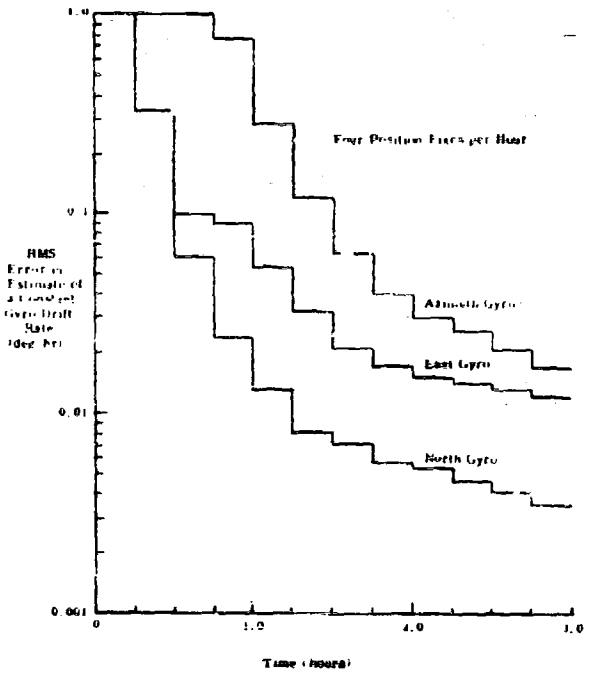

FIG. 4. Time History of RMS Errors in the Estimate of Constant Gyro Drift Rate (Ref. 3).

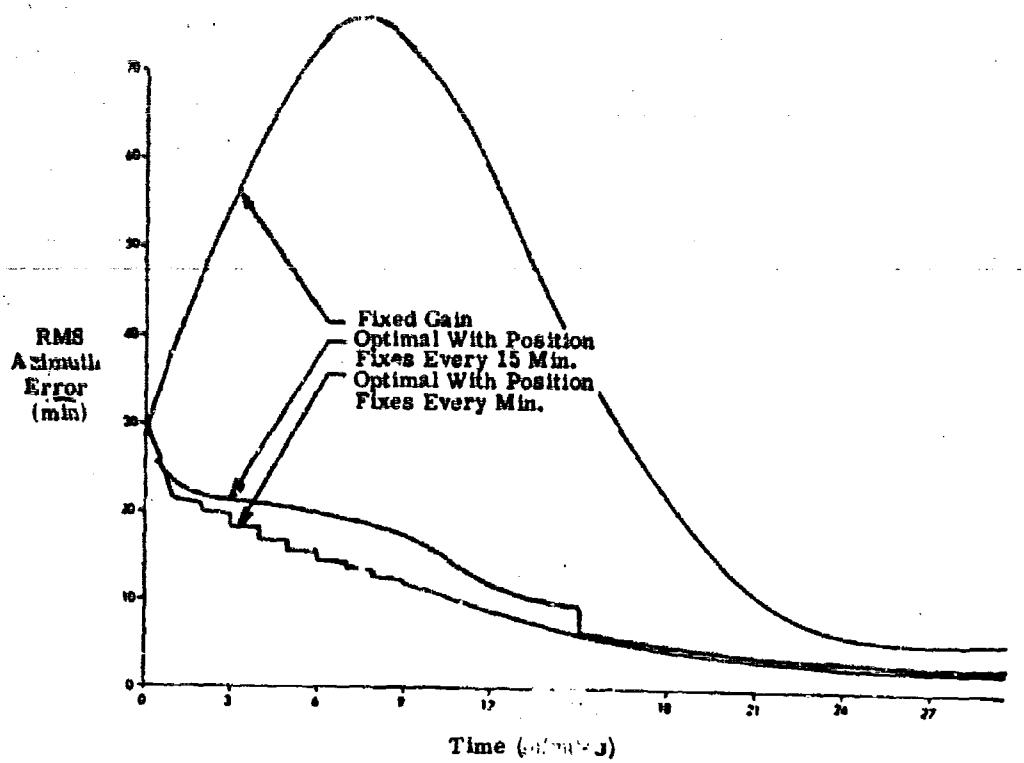

FIG. 5. Optimal Versus Conventional Airborne Alignment Accuracy (Ref. 2).

Section 4 describes the correlation properties of errors in inertial sensors and external measurements. It illustrates the steps necessary to formulate these errors in the manner required by the Kalman Filter. Section 5 describes three important mechanizations of inertial navigation systems and develops the expressions necessary to apply Kalman Filtering to them. Whenever the inertial navigation system errors are estimated they are applied as corrections to the navigator. Section 6 discusses the use of the Kalman Filter output to minimize inertial navigator errors at all times. Section 7 describes the use of the Kalman Filter for self-alignment, while Section 8 concerns the transfer alignment of one inertial system to another. Practical considerations which arise in the use of the Kalman Filter are discussed in Section 9. They include computer requirements, observability of state variables, suboptimal filtering to reduce complexity, and sensitivity analyses.

Section 2. KALMAN FILTER CONCEPTS

In the late 1940's, Norbert Wiener first specified the linear filter which has the capability of separating a single signal from additive noise, minimizing the mean square error in the indicated signal--filter output or estimate (see Ref. 4). The "Wiener Filter" is time invariant and the minimum mean-squared error criterion is theoretically achieved only after the stationary signal and noise have been operated upon for an infinite time.

In the decade that followed Wiener's first results, his theory was extended to cover the cases where filtering was conducted over a finite period, the filter received inputs at discrete instants of time, the filter and its inputs were nonstationary, and several signals (states) were to be detected. In the early 1960's, Kalman and others (Ref. 5, 6, and 7) provided a unified body of linear filter theory which handles all of these situations and is expressed entirely in the time domain. The Kalman Filter, as it has come to be called, provides an essentially real-time reduction of its input data to give a minimum variance (i.e., least squares) estimate of the state variables in a nonstationary linear system. It can be derived in many different ways. Under identical assumptions, the following approaches all yield the same filter: least squares estimation, Bayesian estimation, maximum likelihood, and conditional expectation.

LINEAR DYNAMIC SYSTEMS

The Kalman Filter is formulated using state vector, time domain notation. The state of a dynamic system is any complete set of quantities necessary to describe the unforced motion of that system at all future times. Given the state at any time and a history of the system forcing functions, the state at any subsequent time can be computed. If the linear system behavior is described by an n^{th} order linear differential equation in the dependent variable, driven by f(t), a function of the independent variable, t,

$$\lambda^{(n)}(t) + \cdots + a_2\lambda^{(1)}(t) + a_1\lambda(t) = f(t) \qquad (1)$$

the system state can be described by the dependent variable, λ, and its first (n-1) derivatives. A more compact formulation is introduced in the following example.

Example: The linear second-order differential equation for the variable λ is expressed by

$$\ddot{\lambda} + a_2(t)\,\dot{\lambda} + a_1(t)\,\lambda = \alpha(t) + \beta(t)$$

where the time functions α and β are driving the equation. Any number of driving functions are possible in the general case. Appropriate state variables can be defined as

$$x_1 = \lambda$$

$$x_2 = \dot{\lambda}$$

Then

$$\dot{x}_1 = \dot{\lambda} = x_2$$

$$\dot{x}_2 = \ddot{\lambda} = -a_2(t)\,x_2 - a_1(t)\,x_1 + \alpha(t) + \beta(t)$$

In vector-matrix form, the equation is

$$\begin{bmatrix} \dot{x}_1 \\ \dot{x}_2 \end{bmatrix} = \begin{bmatrix} 0 & 1 \\ -a_1(t) & -a_2(t) \end{bmatrix} \begin{bmatrix} x_1 \\ x_2 \end{bmatrix} + \begin{bmatrix} 0 & 0 \\ 1 & 1 \end{bmatrix} \begin{bmatrix} \alpha(t) \\ \beta(t) \end{bmatrix}$$

which is a first-order vector differential equation. This compact formulation can be generalized to an n^{th} order system.

The state variables of a linear system, $x_1, \cdots x_n$, are written in the form of a state vector for ease in manipulation

$$\underline{x} = \begin{bmatrix} x_1 \\ \cdot \\ \cdot \\ \cdot \\ x_n \end{bmatrix}$$

The state variables of any n^{th} order continuous linear system can be defined in such a manner that the system dynamics are expressed in the form of a first-order linear differential equation in the state vector $\underline{x}$.

The vector notation permits the equation to be written in a compact vector-matrix form

$$\dot{\underline{x}}(t) = F(t)\ \underline{x}(t) + G(t)\ \underline{u}(t) \qquad (2)$$

The vector $\underline{u}$ contains the independent variables that are forcing the system differential equations. If $\underline{x}$ has n elements and $\underline{u}$ has r elements, F and G are n x n and n x r matrices, respectively. Figure 6 is a block diagram illustration of Eq. 2.

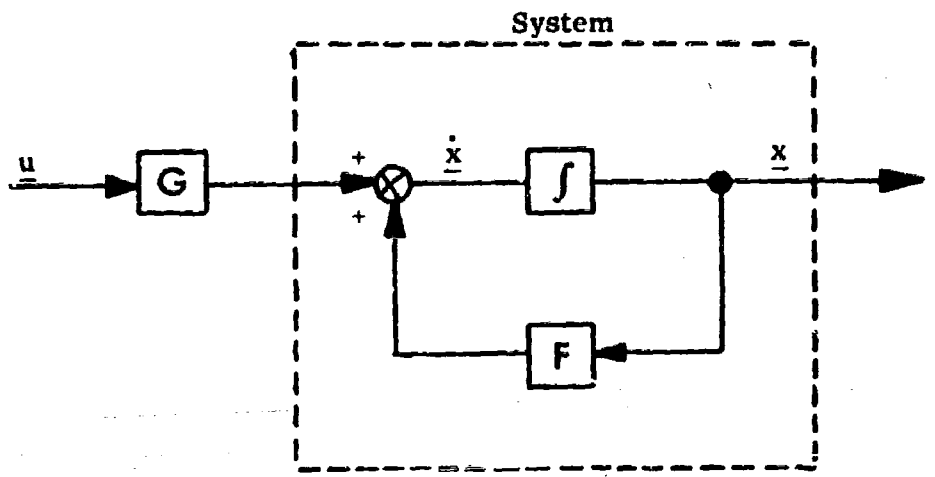

FIG. 6. Block Diagram of First-Order Linear Differential Equations in State Space Notation.

Given the state at time t_n, denoted $\underline{x}(t_n)$, and the vector forcing function $\underline{u}(t)$ for all time greater than t_n, the state at any subsequent time, t, can be found by solving the state differential equation, Eq. 2. Another, frequently more useful, way to express the state vector behavior uses the state transition matrix, denoted $\Phi\ (t, t_n)$ to describe the effect of the state at t_n on the state at some other time, t. The transition matrix is an influence function. In the absence of forcing terms, the influence of $\underline{x}(t_n)$ on $\underline{x}(t)$ is displayed through the relation

$$\underline{x}(t) = \Phi(t,t_n)\ \underline{x}(t_n) \qquad (3)$$

The state transition matrix is computed from the system dynamics as expressed in the system matrix, F. When F is a constant, Φ is a function of the time difference $(t-t_n)$ and is given by

$$\Phi(t-t_n) = e^{F(t-t_n)} \tag{4}$$

The matrix exponential in Eq. 4 is a legitimate operation and can be expressed, by analogy with the scalar exponential, as

$$e^{F(t-t_n)} = I + (t-t_n)\,F + \frac{(t-t_n)^2}{2!}\,F^2 + \ldots$$

$$= \sum_{j=0}^{\infty} \frac{(t-t_n)^j}{j!}\,F^j \tag{5}$$

where I is the n x n identity matrix. When F is time-varying, the state transition matrix must be calculated from the differential equation

$$\frac{d[\Phi(t,t_n)]}{dt} = F(t)\,\Phi(t,t_n) \;;\quad \Phi(t_n,t_n) = I \tag{6}$$

Further details on computing Φ are available in Ref. 8.

When F is time-varying and forcing terms are available, the state vector can be expressed in terms of $\underline{x}(t_n)$ and the state transition matrix by

$$\underline{x}(t) = \Phi(t,t_n)\,\underline{x}(t_n) + \int_{t_n}^{t} \Phi(t,\tau)\,G(\tau)\,\underline{u}(\tau)\,d\tau \tag{7}$$

where

$$\frac{d}{d\tau}\,[\Phi^T(t,\tau)] = -F^T(\tau)\,\Phi^T(t,\tau) \;;\quad \Phi(t,t) = I$$

If interest is focused on the system state vector only at discrete points in time, Eq. 7 can be expressed as a difference equation

$$\underline{x}_{n+1} = \Phi_n\,\underline{x}_n + \underline{w}_n \tag{8}$$

where the notation $\underline{x}_n$ indicates the state vector at t_n. Unless the system dynamics are stationary (not time-varying) and the time interval is fixed, Φ_n will be a function of time and of the interval between the instants represented by t_n and t_{n+1}. The term $\underline{w}_n$ represents the effect of the forcing function $\underline{u}$ over the interval t_n to t_{n+1}.

$$\underline{w}_n = \int_{t_n}^{t_{n+1}} \Phi(t_{n+1}, \tau)\, G(\tau)\, \underline{u}(\tau)\, d\tau \qquad (9)$$

The expression given in Eq. 8 will be used extensively in the discussion which follows.

STATE ESTIMATION WITHOUT MEASUREMENTS

In the absence of random forcing terms, the system state behaves in a deterministic (directly calculable) manner described by Eq. 7. However, when random disturbances are present, the system exhibits random behavior and, if exact measurement of $\underline{x}(t)$ is not always possible, it becomes necessary to estimate the state vector. If an estimate is provided at some point in time, t_n, and the system is not observed (i.e., no measurements of the state are available), the best estimate of the state at all subsequent times is provided by solving the deterministic portions of Eq. 8. The estimate at t_n is used as the initial condition. Two factors contribute to errors in the estimate at times later than t_n; the errors in the initial estimate propagate in a manner described by Φ and random uncertainties in knowledge of the forcing functions provide additional errors.

Thus far we have dealt with deterministic quantities. By definition, random processes cannot be specified quantitatively as functions of time. It is necessary to describe them in a statistical manner. In particular, it is sufficient to describe random quantities (assumed Gaussian) by their first and second moments in order to apply the Kalman Filter. The first statistical moment, or mean, is described and removed from consideration by specifying it to be zero. Any quantity which is biased by a known amount can be replaced by a zero-mean variable through simple redefinition. The second statistical moments between processes are described in the state vector notation by the covariance matrix. Convariance matrices are discussed in Appendix A. Conceptually their diagonal elements are measures of the "size" of the random signals they describe, while the off-diagonal elements provide a measure of the interrelation between different random processes. It is assumed throughout this discussion that covariances between random quantities are zero

if not explicitly stated to be otherwise. Because ensemble averages or expectations are taken in defining the covariances, the results of the calculations are a valid representation only of the ensemble average behavior of the filter and its estimates.

The estimate of the state at t_n is designated by $\hat{\underline{x}}_n$ and the random error in that estimate is defined by

$$\tilde{\underline{x}}_n = \hat{\underline{x}}_n - \underline{x}_n \tag{10}$$

The covariance matrix of $\tilde{\underline{x}}_n$ is denoted by P_n. For zero-mean variables,

$$P_n = E\left(\tilde{\underline{x}}_n \tilde{\underline{x}}_n^T\right)^* \tag{11}$$

If Q_n is the covariance matrix for the random portion of $\underline{w}_n$, a difference equation can be obtained from Eq. 8, 10, and 11 which describes the growth of the estimation error covariance

$$P_{n+1} = \Phi_n P_n \Phi_n^T + Q_n \tag{12}$$

In arriving at Eq. 12, use is made of the fact that

$$E\left(\tilde{\underline{x}}_n \underline{w}_n^T\right) = 0 \tag{13}$$

since $\underline{w}_n$ is uncorrelated in time.

It can be seen that the random uncertainties in $\underline{w}_n$ (described by Q_n) can only increase the errors in the estimate of the system state as described by P; this is a reasonable conclusion. Mathematically it results from the fact that Q_n is a non-negative definite matrix. In continuous notation a differential equation for the error covariance matrix results (see Appendix A)

$$\dot{P} = FP + PF^T + GQG^T \tag{14}$$

where Q is the covariance matrix for the random portion of $\underline{u}$.

It should be noted that the random quantities forcing the system can take two very distinct forms. One is errors in the control applied to the system. The other represents random disturbance of the system.

*Throughout the report the symbol E preceding a vector product is used to denote the ensemble average of the quantity enclosed in the brackets.

When a known control or forcing function, $\underline{p}(t)$, is used in the presence of system disturbances, Eq. 2 can be written as

$$\dot{\underline{x}}(t) = F(t)\,\underline{x}(t) + G(t)\,\underline{u}(t) + L(t)\,\underline{p}(t) \tag{15}$$

to demonstrate the separate effects. Then, when the two effects are uncorrelated, Eq. 12 and 14 can be written as

$$P_{n+1} = \Phi_n P_n \Phi_n^T + Q_n + S_n \tag{16}$$

and

$$\dot{P} = FP + PF^T + GQG^T + LSL^T \tag{17}$$

Here the S matrices are the covariance of the errors in application of the control, while the Q matrices describe the effect of the random disturbances. Since the two random driving functions have analogous effects on the error covariance, only random system disturbances will be considered in the subsequent discussions.

KALMAN FILTER

When use is made of measurements to change the estimate of $\underline{x}$, the error in the estimate is also changed. Hopefully this error, or rather the statistical description of it, is in some way reduced. In the Kalman Filter the measurements are taken as linear combinations of the system state variables, corrupted by uncorrelated noise. The measurement equation is written in vector-matrix notation

$$\underline{z}_n = H_n \underline{x}_n + \underline{v}_n \tag{18}$$

where $\underline{z}_n$ is the set of measurements at time t_n, $z_1, \ldots, z_q$, arranged in vector form

$$\underline{z}_n = \begin{bmatrix} z_1 \\ \cdot \\ \cdot \\ \cdot \\ z_q \end{bmatrix} \tag{19}$$

H_n is a q x n matrix describing the linear combinations of state variables which comprise z_n in the absence of noise. Also, v_n is a vector of random noise quantities corrupting the measurements.

Example: Suppose it is desired to estimate the constant scalar quantity x based on n noise-corrupted measurements. The noise has zero mean and is uncorrelated. An unbiased, minimum variance estimate results when $\hat{x}$ is taken as the average of the measurements, z_i,

$$\hat{x}(n) = \frac{1}{n} \sum_{i=1}^{n} z_i$$

When an additional measurement becomes available,

$$\hat{x}(n+1) = \frac{1}{n+1} \sum_{i=1}^{n+1} z_i$$

However, the estimate based on n + 1 measurements can be computed employing only $\hat{x}(n)$ and the (n + 1)st measurement

$$\hat{x}(n+1) = \frac{n}{n+1} \frac{1}{n} \sum_{i=1}^{n} z_i + \frac{1}{n+1} z_{n+1}$$

$$= \frac{n}{n+1} \hat{x}(n) + \frac{1}{n+1} z_{n+1}$$

$$= \hat{x}(n) + \frac{1}{n+1} [z_{n+1} - \hat{x}(n)]$$

The new estimate is the old estimate modified by a weighted difference between the old estimate and the most recent measurement. This is a recursive formulation, eliminating the need to store past measurements.

By analogy with the example, one logical way to use the measurement vector z_n is to anticipate it based on knowledge of the measurement matrix H_n and the estimate of the state vector at the instant the measurements are taken. If z_n and $H_n \hat{x}_n$ do not agree, the difference must result from the measurement noise v_n or an error in the estimate. The state

variable estimates can then be changed according to statistical knowledge of the errors in $\underline{\hat{x}}_n$ and of the measurement errors. It would be appropriate to cause $\underline{\hat{x}}_n(+)$, the state vector estimate after consideration of the measurement, to be related to $\underline{\hat{x}}_n(-)$ by

$$\underline{\hat{x}}_n(+) = \underline{\hat{x}}_n(-) + K_n[\underline{z}_n - H_n \underline{\hat{x}}_n(-)] \tag{20}$$

Between measurements, the state vector estimate will obey the deterministic part of Eq. 8. This behavior of $\underline{\hat{x}}$ is illustrated in Fig. 7. It can be seen that the state estimate between measurements is obtained by mathematical modeling of the system.

The use of measurements provided at discrete instants of time causes the error covariance to be discontinuous, having different values before and after the measurements. This is illustrated in Fig. 2, 3, and 4. For this reason, the error covariance matrix immediately before the measurements taken at the n^{th} instant are used is designated $P_n(-)$. The same matrix after the measurements are employed is called $P_n(+)$. The matrix $P_n(-)$ is computed according to Eq. 12

$$P_{n+1}(-) = \Phi_n P_n(+) \Phi_n^T + Q_n \tag{21}$$

If Eq. 20 is used to improve the state vector estimate, the new error covariance is expressed (see Appendix B) by

$$P_n(+) = \left(I - K_n H_n\right) P_n(-) \left(I - K_n H_n\right)^T + K_n R_n K_n^T \tag{22}$$

where I is the square identity matrix and R_n is the covariance matrix of the measurement errors $\underline{v}_n$.

The Kalman Filter was originally derived under assumptions that permit the *a priori* specification of a linear structure (Ref. 9). The optimum filter was found to have the structure shown in Fig. 7. That is, it processes the measurements sequentially according to Eq. 20. In addition, it estimates between measurements according to Eq. 3 and the filter gain matrix is specified by

$$K_n = P_n(+) H_n^T R_n^{-1} \tag{23}$$

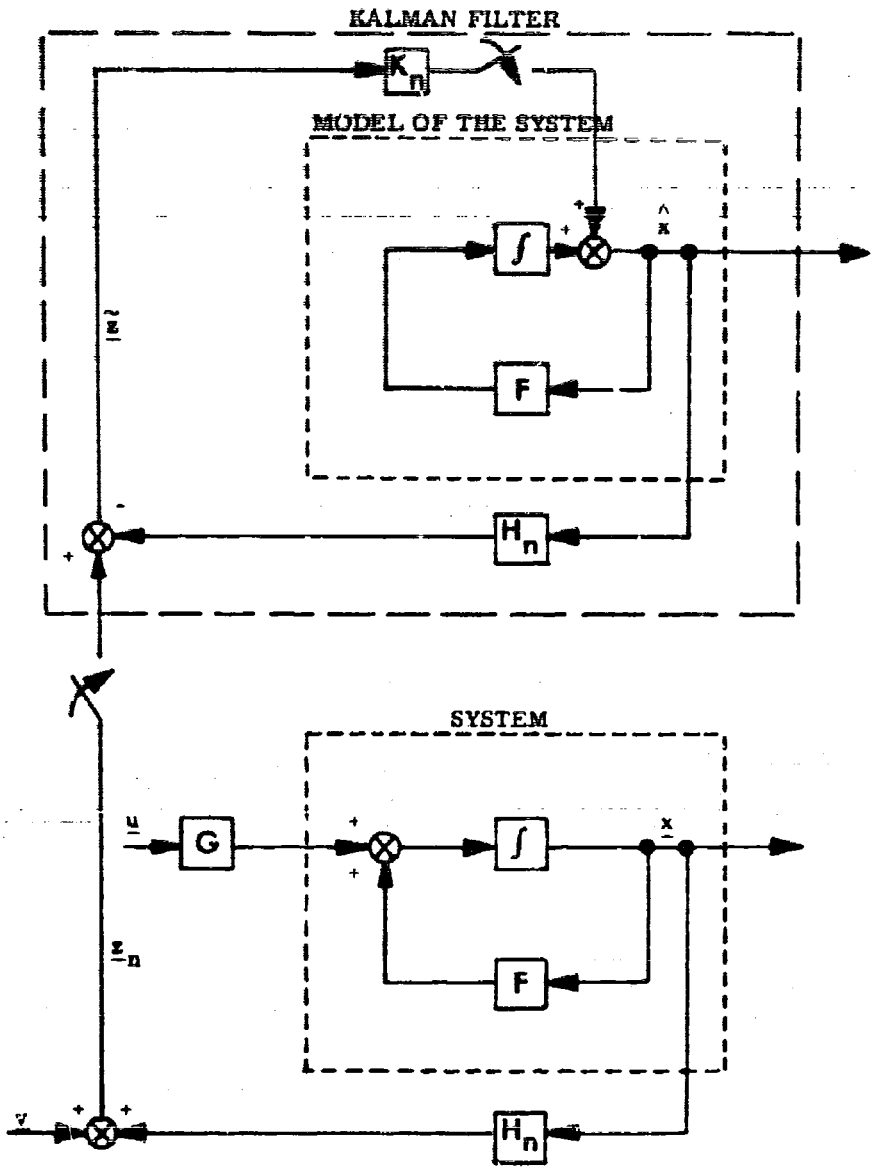

Note: The switches are synchronized.

FIG. 7. Block Diagram of the Discrete Estimation Equations.

An alternate form of Eq. 23 which can avoid the consequences of a singular R matrix is

$$K_n = P_n(-)\, H_n^T \left[H_n\, P_n(-)\, H_n^T + R_n\right]^{-1} \tag{24}$$

(See Appendix B.) Substitution of Eq. 23 or 24 into 22 provides an expression for the new error covariance matrix entirely in terms of the measurement matrix H_n and the measurement error covariance

$$P_n(+) = P_n(-) - P_n(-)\, H_n^T \left[H_n P_n(-)\, H_n^T + R_n\right]^{-1} H_n P_n(-) \tag{25}$$

$$= \left(I - K_n H_n\right) P_n(-)$$

Using Eq. 21 and 25, the error covariance can be calculated for any measurement time. Equation 23 or Eq. 24 then provides the filter gain matrix and Eq. 20 updates $\hat{\underline{x}}$. The state vector estimate is carried forward to the next measurement by Eq. 3. The optimum estimation procedure is illustrated in Fig. 8.

The continuous version of the Kalman Filter is illustrated in Fig. 9. The measurements are described by

$$\underline{z}(t) = H(t)\, \underline{x}(t) + \underline{v}(t) \tag{26}$$

Measurements are employed to change the derivative of the state vector estimate according to the equation

$$\dot{\hat{\underline{x}}} = F\, \hat{\underline{x}} + K\left(\underline{z} - H\, \hat{\underline{x}}\right) \tag{27}$$

The Kalman Filter gain matrix is specified by

$$K = P\, H^T\, R^{-1} \tag{28}$$

and the differential equation for the error covariance is

$$\dot{P} = FP + PF^T - PH^T\, R^{-1}\, HP + GQG^T \tag{29}$$

Inspection of Eq. 21, 25, and 29 and the knowledge that Q, R and the initial error covariance are all symmetric matrices reveals that P, $P_n(+)$, $P_n(-)$ are always symmetric. Steady-state values of the error covariance (and thus the filter gain) can be calculated for many stationary systems with stationary noises without specification of the initial value of P (Ref. 5).

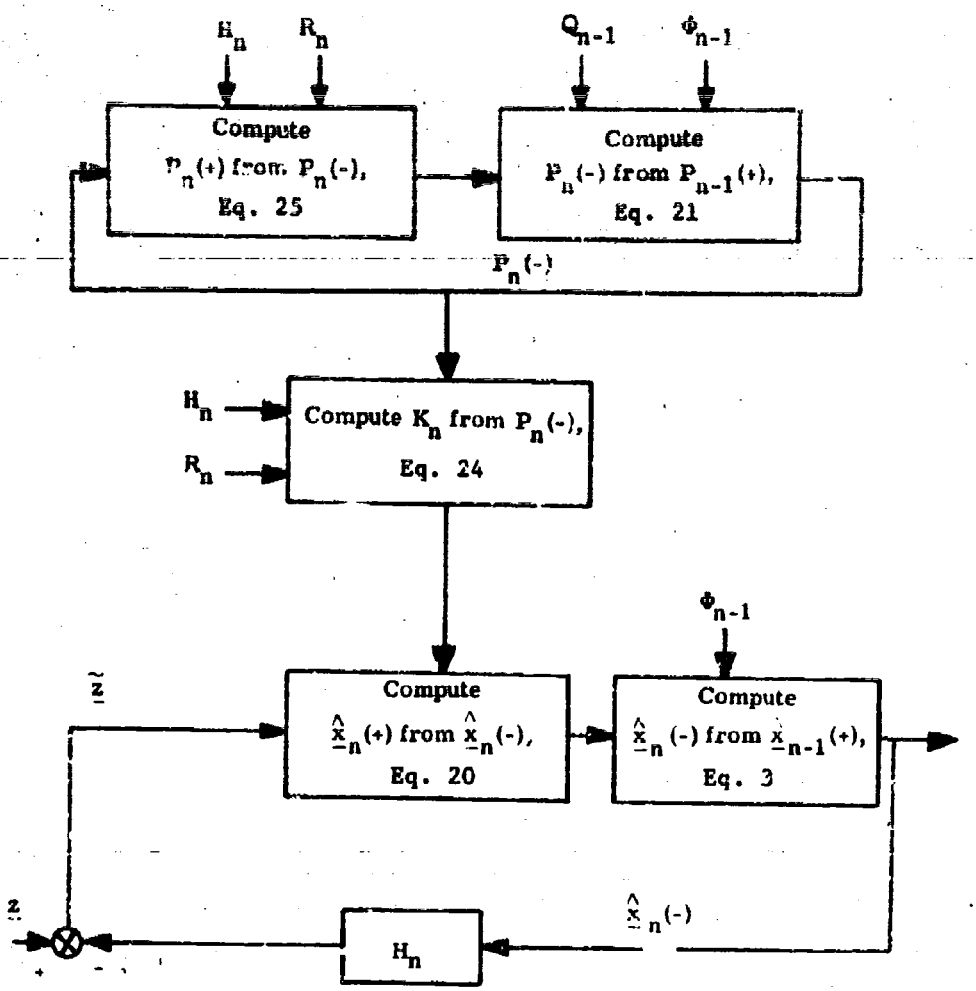

FIG. 8. Information Flow Diagram for Discrete Kalman Filter.

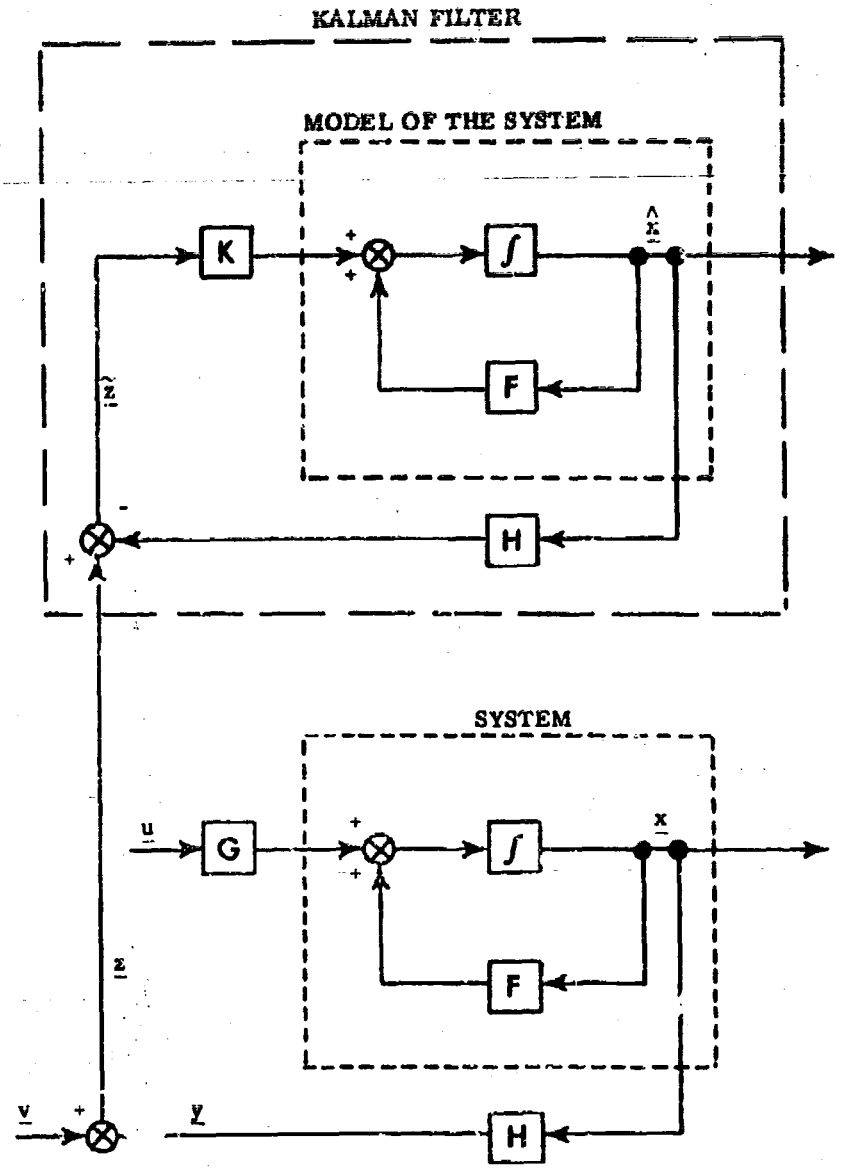

FIG. 9. Block Diagram of the Continuous Estimation Equations.

Intuitive Concepts

Inspection of the equations describing the behavior of the error covariance matrix reveals several observations which confirm our intuition about the filter operation. The effect of system disturbances on the growth of the error covariance can be seen from Eq. 21 and 29 to be the same as that observed when measurements were not available (Eq. 12 and 14). The larger the statistical parameters of the disturbances as reflected in the "size" of the Q matrix and the more pronounced the effect of the disturbances as reflected in the "size" of the G matrix, the more rapidly the error covariance will grow.

The effect of measurement noise on the error covariance of the discrete filter is observed better in an alternate form of Eq. 25 (Ref. 10)

$$P_n^{-1}(+) = P_n^{-1}(-) + H_n^T R_n^{-1} H_n \qquad (30)$$

Large measurement noise (R_n^{-1}) provides only a small increase in the inverse of the error covariance (a small decrease in the error covariance) when the measurement is used; the associated measurements contribute little to reduction in estimation errors. On the other hand, small measurement errors (large R_n^{-1}) cause the error covariance to decrease considerably whenever a measurement is utilized. When measurement noise is absent, Eq. 25 must be used because R_n^{-1} does not exist.

The effect of measurement noise on the ability of the continuous Kalman Filter to provide accurate estimates of the state appears in the third term on the right side of Eq. 29. If noise occurs in every element of the measurement, R and R^{-1} are positive definite matrices. The term

$$PH^T R^{-1} HP \qquad (31)$$

is also positive definite and the negative of this will always cause a decrease in the "size" of a non-zero error covariance matrix P. The magnitude of this term is inversely proportional to statistical parameters of the measurement noise. Larger measurement noise will cause the error covariance to diminish less rapidly or to grow, depending on the system dynamics, disturbances, and the initial value of P. Smaller noise will cause the filter estimates to converge on the true values more rapidly. In the absence of measurement noise in any of the elements of $\underline{z}$, R^{-1} does not exist. This case is treated in Ref. 6. The effects of system disturbances and measurement noises of different magnitudes can be described graphically by considering the standard deviation of the error in the estimate of representative state variable. This is presented in Fig. 10 for a hypothetical system.

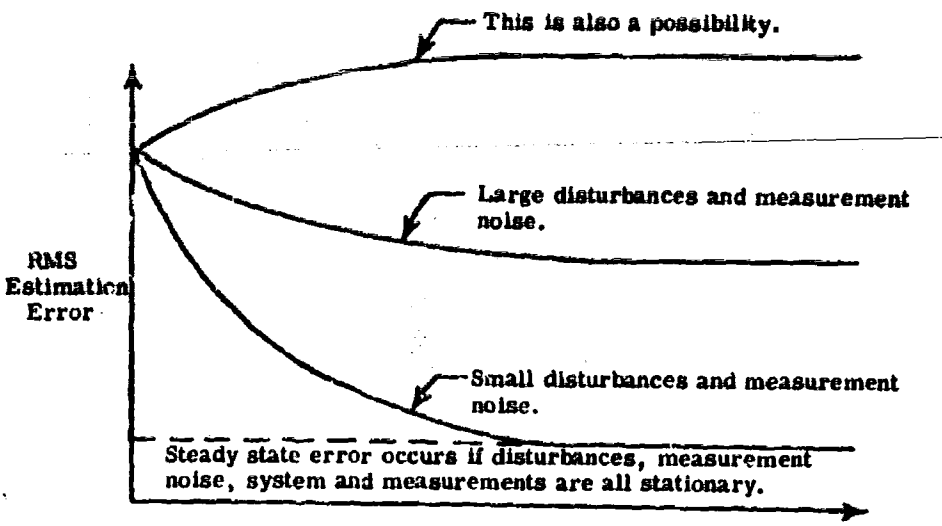

(a) Continuous Filter

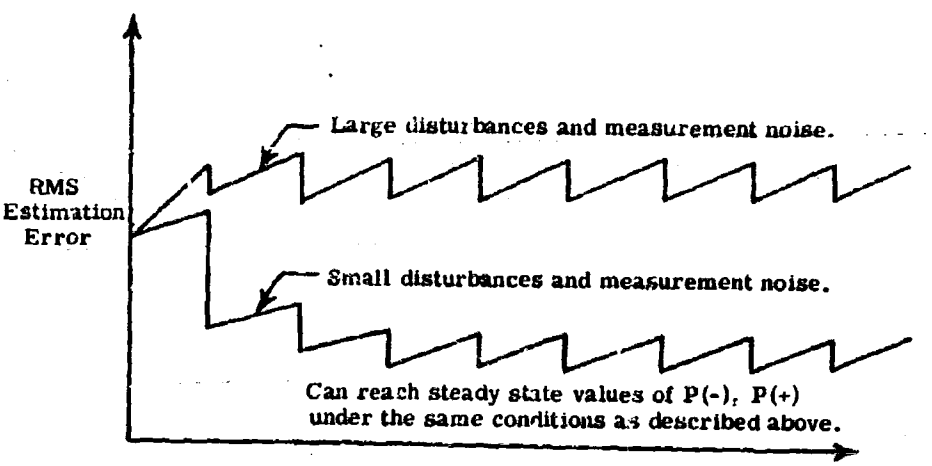

(b) Discrete Filter

FIG. 10. Behavior of the RMS Error in the Kalman Filter Estimate of a Particular State Variable.

Equations 21, 25, and 29 are similar to difference and differential equations that appear frequently in optimization problems. Some work has been accomplished which demonstrates that the Φ (or F), G, and H matrices may be manipulated in order to minimize certain elements of the error covariance matrix (Ref. 11 and 12). This provides a complementary improvement of the Kalman Filter.

Kalman Filter Gain Matrix

It was pointed out earlier that the optimality of the Kalman optimal linear filter is contained in the structure of the filter as displayed in Fig. 7 and 9 and in the specification of the gain matrices by Eq. 23 or 24 and 28. There is an intuitive logic behind the Kalman Filter equations for the gain matrix. It can be seen from Eq. 23

$$K_n = P_n(+)\ H_n^T\ R_n^{-1}$$

but the same ideas apply to Eq. 28. In order to better observe the meaning of the relation, assume that H_n is the identity matrix. It is simply the transformation matrix relating the ideal measurements to the system state according to Eq. 18. When H_n is the identity matrix, both $P_n(+)$ and R_n^{-1} are n x n matrices. If R_n^{-1} is a diagonal matrix (no cross-correlation between noise terms), K_n results from multiplying each column of the error covariance matrix by the appropriate inverse of mean square measurement noise. Each element of the filter gain matrix is essentially the ratio between statistical measures of the uncertainty in the state estimate and the uncertainty in a measurement. If measurement noise is large and state estimate errors are small, the quantity $\underline{z}$ in Fig 7 and 9 is due chiefly to the noise and only small changes in the state estimates should be made. On the other hand, small measurement noise and large uncertainty in the state estimates suggest that $\underline{z}$ contains considerable information about errors in the estimates. Therefore the difference between the actual measurement and that predicted from $H\hat{\underline{x}}$ will be used as the basis for strong corrections to the estimates. Equations 23 and 28 specify the filter gain matrix in a way which agrees with an intuitive approach to improving the estimate.

Correlated Random System Disturbances or Measurement Noise

The requirement that system disturbances and measurement noises be strictly "white noise" or uncorrelated in time can be relaxed to include those random quantities whose correlation time is much less than any characteristic time constant of the system or measurement process. However, the situation frequently arises where the random vectors $\underline{u}$ or $\underline{v}$ do not satisfy this requirement. In order to make the Kalman Filter useful in these cases it is necessary to augment the state vector, i.e, to add new quantities to those which are estimated. In essence, because the random disturbance or measurement error is slowly varying, we are

forced to estimate it in order to correctly evaluate its effect on the estimates of the system state. Correlated signals can be described as resulting from the application of an uncorrelated input to a linear dynamic system. In particular, a zero-mean, exponentially-correlated disturbance is represented by the output of a first-order linear system excited by white noise (see Section 4). The additional state variable in the estimate provided by the Kalman Filter is the output of this first-order system, and the original correlated system disturbance is replaced by the uncorrelated input. In this way the augmented equations for the system and measurement can again be put in the form described earlier for uncorrelated random disturbances and measurement noises. A second-order representation of the correlated quantity would require two additional state elements, etc. Correlated measurement noises can be treated in a similar manner, but in the continuous filter application a more complicated problem arises because augmenting the state vector results in a singular R matrix (Ref. 6).

Optimum Prediction, Smoothing, and Parameter Identification

Several modifications and extensions of the Kalman Filter presently exist. At the same time that the filter was developed it was demonstrated that the optimum prediction of the system state for some time subsequent to the latest measurement is provided by making the state vector estimate obey the deterministic portion of the state differential equation. The initial condition for this equation is given by the estimate immediately after processing the most recent measurement. The error covariance for the predicted state obeys Eq. 12 or 14 (if continuous formulation is desired) with the initial covariance also given by the value immediately following the most recent measurement.

The Kalman Filter has been extended to the area of post-data analysis or optimum smoothing (Ref. 13). The opportunity to use data taken both prior to and subsequent to the point in time at which we want to estimate the system state inevitably permits better estimation accuracy. Additional calculations aggravate a computer-size problem that is often serious with the Kalman Filter alone. Work has also been accomplished on the problem of estimating the parameters of a system by measuring a noise-corrupted linear function of its state variables. Simultaneous refinement of our knowledge of system parameters and random forcing functions is also the subject of much work (see Ref. 14).

AN EXAMPLE

A simple and amusing example will help clarify some of the ideas discussed above. Figure 11 illustrates the example. The observer is attempting to establish (estimate) the position of a drunk relative to a lamp post by observing both through a telescope. The drunk is

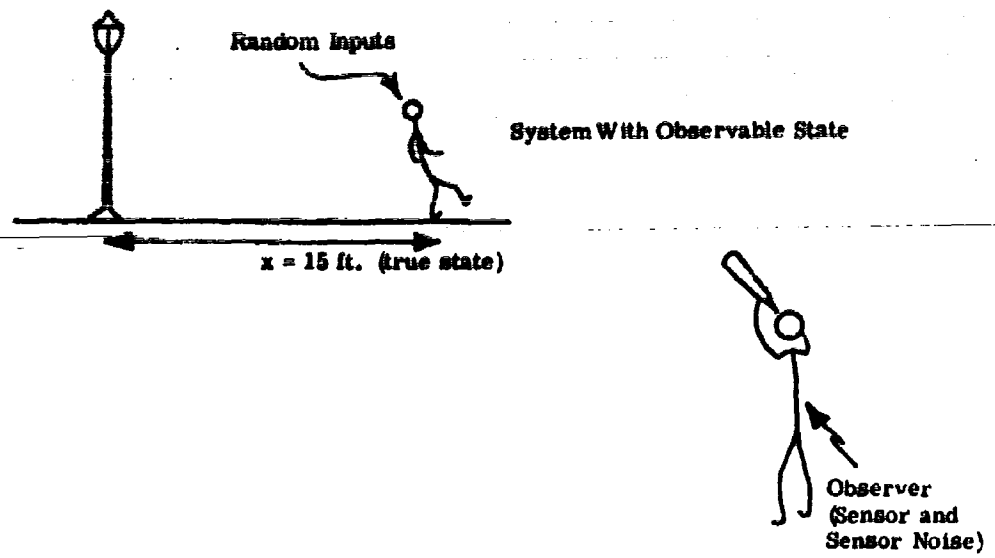

(a) Scenario

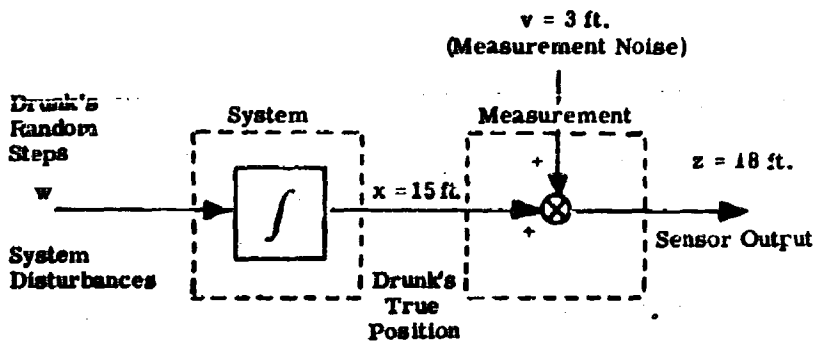

(b) Mathematical Model

FIG. 11. Example: Drunk Near Lamp Post.

constantly taking random length steps in random directions. The observer's measurements are actually non-linear, based on measured angle multiplied by a varying range. However, it will be assumed that the distance to the drunk has an average value and deviations about that value are small compared to the total distance. As a result, the angle between the drunk and the lamp post is taken to be linearly related to the component of the distance between them which is normal to the line of sight. Notice that the component parallel to the line of sight is not observable. (See Section 9.) The single state variable involved in the problem is the position x. The F matrix is zero. Φ and G are scalar (1 x 1) identity matrix. H is the scalar ℓ, the mean distance to the drunk. The drunk's steps and the measurement noise are both assumed to be uncorrelated. Q and R are the mean square values of w and v, respectively. If measurements are taken at discrete points in time which are widely separated compared to the frequency of the drunk's steps, the estimates of his position will deteriorate between observations. Correlated measurement errors would result if the observer was on a structure that was swaying slowly compared to the measurement frequency. Given an initial value for the mean square error in *a priori* knowledge of the drunk's position, the corrections to be made to the estimate as a result of the measurements could be calculated.

If the measurements are equally spaced and if the drunk's steps in the observable direction x provide an RMS position change of q each period, the error covariance of our position estimate between measurements can be written from Eq. 12 as

$$p_n(-) = q^2 + p_{n-1}(+) \tag{32}$$

where the lower case notation is used to indicate scalar quantities. As a measurement is incorporated, the error covariance changes according to Eq. 30

$$\frac{1}{p_n(+)} = \frac{1}{q^2 + p_{n-1}(+)} + \frac{1}{r_n^2} \tag{33}$$

where r_n is the RMS of the measurement error, expressed as a distance. Simplifying Eq. 33 and substituting into Eq. 23, the filter gain is

$$k_n = \frac{p_n(+)}{r_n^2} = \frac{q^2 + p_{n-1}(+)}{q^2 + p_{n-1}(+) + r_n^2}$$

$$= \frac{1}{1 + \dfrac{r_n^2}{p_{n-1}(+) + q^2}} \tag{34}$$

The estimate of the distance x is corrected with each measurement according to

$$\hat{x}_n(+) = \hat{x}_n(-) + k_n \left[z_n - \hat{x}_n(-) \right] \tag{35}$$

From Eq. 34 it can be seen that, if the measurement noise is much less than either the effect of the subject's movement between measurements or the uncertainty in position after the last measurement, $\left\{ p_{n-1}(+) \right\}$, then

$$k_n \approx 1$$

and the estimate of present position closely approximates the most recent observation. On the other hand, if r_n^2 is much greater than the sum of q^2 and $p_{n-1}(+)$,

$$k_n << 1$$

and each observation improves the estimate very little.

EXTENSION TO NONLINEAR SYSTEMS

Though the Kalman Filter is optimum only when the system differential equations and measurements are linear, it has found considerable use in estimating the state variables of nonlinear systems with measurements that are noise-corrupted nonlinear functions of the state variables. This employment of the Kalman Filter is frequently referred to as the "Extended Kalman Filter" (Ref. 15). It is an intuitive but frequently successful application of the Kalman Filter in the absence of truly optimum filters for nonlinear systems.

Suppose the system whose state it is desired to estimate obeys the nonlinear differential equation

$$\dot{\underline{x}} = \underline{f}\ (\underline{x},\ \underline{u},\ t) \tag{36}$$

and the measurements are noise-corrupted nonlinear functions of the state according to

$$\underline{z} = \underline{h}\ (\underline{x},\ t) + \underline{v} \tag{37}$$

If our knowledge of the system state is such that the matrices

$$F = \left.\frac{\partial \underline{f}}{\partial \underline{x}}\right|_{\hat{\underline{x}}}$$

$$G = \left.\frac{\partial \underline{f}}{\partial \underline{u}}\right|_{\hat{\underline{x}}} \qquad (38)$$

$$H = \left.\frac{\partial \underline{h}}{\partial \underline{x}}\right|_{\hat{\underline{x}}}$$

are approximately constant over the range of uncertainty in $\hat{\underline{x}}$, then the continuous Kalman Filter gain matrix can be computed from the above linearization according to Eq. 28 and 29 or Φ can be determined from Eq. 6 and the discrete filter gain calculated. It should be noted that the F, G, and H matrices computed from Eq. 38 can be nonlinear functions of $\hat{\underline{x}}$. The continuous estimate of the state vector is found from the equation

$$\dot{\hat{\underline{x}}} = \underline{f}(\hat{\underline{x}}, t) + K[\underline{z} - \underline{h}(\hat{\underline{x}}, t)] \qquad (39)$$

Equation 39 is similar to that used when the system is linear and linear measurements are prescribed. It differs only in the use of nonlinear system and measurement functions $\underline{f}$ and $\underline{h}$. Figure 12 illustrates the continuous Kalman Filter for a nonlinear system. An alternative approach is to precompute a nominal state trajectory and evaluate F, G, and H in advance. This reduces the on-line computation necessary, but it suffers further errors if the true and nominal state differ significantly.

These techniques are only approximate. They require that the disturbances, measurement noises, and uncertainties in the state be of such a size that the higher-order terms ignored in computing the error covariance are insignificant. If this condition is not satisfied, the application of the Kalman Filter to nonlinear systems may be useless. An iterative technique may be useful in reevaluating the matrices in Eq. 38 based on making a first estimate, $\hat{\underline{x}}_n$, evaluating Eq. 38, then recomputing the state estimate, etc. (Ref. 16 and 17).

Another approach to linear filtering for systems with nonlinear dynamics and nonlinear observations is the use of a one-to-one nonlinear transformation to map the nonlinear problem into a space in which the transformed problem is linear (Ref. 18). However, the assumption of Gaussian noise in the transformed problem is frequently incorrect.

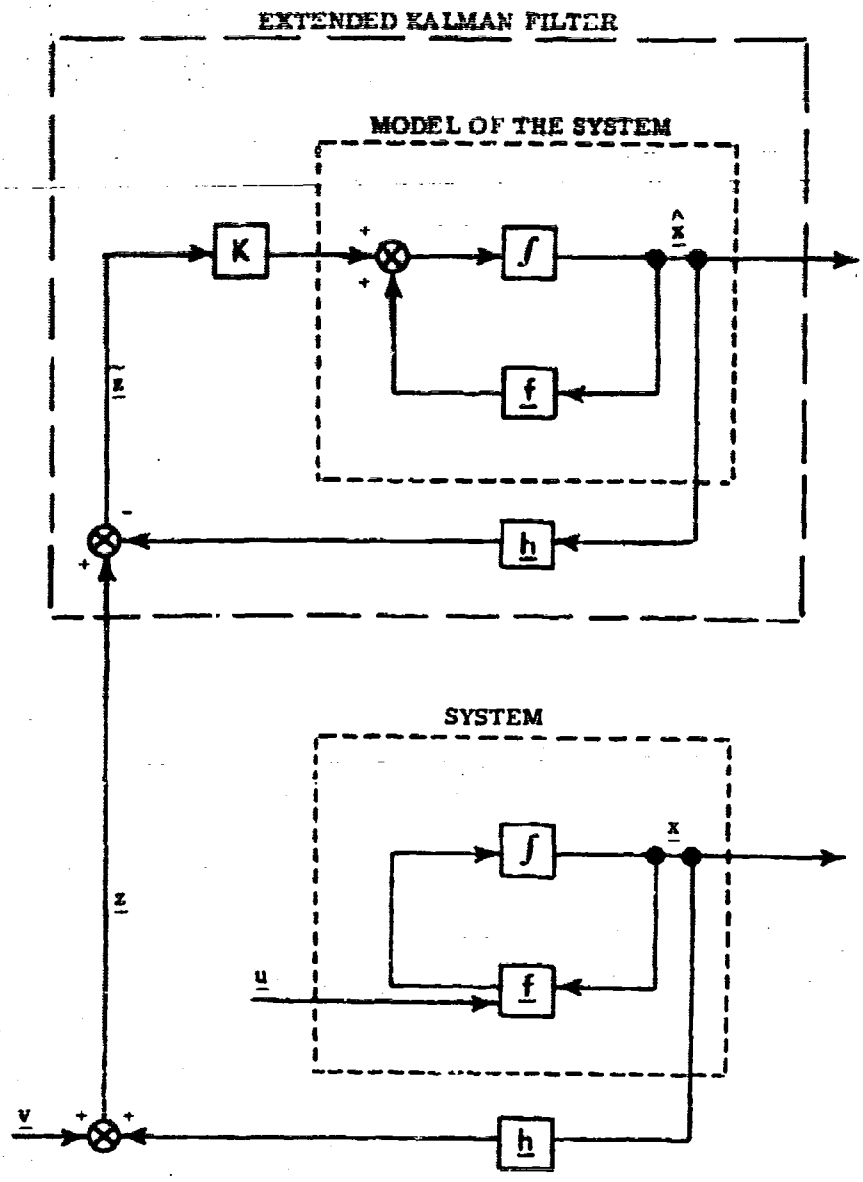

FIG. 12. Block Diagram of the Estimation Equations for the Extended Kalman Filter.

In brief, the Kalman Filter can be quite useful in estimating the state variables of nonlinear systems. However, more care must be exercised in checking theoretical results by means of simulation. Because the error covariance equations provide only an approximate evaluation of the estimation error statistics, Monte Carlo techniques are required to verify the use of the Extended Kalman Filter for nonlinear systems. When the Kalman Filter produces poor estimates of the state of a nonlinear system, ingenious changes can often produce a useful modified version (Ref. 19).

SUMMARY

The Kalman Filter is a systematic approach to estimating the state variables of a linear system. It provides the minimum variance estimates based on:

1. Repeated external measurements
2. An understanding of system and measurement dynamics
3. A statistical knowledge of the system disturbances
4. A statistical knowledge of measurement errors
5. A statistical knowledge of the errors in determining the initial state.

Figure 13 contains a summary of the Kalman Filter equations.

KALMAN FILTER WITH DISCRETE MEASUREMENTS

System Model:

$$\underline{x}_{n+1} = \Phi_n \underline{x}_n + \underline{w}_n \qquad E\left[\underline{w}_n \underline{w}_m^T\right] = Q_n \delta_{nm}, \; E\left[\underline{w}_n\right] = 0$$

Measurement Model:

$$\underline{z}_n = H_n \underline{x}_n + \underline{v}_n \qquad E\left[\underline{v}_n \underline{v}_m^T\right] = R_n \delta_{nm}, \; E\left[\underline{v}_n\right] = 0$$

Kalman Filter:

$$\hat{\underline{x}}_{n+1} = \Phi_n \hat{\underline{x}}_n + K_n \left[\underline{z}_n - H_n \Phi_n \hat{\underline{x}}_n\right]$$

$$K_n = P_n (+) H_n^T R_n^{-1}$$

$$P_{n+1}^{-1} (+) = P_{n+1}^{-1} (-) + H_{n+1}^T R_{n+1}^{-1} H_{n+1}; \text{ one step transition (updating only)}$$

$$P_{n+1} (-) = \Phi_n P_n (+) \Phi_n^T + Q_n; \text{ growth between measurements (does not involve measurements)}$$

KALMAN FILTER WITH CONTINUOUS MEASUREMENTS

System Model:

$$\dot{\underline{x}} = F\underline{x} + G\underline{u}, \qquad E\left[\underline{u}(t)\,\underline{u}(t')^T\right] = Q\,\delta(t - t'), \; E\left[\underline{u}(t)\right] = 0$$

Measurement Model:

$$\underline{z} = H\underline{x} + \underline{v}, \qquad E\left[\underline{v}(t)\,\underline{v}(t')^T\right] = R\,\delta(t - t'), \; E\left[\underline{v}(t)\right] = 0$$

Kalman Filter:

$$\dot{\hat{\underline{x}}} = F\hat{\underline{x}} + K\left[\underline{z} - H\hat{\underline{x}}\right]$$

$K = PH^T R^{-1}$ = Kalman optimum weighting matrix

$\dot{P} = FP + PF^T + GQG^T - PH^T R^{-1} HP$
(covariance matrix riccati equation)

EXTENSION TO NONLINEAR SYSTEMS

System:

$$\dot{\underline{x}} = \underline{f}(\underline{x}, \underline{u}, t)$$

Measurement:

$$\underline{z} = \underline{h}(\underline{x}, t) + \underline{v}$$

Linearization: (about the best estimate)

$$F = \left.\frac{\partial \underline{f}}{\partial \underline{x}}\right|_{\hat{\underline{x}}}, \; G = \left.\frac{\partial \underline{f}}{\partial \underline{u}}\right|_{\hat{\underline{x}}}, \; H = \left.\frac{\partial \underline{h}}{\partial \underline{x}}\right|_{\hat{\underline{x}}}$$

Estimate:

$$\dot{\hat{\underline{x}}} = \underline{f}(\hat{\underline{x}}, t) + K\left[\underline{z} - \underline{h}(\hat{\underline{x}}, t)\right]$$

$K = PH^T R^{-1}$

FIG. 13. Summary of Kalman Filter Forms.

Section 3. MODELS OF INERTIAL NAVIGATION SYSTEMS AND ERROR DYNAMICS

Engineers using the Kalman Filter to improve the accuracy of inertial navigators have, in part, been successful because they possessed a good understanding of the physical principles underlying inertial navigation. Consequently, the succeeding sections discuss basic inertial sensors, strapdown and gimballed inertial measuring units, navigation using inertial measurements, the propagation of errors in an inertial navigation system, and the external measurements used to recalibrate.

INERTIAL SENSORS

It was noted earlier that the concept of inertial navigation is quite simple; measurement of linear acceleration, velocity and angular rate, and application of Newton's laws of motion. There are two kinds of sensors which are basic to inertial systems--those which measure linear motion and those which measure angular motion.

Accelerometers

Linear motion is indicated by accelerometers. As the name implies, they measure linear acceleration though frequently the instrument output signal is the integral of the measured acceleration (i.e., velocity difference). Accelerometers operate by sensing the forces acting on a proof mass. This force may be indicated by a linear displacement, torque (through a moment arm), change in the natural frequency of a vibrating element, etc. Figure 14 illustrates a pendulous accelerometer which converts force along the input axis to torque about the output axis. The quantity measured by an ideal accelerometer is often called specific force and represents the acceleration of the proof mass less that portion due to mass attraction (gravitation). It is expressed by the equation[1]

$$\bar{f} = m\,(\bar{a} - \bar{G}) \qquad (40)$$

where $\bar{f}$ is specific force, $\bar{a}$ is the acceleration of the proof mass, m, and $\bar{G}$ is the gravitational attraction acceleration. If m and $\bar{G}$ are known, acceleration can be calculated from the specific force. Accelerometers typically measure specific force along one axis fixed in the instrument and three such devices are necessary to imply total acceleration in three-dimensional navigation space. It is customary, though not necessary, to orient their input axes to be mutually perpendicular.

[1] In the equations of inertial navigation systems, physical vectors will be designated by an overbar to distinguish them from the vector notation (underbar) used in discussions of the Kalman Filter.

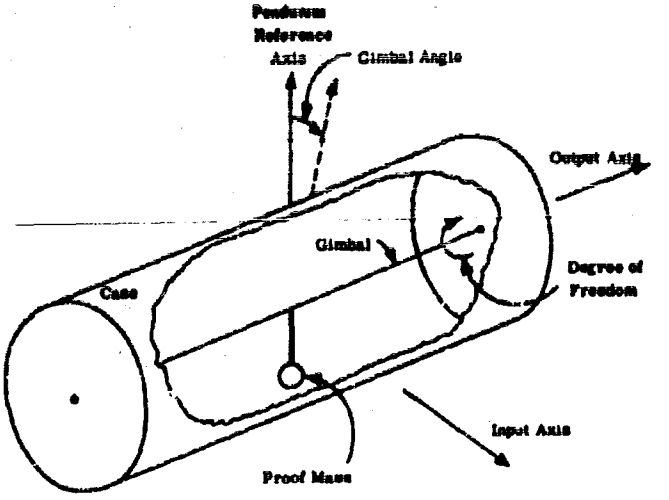

FIG. 14. Single-Degree-of-Freedom Accelerometer.

Gyroscopes

The angular motion sensor used in inertial navigation systems is the gyroscope. Two basic types of gyroscope exist: the so-called free or two-degree-of-freedom gyro and the restrained or single-degree-of-freedom gyro.

The single-degree-of-freedom (SDF) gyro is illustrated in Fig. 15. Its basic operation results from the fact that an angular rate about the input axis creates a torque about the output axis. The torque is expressed by the equation

$$\tau_o = H\omega_i \tag{41}$$

where ω_i is the input angular rate and H is the rotor spin angular momentum. The single degree of freedom is provided by permitting the gimbal to rotate relative to the case about the output axis. The gimbal angle is the angle between the angular momentum vector and some nominal orientation of H relative to the case. If damping is provided between the gimbal and the case, the gimbal angle represents the integral of the angular rate, ω_i, and a rate-integrating gyro results. If a restoring torque proportional to the gimbal angle is provided, the device is called a rate gyro. In either case the sensor output is provided by measuring the gimbal angle. A torque generator which provides torque to the gimbal about the output axis is also present in most applications.

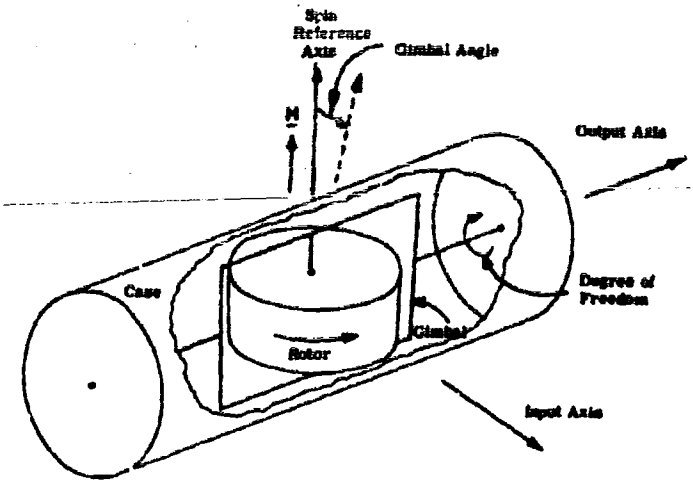

FIG. 15. Single-Degree-of-Freedom Gyro.

With the two-degree-of-freedom gyro, use is made of the fact that, in the absence of torques, the angular momentum vector keeps a fixed direction in inertial space. Therefore, gyro case motions are detected from the relative orientation between rotor and case. Three SDF gyros are used to sense the total angular motion of an instrument package. They are customarily oriented with their input axes orthogonal. If free gyros are used, only two instruments are required.

INERTIAL MEASUREMENT UNITS

Inertial navigation systems require an indication of acceleration as the input to the navigation equations. Furthermore, these accelerations (or rather the acceleration vector) must be resolved into the coordinate frame in which the navigation equations are computed. Two general approaches, described below, are taken to the problem of indicating inertial acceleration in the desired coordinate frame. Both techniques employ an instrument cluster or inertial measurement unit (IMU) which consists of the necessary number of gyros and accelerometers. The inertial sensors measure acceleration and angular motion in a coordinate system fixed in the IMU. The two schemes differ only in the way they provide acceleration measurements resolved in navigation coordinates.

Gimballed Platforms

The first practical inertial navigation systems mounted their sensor clusters on gimballed platforms. Gimbals permit isolation of the instruments from angular motions of the carrying vehicles. This isolation is

accomplished with the help of the gyros. They indicate changes in the angular orientation of the platform relative to inertial space and, by means of gimbal servos, the platform is returned to its proper attitude. When a rotation of the platform relative to inertial space is desired, output axis torque generators on the gyros are used to cause false indications of angular rotation. Because they cannot be distinguished from actual inputs, these fictitious rotations provide platform reorientation in a manner similar to that described above. For more detail, the concept of the space integrator is useful (Ref. 20 and 21). The gimballed platform permits accelerometer measurements to be used directly because the sensor input axes can be oriented parallel to the navigation axes.

Strapdown Systems

The simplest way to mount the instrument cluster is to attach it rigidly to the vehicle. This approach saves the weight and power associated with gimbals and gimbal servos. But as a result of the fact that the navigation equations are seldom implemented in vehicle-fixed coordinates, the accelerometer outputs must be resolved into the navigation axis system. The relative orientation between orthogonal sensor input axes and the navigation coordinate system is described by a transformation matrix. If the initial value of this matrix is known, the gyros provide the necessary information to calculate it for all subsequent times during system operation. The acceleration vector, measured in the vehicle axes, is then transformed into navigation axes; subsequent data processing is identical with that of gimballed systems. While the strapdown system simplifies the hardware requirements for an IMU, it increases the requirements for computer size, speed, and accuracy because of the transformation matrix calculations. In addition, because high input angular rates are experienced, SDF gyros in strapdown applications must be provided with high-level torque generators.

Whatever their mechanization, IMU's use groups of inertial sensors to indicate acceleration resolved in the navigation coordinate frame. The two schemes discussed above are illustrated in Fig. 16.

INERTIAL NAVIGATION SYSTEMS

The simplest form of navigation using inertial instruments is expressed by the equation

$$\left(\frac{d^2\,\overline{R}}{dt^2}\right)_I = \frac{\overline{f}}{m} + \overline{G} \qquad (42)$$

The vector $\overline{R}$ describes a position relative to the earth's center. Its second derivative as seen in inertial coordinates is given by the properly resolved accelerometer measurements, with the gravitational acceleration

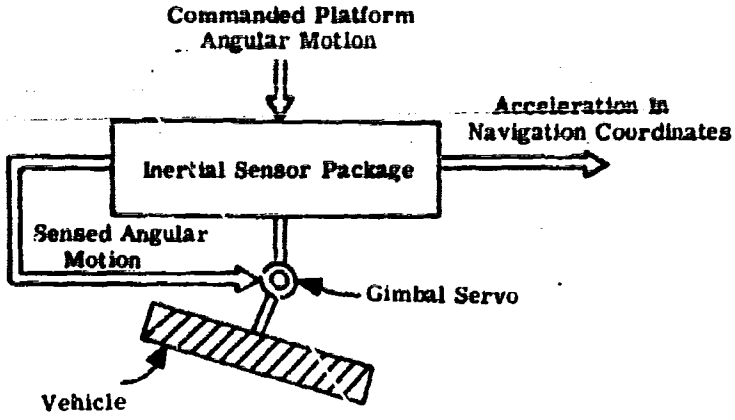

(a) Gimballed IMU

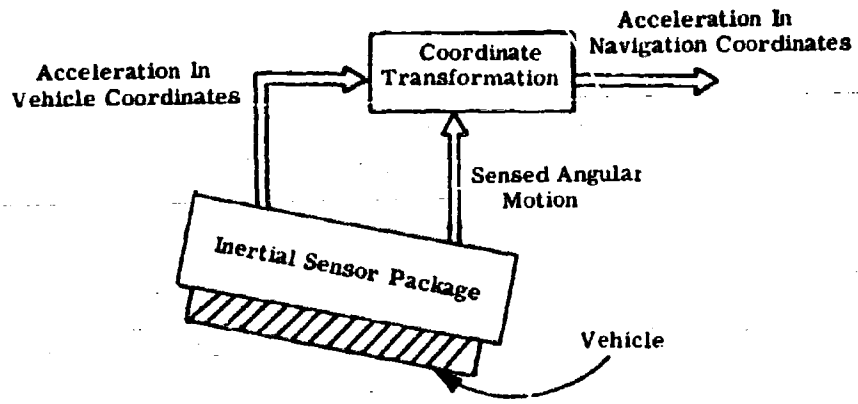

(b) Strapdown IMU

FIG. 16. Inertial Measurement Unit Concepts.

added. Double integration of Eq. 42 will provide indications of the changes in $\bar{R}$. In addition, if the results are to be correct, the guidance computer must indicate $\bar{G}$ exactly, the accelerometer must have no errors, and the initial conditions on $\bar{R}$ and $d\bar{R}/dt$ must be known.

Most of the discussion in this report involves navigation near the earth. For this problem three reference frames are useful. The first is the inertial frame already mentioned. In addition, a reference frame with origin at earth's center is defined. This frame is inertially non-accelerating but fixed to the earth and therefore rotating relative to inertial space at a constant rate of approximately 15 degrees per hour. The rotation rate is represented by a vector, $\bar{\Omega}$. The third reference frame is that of the particular inertial system. It has its origin near the earth's surface, usually at the position of the vehicle carrying the sensors. It can rotate relative to the earth-fixed frame at a rate designated ρ. For convenience the three frames are called I, E, and C, respectively (see Fig. 17). Ideally, the accelerometer measurements are resolved into the C frame.

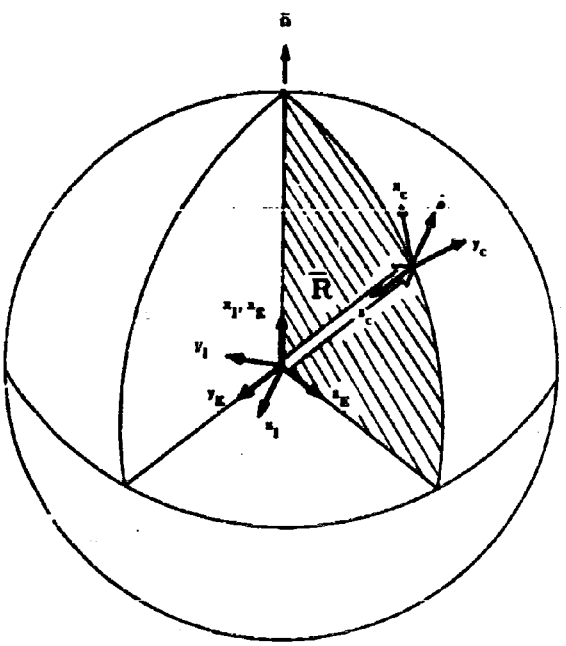

FIG. 17. Reference Coordinate Frames for Near-Earth Inertial Navigation.

The position of a vehicle near the surface of the earth is usually described by the position vector resolved in the earth-fixed or E coordinate frame. The velocity of the vehicle with respect to the earth is designated $\bar{v}$ and expressed by

$$\bar{v} = \left(\frac{d\bar{R}}{dt}\right)_E$$

$$= \left(\frac{d\bar{R}}{dt}\right)_I - \bar{\Omega} \times \bar{R} \tag{43}$$

Equation 43 makes use of a theorem of Coriolis. The derivative of $\bar{v}$ with respect to the C or navigation coordinate frame is given by

$$\left(\frac{d\bar{v}}{dt}\right)_C = \left(\frac{d\bar{v}}{dt}\right)_E - \bar{\rho} \times \bar{v} \tag{44}$$

The derivative of $\bar{v}$ with respect to the E frame is related by

$$\left(\frac{d\bar{v}}{dt}\right)_E = \left(\frac{d^2\bar{R}}{dt^2}\right)_E$$

$$= \left(\frac{d^2\bar{R}}{dt^2}\right)_I - 2\bar{\Omega} \times \left(\frac{d\bar{R}}{dt}\right)_E - \bar{\Omega} \times (\bar{\Omega} \times \bar{R}) \tag{45}$$

Substituting from Eq. 45 into Eq. 44,

$$\left(\frac{d\bar{v}}{dt}\right)_C = \left(\frac{d^2\bar{R}}{dt^2}\right)_I - 2\bar{\Omega} \times \bar{v} - \bar{\Omega} \times (\bar{\Omega} \times \bar{R}) - \bar{\rho} \times \bar{v} \tag{46}$$

Defining

$$\bar{\omega} = \bar{\Omega} + \bar{\rho} \tag{47}$$

Eq. 46 becomes

$$\left(\frac{d\bar{v}}{dt}\right)_C = \left(\frac{d^2\bar{R}}{dt^2}\right)_I - (\bar{\omega} + \bar{\Omega}) \times \bar{v} - \bar{\Omega} \times (\bar{\Omega} \times \bar{R}) \tag{48}$$

Substituting from Eq. 42,

$$\left(\frac{d\bar{v}}{dt}\right)_C = \frac{\bar{f}}{m} - (\bar{\omega} + \bar{\Omega}) \times \bar{v} + \bar{G} - \bar{\Omega} \times (\bar{\Omega} \times \bar{R}) \tag{49}$$

When considering navigation near the surface of the earth, it is convenient to define a new vector, gravity. Because of the earth's rotation, the local vertical or plumb line is parallel to the gravitation vector $\bar{G}$ only at the poles. At any other latitude the earth's rotation tilts the local vertical, $\bar{g}$, so that it is related to the gravitation vector by

$$\bar{g} = \bar{G} - \bar{\Omega} \times (\bar{\Omega} \times \bar{R}) \tag{50}$$

This is illustrated in Fig. 18. Equation 49 can be written in terms of the gravity vector

$$\left(\frac{d\bar{v}}{dt}\right)_C = \frac{\bar{f}}{m} - (\bar{\omega} + \bar{\Omega}) \times \bar{v} + \bar{g} \tag{51}$$

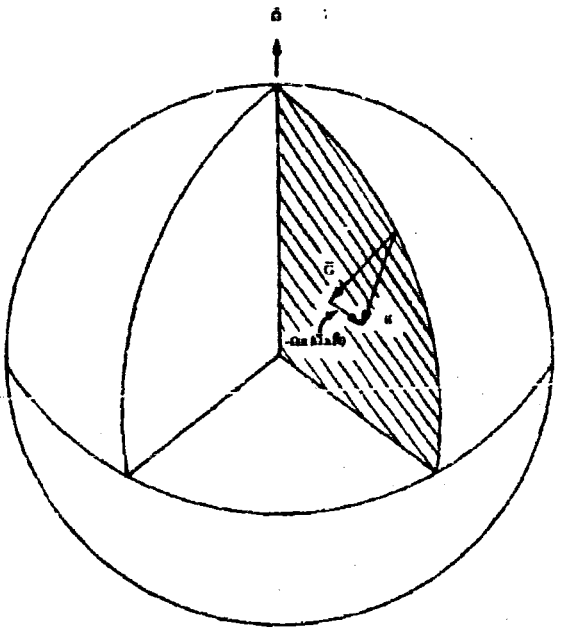

FIG. 18. Definition of Gravity Vector.

Equation 51 is one of the most convenient forms of the navigation equations to implement. The left side of the equation is the derivative of earth-fixed velocity with respect to the navigation frame. The first term on the right is provided by the accelerometers and the remaining two terms can be calculated from position and knowledge of ρ. The computer solves Eq. 51 for the vehicle velocity vector in the navigation frame. Then a second integration provides changes in $\bar{R}$ relative to the earth-fixed coordinate frame.

Several choices of the navigation frame, C, are commonly used for near-earth navigation. They differ basically in the way the vector $\bar{\omega}$ is prescribed. The three most popular are:

1. North--vertical

   Center at present vehicle location
   x--horizontal, north
   y--horizontal, east
   z--vertical (down)

2. Free azimuth[2]

   Center at present vehicle location
   x--horizontal, at known (variable) angle with north
   y--horizontal, at known (variable) angle with east
   z--vertical (down)

3. Tangent plane

   Center at a nominal vehicle location
   x--initial north
   y--initial east
   z--initial vertical (down)

The first two coordinate systems are called "locally level" because their x-y planes are always tangent to the earth at the vehicle position. These are usually found in cruise vehicles (aircraft, submarines, ships) which travel long distances. The third system is referred to as "launch point level" and is used in missile applications and for navigation over small areas.

ERRORS IN INERTIAL NAVIGATION SYSTEMS

It is impossible to implement inertial navigation systems without errors. However, these errors can be kept within acceptable bounds through the use of external measurements. Presently, the predominant error sources are imperfect indications of motion as provided by the gyros and accelerometers as well as limited knowledge of the direction of g. Gyro errors, called drift rates, will be designated in vector form by $\bar{\epsilon}$, and accelerometer errors are designated $\bar{\nabla}$. Many inertial

[2] In this case the z component of $\bar{\omega}$ is zero. A related system, often called "wander azimuth," has the z component of $\bar{\omega}$ equal to the z component of $\bar{\Omega}$.

navigation system errors not due to false initial conditions are caused by effects which can be lumped into the terms $\bar{\epsilon}$ and $\bar{\nabla}$.

Using standard perturbation techniques, the effect of these errors on the navigation computations can be determined. Appendix C derives the inertial navigator error equations for near-earth systems. It also demonstrates the basic instability that appears in the navigation equations for the vertical direction. The error equations are expressed in vector form in terms of the position vector in an earth-fixed coordinate frame, $\bar{R}$; inertial angular rate vector of the navigation coordinate frame, $\bar{\omega}$; earth rotation rate vector, $\bar{\Omega}$; angle between computer indication of the navigation coordinates and the axis system in which accelerometer outputs are actually resolved, $\bar{\psi}$; and the specific force vector and instrument errors

$$\left\{\begin{array}{l} \ddot{\delta R} + 2\bar{\omega} \times \dot{\delta R} + \dot{\bar{\omega}} \times \delta R \\ \\ + \bar{\omega} \times (\bar{\omega} \times \delta R) - \bar{\Omega} \times (\bar{\Omega} \times \delta R) \\ \\ + \omega_s^2 \, \delta R \end{array}\right\} = - \bar{\psi} \times \frac{\bar{f}}{m} + \bar{\nabla} - 2\omega_s \, (\delta\omega_s) \, \bar{R} \qquad (52)$$

where

$$\omega_s = \sqrt{\frac{|\bar{g}|}{|\bar{R}|}} \qquad (53)$$

and the dynamics of $\bar{\psi}$ are described (see Appendix C) by

$$\dot{\bar{\psi}} = \bar{\psi} \times \bar{\omega} + \bar{\epsilon} \qquad (54)$$

The errors in navigation quantities are the state variables in the Kalman Filter. By substituting the proper relation for $\bar{\omega}$ into Eq. 52 and 54, the F or Φ matrices required in Eq. 12 and 14 can be defined. The error relations can also be diagramed. Figure 19 illustrates the propagation errors in a north-vertical system.

EXTERNAL MEASUREMENTS

In order to keep the errors generated in an inertial navigation system within acceptable levels, it is necessary to recalibrate the system periodically. The recalibration or correction of system errors is

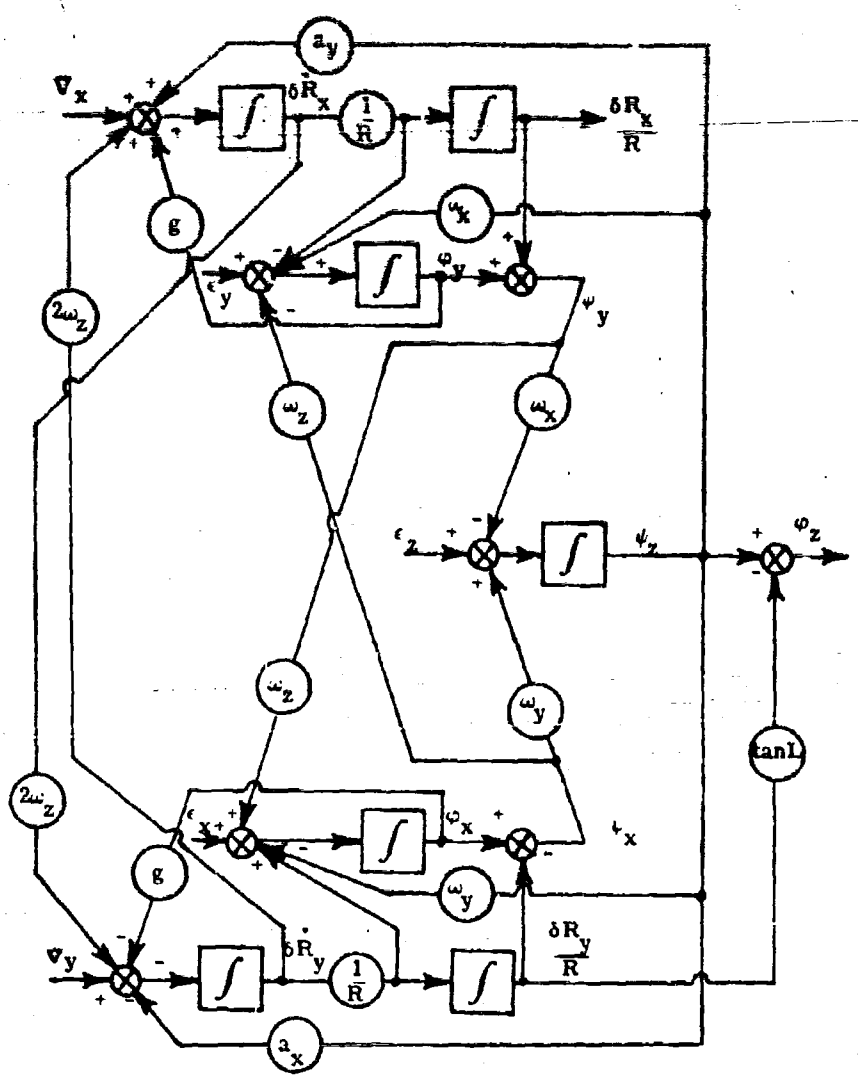

FIG. 19. Block Diagram of Error Dynamics for a North-Vertical Inertial Navigation System.

achieved with the use of independent sources of information. Those external measurements include position, velocity, attitude, and combinations thereof. Typical sources are:

Position--Radio navigation aids (Loran, Omega, Tacan, etc.)
Navigation satellites
Star sights
Landmarks, identified and unidentified
Radar
Map matching

Velocity--Doppler radar
Electromagnetic speed log

Attitude--Star sight
Horizon measurements

The external measurements are compared to corresponding quantities indicated by the inertial navigation system, and system and random measurement errors are related linearly to the difference. This linear relation between inertial system errors and the formed differences between measured and indicated values of position, velocity, and attitude specifies the H matrices in Eq. 18 and 26. The Kalman Filter uses the differences between indicated and measured quantities to provide the optimum estimate of the inertial navigation system errors. Inertial sensor errors such as gyro drift rate and accelerometer errors are also estimated. Corrections may then be applied to the system, based on the error estimates. Figure 20 illustrates the procedure. A more detailed description of the manner in which the corrections are applied is found in Section 6.

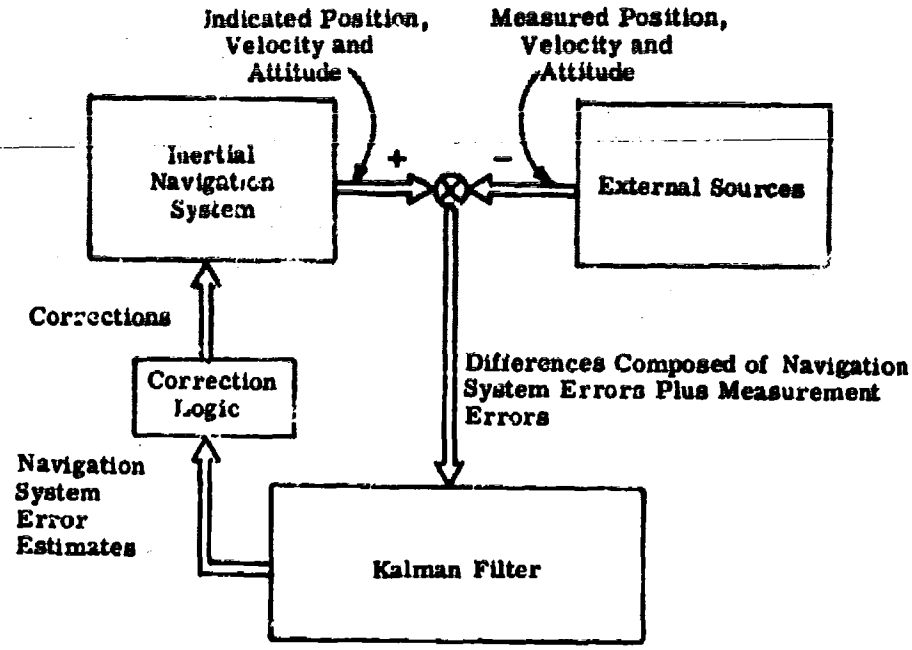

FIG. 20. Block Diagram of Recalibration Scheme.

Section 4. CORRELATED ERROR DYNAMICS FOR SENSORS

The Kalman Filter equations displayed in Section 2 were developed with the assumption that the system disturbances ($\underline{u}(t)$ or $\underline{w}_n$) and measurement errors ($\underline{v}(t)$ or $\underline{v}_n$) were not correlated in time. The strict requirement of "white noise" disturbances and measurement errors can be relaxed to include those quantities whose correlation time is much less than the characteristic times of the system or of the measurements. In either case, the lack of correlation is an indication that nothing can be gained by estimating the disturbances and errors themselves, i.e., if an accurate estimate was available it would not help predict the state at the next time of interest. However, when the disturbances and measurement errors are not changing rapidly compared with the system state or measurements, the filter accuracy can be enhanced by estimating these additional quantities; the filter estimates of $\underline{u}(t)$ and $\underline{v}(t)$ are used to more accurately predict system behavior.

The estimation of system disturbances and measurement errors which have significant time correlation is frequently described as "state vector augmentation." That is, the number of state variables to be estimated is increased by including these quantities. Also, their dynamic behavior is described in the appropriate rows of an enlarged F (or Φ) matrix which specifies the unforced behavior of the augmented state vector. Because these quantities are random, their behavior cannot be described deterministically. Instead, they are usually taken to be the state variables of a fictitious linear dynamic system which is excited by white noise. This model serves two purposes; it provides the proper autocorrelation characteristics through specification of the linear system and the strength of the driving noise, and, in addition, the random nature of the signal follows from the random excitation. The differential equation for the augmented state is in the proper form for the Kalman Filter--a deterministic system excited by an uncorrelated random signal. When measurement noise quantities are included in the augmented state vector, some of the newly-defined measurement vector elements do not contain noise. As a result, the matrix R^{-1} is undefined and modifications must be made to the equations of Section 2 for the continuous filter (see Ref. 6). All correlated system disturbances and measurement errors for inertial navigation systems can be described to a good approximation by a combination of one or more of the several types of behavior described in this section.

STATE VECTOR AUGMENTATION

The augmentation of the state vector to account for correlated disturbances can be illustrated using Eq. 2

$$\dot{\underline{x}} = F\underline{x} + G\underline{u} \tag{55}$$

Suppose $\underline{u}$ was composed of correlated quantities $\underline{u}_1$ and uncorrelated quantities $\underline{u}_2$,

$$\underline{u} = \underline{u}_1 + \underline{u}_2 \tag{56}$$

If $\underline{u}_1$ can be modeled to obey a differential equation

$$\dot{\underline{u}}_1 = F_u \underline{u}_1 + \underline{u}_3 \tag{57}$$

where $\underline{u}_3$ is a vector composed of uncorrelated quantities, then the augmented state vector $\underline{x}'$ is given by

$$\underline{x}' = \begin{bmatrix} \underline{x} \\ \hline \underline{u}_1 \end{bmatrix} \tag{58}$$

and the augmented state differential equation, driven only by uncorrelated disturbances, is given by

$$\dot{\underline{x}}' = \begin{bmatrix} \dot{\underline{x}} \\ \hline \dot{\underline{u}}_1 \end{bmatrix} = \left[\begin{array}{c|c} F & G \\ \hline O & F_u \end{array}\right] \begin{bmatrix} \underline{x} \\ \hline \underline{u}_1 \end{bmatrix} + \left[\begin{array}{c|c} G & O \\ \hline O & I \end{array}\right] \begin{bmatrix} \underline{u}_2 \\ \hline \underline{u}_3 \end{bmatrix} \tag{59}$$

To illustrate state vector augmentation to account for correlated measurement noise, suppose

$$\begin{aligned} \dot{\underline{x}} &= F\underline{x} + G\underline{u} \\ \underline{z} &= H\underline{x} + \underline{v} \end{aligned} \tag{60}$$

where $\underline{u}$ is a vector of uncorrelated disturbances, but $\underline{v}$ is the sum of a correlated measurement noise vector, $\underline{v}_1$, and uncorrelated errors, $\underline{v}_2$,

$$\underline{v} = \underline{v}_1 + \underline{v}_2 \tag{61}$$

If the correlated measurement errors are modeled to obey the white-noise driven differential equation

$$\dot{\underline{v}}_1 = F_v \underline{v}_1 + \underline{u}_v \tag{62}$$

the augmented state vector $\underline{x}'$ obeys the differential equation

$$\dot{\underline{x}}' = \begin{bmatrix} \dot{\underline{x}} \\ \dot{\underline{v}} \end{bmatrix} = \left[\begin{array}{c|c} F & O \\ \hline O & F_v \end{array}\right] \begin{bmatrix} \underline{x} \\ \underline{v} \end{bmatrix} + \left[\begin{array}{c|c} G & O \\ \hline O & I \end{array}\right] \begin{bmatrix} \underline{u} \\ \underline{u}_v \end{bmatrix} \tag{63}$$

and the measurement obeys

$$\underline{z} = \left[H \mid I\right] \underline{x}' + \underline{v}_2 \tag{64}$$

If $\underline{v}_2$ has one or more zero elements (one or more measurements do not contain uncorrelated errors) the R matrix has a corresponding number of zero rows and columns. As a result, R^{-1} does not exist and a modification to the continuous Kalman Filter is necessary (Ref. 6).[3]

CORRELATION MODELS

Random Constant

The random constant is a nondynamic quantity with a random amplitude. Nevertheless, if it is known to exist, the random constant must be included among the elements of the augmented state vector.

$$\dot{x} = 0 \tag{65}$$

Its constant nature is indicated by the fact that the rows of the F and G matrices corresponding to this quantity contain only zeros. In the discrete formulation, the element at the intersection of the corresponding row and column of the Φ_n matrix is unity while the remaining elements of the pertinent row are zeros. The corresponding row and column of the matrices $G\,Q\,G^T$ or Q_n contain only zeros. Figure 21 illustrates the nature of Φ_n, $\underline{w}_n$, and Q_n when one state variable is a random constant. The random constant can be pictured as the output of an integrator with no input but having a random initial condition.

[3]Recent work suggests that state vector augmentation may not be necessary when correlated measurement noise is present (Ref. 22).

$$\begin{bmatrix} X_{1_{n+1}} \\ X_{2_{n+1}} \\ X_{3_{n+1}} \end{bmatrix} = \underbrace{\begin{bmatrix} - & - & - \\ 0 & 1 & 0 \\ - & - & - \end{bmatrix}}_{\Phi_n} \begin{bmatrix} X_{1_n} \\ X_{2_n} \\ X_{3_n} \end{bmatrix} + \underbrace{\begin{bmatrix} - \\ 0 \\ - \end{bmatrix}}_{w_n}$$

$$Q_n = \begin{bmatrix} & 0 & \\ 0 & 0 & 0 \\ & 0 & \end{bmatrix}$$

X_2 is a Random Constant

FIG. 21. Illustration of Φ_n, w_n, and Q_n When One State Variable is a Random Constant.

Random Walk

The random walk results when uncorrelated signals are integrated. It derives its name from an illustration involving a man who takes fixed-length steps in arbitrary directions (see p. 24). In the limit, when the number of steps is large and their length is small, the distance travelled in a particular direction looks like the random walk variable. The state variable differential equation for this quantity is given by

$$\dot{x} = u \tag{66}$$

where $E[u(t)u(\tau)] = q(t)\delta(t-\tau)$. A block diagram representation of this equation is shown in Fig. 22(a). The mean square value of the random walk variable grows linearly with time according to

$$\overline{x^2} = qt^* \tag{67}$$

The rows of the F and Φ matrices which correspond to a random walk variable are the same as for a random constant but, in general, $G\underline{u}$ or $\underline{w}_n$ provide finite contributions to changes in the state variable. The corresponding column and row of $G\,Q\,G^T$ can be non-zero and the element at their intersection is given from Eq. 67 by q. For Q_n the appropriate element is

$$q\left(t_{n+1} - t_n\right)$$

The random walk and random bias can be represented together with the use of only one additional state variable. This is illustrated in Fig. 22(b).

*This is readily shown using Eq. 14. Since F is zero and G is unity the derivative of P is Q. Using the lower case to denote scalar quantities,

$$p = qt + p(0)$$

Since there are no measurements, $\hat{x}$ is zero and

$$p = \overline{x^2}$$

(a) The Random Walk

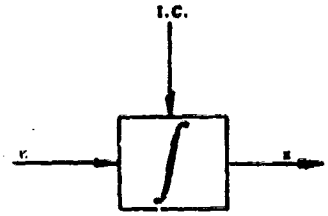

(b) The Random Walk and Random Constant

FIG. 22. Block Diagrams Demonstrating the Combination of Random Constant and and Random Walk in One Additional State Variable.

Exponentially-Correlated Random Variable

A random quantity whose autocorrelation function is a declining exponential

$$\phi_{xx}(\tau) = \sigma^2 e^{-\beta|\tau|} \tag{68}$$

is frequently a useful representation of errors and disturbances in inertial navigation systems. The same quantity provides a reasonable approximation for a band-limited signal whose spectral density is flat for a finite bandwidth of frequency. The exponentially-correlated random variable can be generated by passing an uncorrelated signal through a linear first-order feedback system. A block diagram for the system is shown in Fig. 23. The differential equation of the additional state variable is

$$\dot{x} = -\beta x + u \tag{69}$$

The mean square value of the exponentially-correlated random variable is constant if the mean square initial condition on the integrator is taken as $\overline{x^2}$. The specification of this quantity appears at the intersection of the appropriate row and column in the initial error covariance matrix, $P(t_o)$. The corresponding diagonal element (at the intersection of the appropriate row and column) of the F matrix is $-\beta$. All other elements of the coresponding row are zero. The Φ matrix is similarly arranged with the diagonal element given by

$$e^{-\beta\left(t_{n+1} - t_n\right)}$$

The G, G Q G^T and Q_n matrices have the same characteristics as for the random walk. The mean square value of x is related to q by

$$\overline{x^2} = \frac{q}{2\beta} * \qquad (70)$$

It is interesting to note that, when the period of estimation is much less than the time constant $1/\beta$, an exponentially-correlated quantity can be approximated by the random walk. Under this condition an exponentially-correlated variable and a random constant can be approximated by only one additional variable.

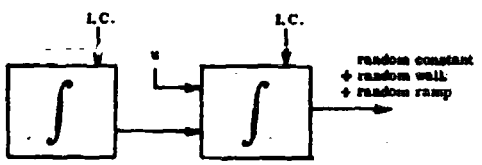

FIG. 23. Block Diagram Showing Generation of Three Random Characteristics by the Addition of Only Two State Variables.

*Again, Eq. 14 can be employed. Since $F = -\beta$ and $G = I$,

$$\dot{p} = -2\beta p + q$$

In the steady state, $\dot{p} = 0$, and $p = \frac{q}{2\beta}$.

Periodic Random Quantities

Random variables which exhibit a periodic nature may also arise in inertial navigation systems. Their autocorrelation functions can be represented by

$$\phi_{xx}(\tau) = \frac{\sigma^2}{\cos \eta} e^{-\zeta \omega_n |\tau|} [\cos(\omega' |\tau| - \eta)] \tag{71}$$

where

$$\omega' = \omega_n (1 - \zeta^2)^{1/2} \tag{72}$$

and the values of ζ and ω_n are chosen to fit empirical autocorrelation data. Two additional state variables are necessary to represent a random signal with this autocorrelation function. One pair of state quantities which provides this relation is given by

$$\begin{aligned} \dot{x}_\ell &= x_{\ell+1} + au \\ \dot{x}_{\ell+1} &= -\omega_n^2 x_\ell - 2\zeta\omega_n x_{\ell+1} + (b - 2a\zeta\omega_n)u \end{aligned} \tag{73}$$

where

$$\begin{aligned} a^2 &= \frac{2\sigma^2}{\cos \eta} \omega_n \sin(\alpha - \eta) \\ b^2 &= \frac{2\sigma^2}{\cos \eta} \omega_n^3 \sin(\alpha + \eta) \\ \alpha &= \tan^{-1}\left(\frac{\zeta}{(1 - \zeta^2)^{1/2}}\right) \end{aligned} \tag{74}$$

and x_ℓ has its autocorrelation function given in Eq. 71 (Ref. 23).

Random Ramp Variables

Frequently, random errors arise in inertial systems which exhibit a definite time-growing value. The random ramp, a function which grows linearly with time, can be used to describe them. The growth rate of the random ramp is a random quantity with a given probability density. Two additional state elements are necessary to describe the random ramp:

$$\begin{aligned} \dot{x}_\ell &= x_{\ell+1} \\ \dot{x}_{\ell+1} &= 0 \end{aligned} \tag{75}$$

where the initial condition on $x_{\ell+1}$ provides the slope of the ramp. This initial condition is exhibited in the form of a mean square slope $\overline{r^2}$, which appears in the corresponding diagonal element of the initial error covariance matrix $P(t_o)$. x_ℓ is the random ramp quantity. The row of the F matrix which corresponds to x_ℓ has a one on the column corresponding to $x_{\ell+1}$ and zeros everywhere else. In the Φ matrix the same element is specified by $(t_{n+1} - t_n)$ and there are ones on the diagonal. The row in the F matrix which is related to $x_{\ell+1}$ contains only zeros. The rows of G and the rows and columns of $G\,Q\,G^T$ or Q_n which correspond to x_ℓ and $x_{\ell+1}$ are also empty. The mean square value of x_ℓ grows as a parabola with time

$$\overline{x_\ell^2} = \overline{r^2}\, t^2 \tag{76}$$

The random ramp, random walk, and random constant can be represented together by the use of only two additional state variables. This is illustrated in Fig. 23.

A summary of the above-described random quantities is given in Fig. 24. Occasionally other more complex random error models arise. For example, Ref. 24 discusses a time- and distance-correlated error whose autocorrelation function is given by

$$\phi(\tau,d) = \sigma^2 \left(e^{-\tau/a}\right)\left(e^{-d/b}\right);\ \tau,\ d > 0 \tag{77}$$

Name	Autocorrelation Function	State Differential Equations	Block Diagram	Mean Square Value
Random Constant		$\dot{x} = 0$	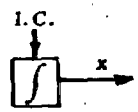	$\overline{x(t_0)^2}$
Random Walk	——	$\dot{x} = u$	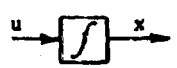	qt
Exponentially Correlated Random Variable	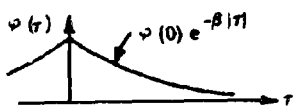	$\dot{x} = -\beta x + u$	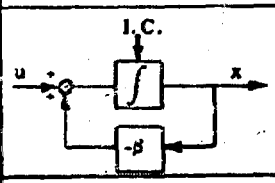	$\frac{q}{2\beta}$
Periodic Random Variable	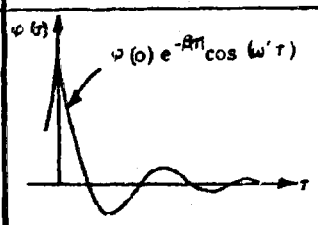 ω' defined in text	$\dot{x}_L = x_{L+1} + au$ $\dot{x}_{L+1} = -\omega_n^2 x_L - 2\beta x_{L+1} + (b - 2a\beta)u$	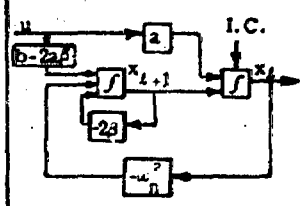 ω_n, a, b defined in text	$\left(\frac{\omega_n^2 a^2 + b^2}{4\beta\omega_n^2}\right) q$
Random Ramp	——	$\dot{x}_L = x_{L+1}$ $\dot{x}_{L+1} = 0$	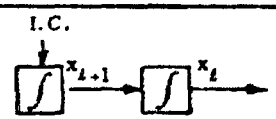	$\overline{(x_{L+1}(t_0))^2 t^2}$

FIG. 24. Random Variables.

where a and b are a first-order correlation time and a first-order correlation distance, respectively. A similar correlation appears to occur in certain radio navigation systems. However, the vast majority of inertial navigation system measurement errors and disturbances can be described by some combination of the random variable relations summarized in Fig. 24.

INERTIAL SENSOR ERRORS

Random inertial sensor errors are produced by many practical and theoretical imperfections in the operation of these instruments. They are among the major random disturbances for inertial navigation systems. Through extensive testing and detailed knowledge of the sensor dynamics many other errors are measured and compensated or removed by careful design. But, when all the tests for predictable errors and the ingenious design tricks have been exhausted, there still remain errors whose source and systematic behavior defy detection. Often additional testing reveals that the statistical behavior of these inertial sensor errors can be described by one or more of the forms presented in the previous section. It should be emphasized that the pertinent statistical parameters (mean square, correlation time, etc.) are only obtained through the analysis of large amounts of data. Frequently the error behavior observed is highly dependent on the individual instrument tested or the period of observation. Therefore, it is not surprising that complete agreement on inertial sensor error models does not exist.

The statistical model of inertial sensor errors also depends greatly on the operating situation. If the errors in a cruise inertial navigator are being estimated, a very detailed model may be required. On the other hand, errors in a tactical missile navigator can be determined accurately with simpler models for sensor error statistics.

Gyro Drift Rate

In one case or another, all of the random variables described in Fig. 24 except the periodically-correlated quantity have been found to be good descriptions of gyro drift rate. Reference 25 proposes the combination of random bias, exponentially-correlated error, and a random walk as a good statistical model of the gyro drift rate. In this case the initial condition for the integrator in the system generating the exponentially-correlated component is taken as zero. Further studies reveal that the random ramp may be a necessary addition in order to describe gyro drift rate more completely. It can be seen that two or three additional state variables must be added for each gyro.

Accelerometer Error

Accelerometer errors are usually described in terms of random constants and exponentially-correlated errors only. Two additional state variables are required to represent the correlation properties of these errors.

Although it is not an accelerometer error per se, gravity deflection of the vertical can be modeled as an exponentially-correlated disturbance originating in the level accelerometers of an inertial system. This particular geodetic error is of great importance in the long-range or cruise-type vehicle. While the phenomenon is spatially fixed, an equivalent correlation time can be derived by dividing the actual correlation distance by vehicle speed. Vehicle maneuvers, of course, have to be properly treated in this calculation.

MEASUREMENT ERRORS

The measurements of position, velocity, and attitude used by the Kalman Filter to improve the accuracy of inertial navigation systems may also contain errors whose correlation times are significant. The procedure for incorporating additional variables into the system in order to estimate the correlated measurement errors is demonstrated on p. 45.

The statistical properties of measurement errors are obtained in a manner similar to those for sensor errors--physical evaluation and analysis of large quantities of data. Frequently, measurement errors can be reduced by averaging a noisy measurement over a period which is long compared to the error correlation time but short with respect to characteristic times of the quantity being measured.

Position Measurements

Radio position indication schemes such as Loran or Omega contain errors which can be viewed as a random bias plus an exponentially-correlated quantity. The characteristic times of the exponential auto-correlation functions are in the range of 3 to 15 minutes for Loran C and 1 hour for Omega. This model of radio navigation uncertainties is approximate because position itself affects the errors. However, the approximation is valid for slowly-moving vehicles such as ships. The radiometric sextant (i.e., sun or moon tracker) is used to determine position and also serves to illustrate errors which can arise in attitude measurements with radio instruments. Its angle measurements are corrupted by white noise, random constant, and exponentially-correlated errors. These can be converted into similar errors in position indication through knowledge of the measurement geometry.

Velocity Measurement

Doppler velocity measurements contain correlated errors. These errors may differ for along-track velocity measurements and across-track velocity (Ref. 26). However, it has been shown (Ref. 2) that averaging Doppler measurements over a short period of time will reduce the size of the measurement errors and permit them to be considered as uncorrelated. A ship's EM log has an apparent error if any ocean current exists. It is usually modeled as a random constant plus error which is exponentially correlated in position. The position correlation coefficient is then converted into a characteristic time by dividing it by ship's speed.

Attitude Measurement

Attitude measurement errors in a radio sextant have already been discussed. They are characteristic of all attitude sensors which measure electromagnetic radiation below the visible range. Optical measurements of attitude in which the light path passes through an atmosphere are also subject to exponentially-correlated errors. Attitude measurement instruments (possibly including effects due to the man operating them) also provide random constant and uncorrelated errors.

A discussion of random system disturbances and measurement errors is necessarily incomplete. Each inertial sensor and measurement device to be used in a system employing the Kalman Filter must have its errors carefully analyzed before a proper error model can be determined.

Section 5. APPLICATION TO NAVIGATION SYSTEMS

Differential equations describing the propagation of inertial navigation system errors have been developed and the use of the Kalman Filter described. As already hinted, the filter will estimate the errors in the inertial navigation system rather than the system variables themselves. It is the error quantities whose dynamics can be described in terms of linear equations which, though not exact, are an excellent approximation. In this section state vectors are defined and the system matrices F, corresponding to different system configurations, are extracted from the error differential equations. Given F, it is possible to compute the Φ matrices of the discrete filter formulation.

In addition, the measurement matrices, H, are specified for common external measurements. Also, the effects of random system disturbances and measurement errors are described in terms of the G, Q, and R matrices. The section is concluded by stating all of the matrices required to estimate the errors in a north-vertical inertial navigation system and displaying some results from the Kalman Filter error covariance equation for that case.

NAVIGATION COORDINATE SYSTEMS

To begin, a more detailed exposition is made of the three inertial navigation coordinate frames outlined under Inertial Navigation Systems (p. 35) and in Appendix C.

North-Vertical Coordinates

Currently, the most common set of coordinate axes used for inertial navigation in long-term cruise systems such as SINS is the orthogonal triad-oriented north horizontal (x), east horizontal (y), and vertical downward (z). These axes, subsequently called north-vertical coordinates, or a similar set oriented north horizontal, east horizontal, and vertical upward, always have their center at the vehicle position and permit easy calculation of navigation quantities such as longitude and latitude. In a gimballed north-vertical system, the platform is rotated relative to inertial space about its nominal x, y, and z axes according to Eq. 47.

$$\begin{aligned} \omega_x &= (\dot{\lambda} + \Omega) \cos L \\ \omega_y &= -\dot{L} \\ \omega_z &= -(\dot{\lambda} + \Omega) \sin L \end{aligned} \tag{76}$$

where λ and L are the computed values of longitude and latitude and Ω is the magnitude of the earth's angular rate (see Fig. 25). Of course, errors in the implementation of Eq. 78 may arise due to gyro drift rates, etc. If the computed values of λ and L are correct and the platform is initially aligned, Eq. 78, when implemented without error, will keep the two coordinate frames parallel. In a strapdown system, the same rotation is accomplished by supplying the required angular rate to the direction cosine computations.

Free Azimuth Coordinates

Some inertial navigation systems do not provide a platform rotation command about the vertical axis. This eliminates the torquing error associated with the z gyro, which ordinarily displays poorer drift rate characteristics than either of the gyros with horizontal input axes. These "free azimuth" navigation systems indicate the direction of north by calculating the angle between horizontal north and one of the instrumented horizontal platform axes. For calculation of longitude and latitude the accelerometer outputs are resolved into north and east components through this angle. The platform angular rates are:

$$\begin{aligned} \omega_x &= (\Omega + \dot{\lambda}) \cos L \cos \alpha - \dot{L} \sin \alpha \\ \omega_y &= -(\Omega + \dot{\lambda}) \cos L \sin \alpha - \dot{L} \cos \alpha \\ \omega_z &= 0 \end{aligned} \tag{79}$$

where α is the horizontal angle between north and the platform x axis.

In a sense, the free azimuth system is a hybrid of gimballed and strapdown systems, storing one angular relation in the form of the off-azimuth angle and nulling others by keeping the platform level. Several refinements on this scheme occur. These include defining a false north direction in order to avoid high azimuth rates near the earth's geographic poles. Free azimuth coordinates are frequently used for aircraft inertial navigation systems where high platform angular rates about the z axis can be required of a north-vertical system.

Tangent Plane Coordinates

The use of tangent plane coordinates is another technique for eliminating the errors resulting from platform rotation. It takes advantage of the fact that constant platform angular rates can be generated much more accurately than time-varying ones. By defining the navigation axes to be those which coincide with the north-vertical

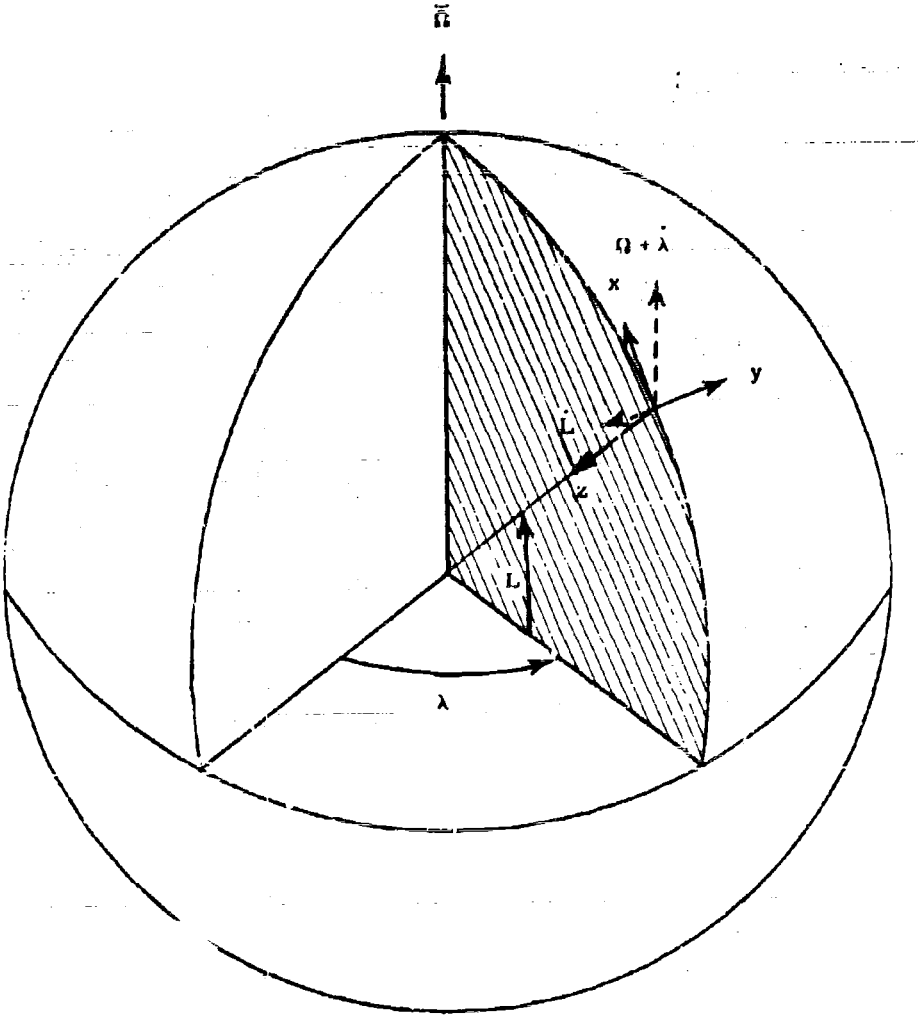

FIG. 25. North-Vertical Coordinates.

axes at a fixed point on the earth (see Fig. 26) only the horizontal and vertical components of the earth rate at this point must be implemented. These rates are constant functions of the fixed-point latitude, L_o, and Ω.

$$\omega_x = \Omega \cos L_o$$

$$\omega_y = 0 \tag{80}$$

$$\omega_z = -\Omega \sin L_o$$

Tangent plane coordinates are usually used in inertial navigators which do not compute latitude and longitude. They are found in short-range vehicles such as airborne tactical missiles whose target location is often measured directly in the tangent plane coordinate frame. If the vehicle carrying a tangent plane inertial navigation system moves more than a few miles from the fixed point, mass attraction forces must be calculated along the x and y axes in order to compensate accelerometer outputs.

SYSTEM STATE DIFFERENTIAL EQUATIONS

The system matrix F describes the unforced behavior of the system state variables according to the equation

$$\dot{\underline{x}} = F\underline{x} \tag{81}$$

When discrete calculations of the state vector are considered, F is used to compute the transition matrix Φ as described in Section 2. Of course F is dependent on the specific state variables chosen and the order in which they appear in the state vector. Reordering the same state variables only requires shifting rows and columns in F. The inertial navigation system error quantities which constitute appropriate state variables can be written in identical form for all three navigation coordinate frames discussed above

$$\underline{x}^T = \left(\delta R_x \ \delta R_y \ \delta \dot{R}_x \ \delta \dot{R}_y \ \phi_x \ \phi_y \ \phi_z\right) \tag{82}$$

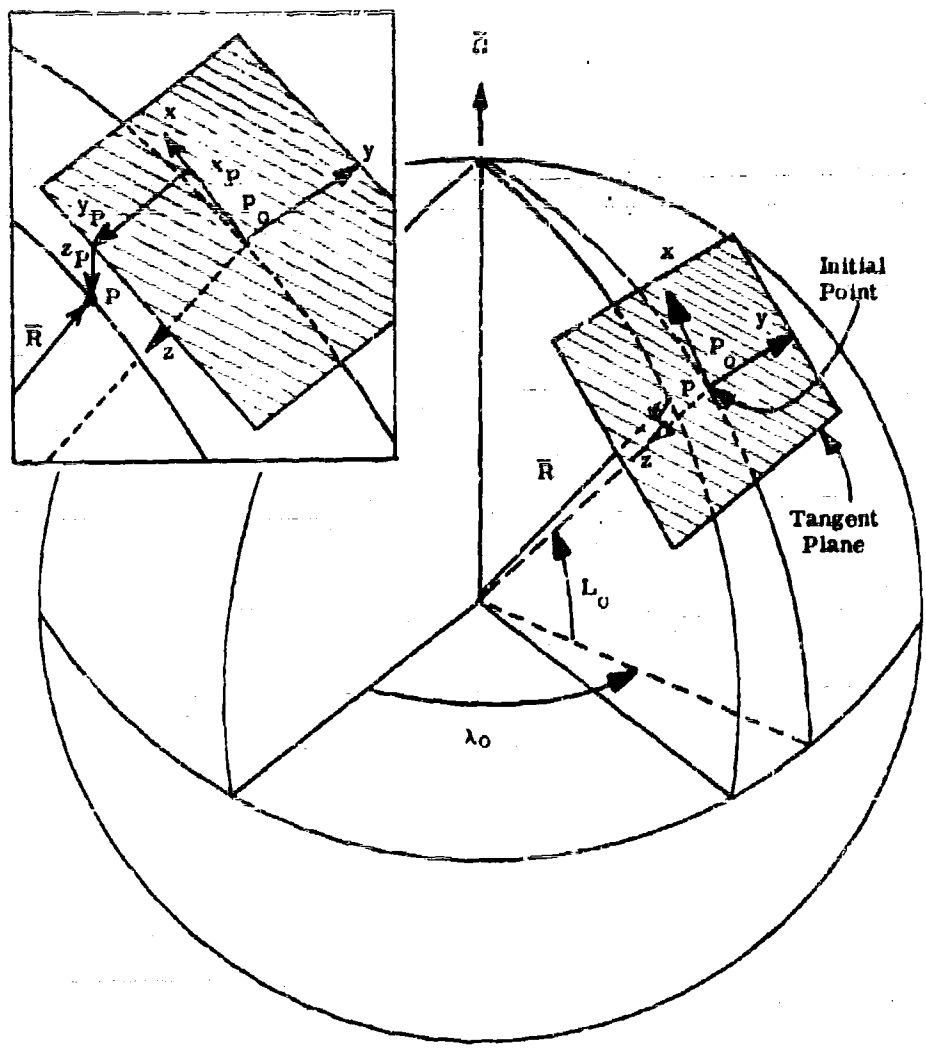

FIG. 26. Tangent Plane Geometry.

Notice that position and velocity in the z or vertical direction are not included as errors of the inertial system. The assumption is made that these quantities are obtained from some other source because of the basic instability which exists in instrumenting the vertical channel of an inertial navigation system (see Appendix C). Special assumptions must be applied to the tangent plane coordinate frame implementation to keep its error equations similar to those of north-vertical and free azimuth systems; the effects of errors due to inaccurate indication of mass attraction forces along the x and y axes are ignored and it is assumed that the local vertical does not differ from the fixed-point vertical by more than a few degrees. Systems employing the tangent plane coordinate axes usually permit these simplifications.

The state vector defined by Eq. 82 exhibits directly the errors in position, velocity, and attitude. Notice that, in a north-vertical system, the same state variables could be specified in terms of longitude and latitude errors through the expressions

$$\begin{aligned} \delta R_x &= R\delta L \\ \delta \dot{R}_x &= R\dot{\delta L} \\ \delta R_y &= R \cos L \, \delta\lambda \\ \delta \dot{R}_y &= R \cos L \, \dot{\delta\lambda} - \dot{L} R \sin L \, \delta\lambda \end{aligned} \tag{83}$$

where R is assumed constant. Similar equations relate the position and velocity errors in a free azimuth system to longitude and latitude errors. However, they involve resolution through the angle between north and the system x axis.

The equations developed in Appendix C provide the F matrix for the state vector of Eq. 82 when north-vertical coordinates are employed

$$F_x = \begin{bmatrix} 0 & 0 & 1 & 0 & 0 & 0 & 0 \\ 0 & 0 & 0 & 1 & 0 & 0 & 0 \\ 0 & \frac{a_y}{R}\tan L & 0 & 2\omega_z & 0 & g & a_y \\ 0 & -\frac{a_x}{R}\tan L & -2\omega_z & 0 & -g & 0 & -a_x \\ \frac{\omega_z}{R} & -\frac{\omega_y}{R}\tan L & 0 & \frac{1}{R} & 0 & \omega_z & -\omega_y \\ 0 & \left(\frac{\omega_z}{R}+\frac{\omega_x}{R}\tan L\right) & -\frac{1}{R} & 0 & -\omega_z & 0 & \omega_x \\ -\frac{\omega_x}{R} & \frac{\omega_y}{R}\tan^3 L & 0 & -\frac{\tan L}{R} & \omega_y & -\omega_x & 0 \end{bmatrix} \quad (84)$$

The system matrix when tangent plane coordinates are used differs from that presented above because the platform axes are not rotated in proportion to velocity

$$F_x = \begin{bmatrix} 0 & 0 & 1 & 0 & 0 & 0 & 0 \\ 0 & 0 & 0 & 1 & 0 & 0 & 0 \\ 0 & 0 & 0 & 2\omega_z & 0 & g & a_y \\ 0 & 0 & -2\omega_z & 0 & -g & 0 & -a_x \\ 0 & 0 & 0 & 0 & 0 & \omega_z & -\omega_y \\ 0 & 0 & 0 & 0 & -\omega_z & 0 & \omega_x \\ 0 & 0 & 0 & 0 & \omega_y & -\omega_x & 0 \end{bmatrix} \quad (85)$$

The subscript is placed on the above matrices in anticipation of later expanding the state vector to include correlated error terms. The elements in F_x include only the most significant terms and the effects of position and velocity along the vertical axis are ignored. Of course, the values of ω_x, ω_y, and ω_z will differ for the three navigation axis systems according to Eq. 78 to 80. As an example of the complexity which can result when more terms are included, Fig. 27 is the complete F_x matrix for north-vertical coordinates written in terms of longitude, latitude, and vertical velocity and acceleration.

SYSTEM DISTURBANCES

The state vector differential equation is driven by inertial sensor errors and incorrect indications of vertical position and velocity. The latter errors can come from one or more of several instruments whose consideration is beyond the scope of this document. The effect of the errors will simply be presented.

Vertical position and velocity errors can be exhibited by rewriting Eq. 81 to include a forcing term

$$\dot{\underline{x}} = F\underline{x} + G\underline{u} \tag{86}$$

Again, specification of G and $\underline{u}$ permits the calculation of $\underline{w}$ for the discrete case. If only δR_z and $\dot{\delta R}_z$ are considered as driving terms,

$$\underline{u} \triangleq \begin{bmatrix} \delta R_z \\ \dot{\delta R}_z \end{bmatrix} \tag{87}$$

G is given, for the state vector defined in Eq. 82, by

$$G^T = \begin{bmatrix} 0 & 0 & 0 & 0 & 0 & 0 & 0 \\ 0 & 0 & -2\omega_y & 2\omega_x & 0 & 0 & 0 \end{bmatrix} \tag{88}$$

$$
\begin{bmatrix}
\dot{R}\delta\dot{L} \\
R\cos L\,\delta\dot{\lambda} \\
R\delta\ddot{L} \\
R\cos L\,\delta\ddot{\lambda} \\
\dot{\varphi}_x \\
\dot{\varphi}_y \\
\dot{\varphi}_z
\end{bmatrix}
=
\begin{bmatrix}
0 & 0 & 1 & 0 & 0 & 0 & 0 \\
0 & 0 & 0 & 1 & 0 & 0 & 0 \\
-(\Omega+\dot{\lambda})^2\cos 2L & 0 & -\frac{2\dot{h}}{R} & -2(\Omega+\dot{\lambda})\sin L & 0 & \ddot{h}-R\dot{L}^2 & R\cos L\,\ddot{\lambda} \\
 & & & & & -R(\Omega+\dot{\lambda})^2\cos^2 L & -2\dot{h}(\Omega+\dot{\lambda})\cos L \\
 & & & & & +g & -2R\dot{L}(\Omega+\dot{\lambda})\sin L \\
\ddot{\lambda}\sin L & & & 2\dot{L}\tan L & -\ddot{h}+R\dot{L}^2 & & -R\ddot{L}-2\dot{h}\dot{L} \\
+2\frac{\dot{h}}{R}(\Omega+\dot{\lambda})\sin L & 0 & 2(\Omega+\dot{\lambda})\sin L & -2\frac{\dot{h}}{R} & +R(\Omega+\dot{\lambda})^2\cos^2 L & 0 & -R(\Omega+\dot{\lambda})^2\frac{\sin 2L}{2} \\
+2\dot{L}(\Omega+\dot{\lambda})\cos L & & & & -g & & \\
-(\Omega+\dot{\lambda})\frac{\sin L}{R} & 0 & 0 & \frac{1}{R} & 0 & -(\Omega+\dot{\lambda})\sin L & \dot{L} \\
0 & 0 & -\frac{1}{R} & 0 & (\Omega+\dot{\lambda})\sin L & 0 & (\Omega+\dot{\lambda})\cos L \\
-(\Omega+\dot{\lambda})\frac{\cos L}{R} & 0 & 0 & -\frac{\tan L}{R} & -\dot{L} & -(\Omega+\dot{\lambda})\cos L & 0
\end{bmatrix}
\begin{bmatrix}
R\delta L \\
R\cos L\,\delta\lambda \\
h\delta L \\
h\cos L\,\delta\lambda \\
\varphi_x \\
\varphi_y \\
\varphi_z
\end{bmatrix}
$$

Note: $h = -R_z$

FIG. 27. Error Propagation Equation for North-Vertical Coordinates in Terms of Latitude and Longitude Errors.

Or, following the notation and extra detail of Fig. 27, the G matrix is

$$G^T = \begin{bmatrix} 0 & 0 & \ddot{L} + \frac{\Omega + \dot{\lambda}}{2} \sin 2L & 2\dot{L} & 0 & 0 & 0 \\ 0 & 0 & -2\dot{L}(\Omega + \dot{\lambda}) \sin L + \ddot{\lambda} \cos L & 2(\Omega + \dot{\lambda}) \cos L & 0 & 0 & 0 \end{bmatrix} \quad (89)$$

In a similar manner, the effects of gyro and accelerometer errors can be exhibited by defining

$$\underline{u}^T \triangleq \left[\nabla_x \; \nabla_y \; \epsilon_x \; \epsilon_y \; \epsilon_z \right] \quad (90)$$

The error sources of Eq. 87 and 90 could be considered together by properly arranging their respective G matrices into one matrix expressing their combined effect on $\underline{x}$. If the inertial sensor errors of Eq. 90 are not correlated in time, no state vector augmentation is needed. In terms of the state vector of Eq. 82, the G matrix for the effects of Eq. 90 is

$$G = \begin{bmatrix} 0 & 0 & 0 & 0 & 0 \\ 0 & 0 & 0 & 0 & 0 \\ 1 & 0 & 0 & 0 & 0 \\ 0 & 1 & 0 & 0 & 0 \\ 0 & 0 & 1 & 0 & 0 \\ 0 & 0 & 0 & 1 & 0 \\ 0 & 0 & 0 & 0 & 1 \end{bmatrix} \quad (91)$$

In truth, the inertial sensor errors are highly correlated quantities and are usually described by one or more of the correlation models given in Section 4. It is therefore necessary to augment the state vector and enlarge the F matrix accordingly. For example, if all inertial sensor errors can be modeled as random walk quantities, random constants, or the sum of both, reference to the preceding section indicates that five additional state variables are necessary. The augmented state vector is given by

$$\underline{x}'^{T} = \left[\delta R_x \; \delta R_y \; \delta \dot{R}_x \; \delta \dot{R}_y \; \varphi_x \; \varphi_y \; \varphi_z \; \nabla_x \; \nabla_y \; \epsilon_x \; \epsilon_y \; \epsilon_z\right] \tag{92}$$

The new F matrix is given by

$$F' = \left[\begin{array}{c:c} F_x & G \\ \hdashline O & O \end{array}\right] \quad (12\times12)^* \tag{93}$$

where the submatrices G and F_x are given in Eq. 91 and 84 or 85. The uncorrelated disturbances which provide the random walk characteristic can be denoted by

$$\underline{u}'^{T} = \left[u_{\nabla_x} \; u_{\nabla_y} \; u_{\epsilon_x} \; u_{\epsilon_y} \; u_{\epsilon_z}\right] \tag{94}$$

and the new G matrix is given by

$$G' = \left[\begin{array}{c} O \\ \hdashline I_5 \end{array}\right] \quad (12\times5) \tag{95}$$

where I_5 is the 5 x 5 identity matrix.

*Frequently, when matrices are expressed in terms of their submatrix elements, the dimensions of the entire array will be noted as shown.

If any of the errors do not exhibit random walk behavior, the corresponding diagonal element of I_5 is changed to zero. The random constant nature of the errors is exhibited by setting the corresponding diagonal elements of the initial error covariance matrix, $P(t_o)$, equal to their mean square values.

If the sensor errors have exponential correlation only, the state vector of Eq. 92 is still used but

$$F' = \left[\begin{array}{c|c} F_x & G \\ \hline O & F_u \end{array}\right] \quad (12x12) \tag{96}$$

where F_u is the matrix whose diagonal elements are composed from the quantities β described in Section 4.

$$F_u = \begin{bmatrix} -\beta_{\nabla_x} & 0 & 0 & 0 & 0 \\ 0 & -\beta_{\nabla_y} & 0 & 0 & 0 \\ 0 & 0 & -\beta_{\epsilon_x} & 0 & 0 \\ 0 & 0 & 0 & -\beta_{\epsilon_y} & 0 \\ 0 & 0 & 0 & 0 & -\beta_{\epsilon_z} \end{bmatrix} \tag{97}$$

The vector $\underline{u}$ and the matrix G are essentially the same for this case. Many other combinations of correlated sensor errors can be prescribed by careful adherence to the rules set down in Section 4.

When state vector augmentation takes place to accommodate correlated system disturbances, the size of the covariance matrix Q_n in the discrete filter also increases. If the quantities forcing the original n-element state vector differential equation are not uncorrelated, the first n rows and columns of Q_n are composed of zeros while an appropriate submatrix in Q_n is the covariance of the uncorrelated quantities, u, described in Section 4. For the two examples of correlated inertial sensor errors given above,

$$Q_n' = \left[\begin{array}{c|c} 0 & 0 \\ \hline 0 & Q_n \end{array}\right] \qquad (12/12) \qquad (98)$$

where

$$Q = E\left|\underline{w}_n \underline{w}_n^T\right| \qquad (99)$$

The discrete forcing vector $\underline{w}_n$ is computed with Eq. 9, using $\underline{u}'$ as defined in Eq. 94. The zero submatrix in the upper left corner of Q_n has dimension 7 x 7 (the original state had seven elements). Other correlation characteristics for inertial sensor errors may require a larger augmented state vector and therefore Q_n and Q_n' matrices. In the continuous filter similar behavior occurs in the matrix product $G\,Q\,G^T$.

MEASUREMENTS

The Kalman Filter detects the buildup of errors in an inertial guidance system through comparison of system indications with external measurements. If the measurement is not given directly in navigation coordinates it must be properly transformed through knowledge of the particular geometry involved. The transformation can either be performed outside the Kalman Filter or take place in the measurement matrix, H. Since direct measurement of inertial sensor errors is not common, the matrices displayed below are for the original 7-element state vector of Eq. 82. Augmentation of the state to account for correlated random disturbances only adds an appropriate number of a zero columns on the right side of the matrices shown. It should be emphasized that H relates the difference between system-indicated and measured values to the system errors.

Position--Measurement of position alone gives a measurement matrix, H_p,

$$H_p = \begin{bmatrix} 1 & 0 & 0 & 0 & 0 & 0 & 0 \\ 0 & 1 & 0 & 0 & 0 & 0 & 0 \end{bmatrix} \qquad (100)$$

If position measurements are given in terms of latitude and longitude they can be compared with system indications of these quantities and

$$H_p = \begin{bmatrix} \frac{1}{R} & 0 & 0 & 0 & 0 & 0 & 0 \\ 0 & \frac{1}{R \cos L} & 0 & 0 & 0 & 0 & 0 \end{bmatrix} \tag{101}$$

for the state vector of Eq. 82.

Velocity--The measurement matrix for velocity measurements is

$$H_v = \begin{bmatrix} 0 & 0 & 1 & 0 & 0 & 0 & 0 \\ 0 & 0 & 0 & 1 & 0 & 0 & 0 \end{bmatrix} \tag{102}$$

Attitude--For most attitude measurements the instrument is pointed according to computed attitude and the angular deviation of a reference point is measured. As a result, the measurement is of $\bar{\psi}$, not $\bar{\phi}$. Consequently not only attitude errors, but position errors as well are measured, because

$$\bar{\psi} = \bar{\phi} - \overline{\delta\theta}$$

$$\delta\theta_x = \frac{\delta R_y}{R} \qquad \delta\theta_y = -\frac{\delta R_x}{R} \tag{103}$$

The measurement matrix is

$$H_a = \begin{bmatrix} 0 & -\frac{1}{R} & 0 & 0 & 1 & 0 & 0 \\ \frac{1}{R} & 0 & 0 & 0 & 0 & 1 & 0 \\ 0 & 0 & 0 & 0 & 0 & 0 & 1 \end{bmatrix} \tag{104}$$

for the free azimuth and tangent plane coordinate systems. For north-vertical coordinates,

$$H_a = \begin{bmatrix} 0 & -\frac{1}{R} & 0 & 0 & 1 & 0 & 0 \\ \frac{1}{R} & 0 & 0 & 0 & 0 & 1 & 0 \\ 0 & \frac{\tan L}{R} & 0 & 0 & 0 & 0 & 1 \end{bmatrix} \tag{105}$$

When combinations of measurements are made, the measurement matrix is constructed by "stacking" the appropriate matrices shown above. For example, if position and velocity are measured at the same time

$$H_{p,v} = \begin{bmatrix} H_p \\ \hline H_v \end{bmatrix} \tag{106}$$

MEASUREMENT ERRORS

Though the "measurements" for the Kalman Filter are accually differences between system-indicated and externally-measured position, velocity, and attitude, the measurement errors are attributed to inaccuracies in the external indications only. As a result, some external measurements--such as position at a surveyed point--are often considered to be essentially error-free. However, when the inertial system is aboard a moving vehicle, important external measurement errors do arise. These are specified statistically by their error covariance matrices, R. When the errors are considered to be uncorrelated between measurements, position, velocity, and attitude measurement error covariance matrices can be denoted

$$R_p = E\left(\underline{v}_p \, \underline{v}_p^T\right) \tag{107}$$

where

$$\underline{v}_p = \begin{bmatrix} v_{R_x} \\ v_{R_y} \end{bmatrix} \tag{108}$$

Similarly,

$$R_v = E\left(\underline{v}_v \underline{v}_v^T\right) \qquad \underline{v}_v = \begin{bmatrix} v_{R_x} \\ v_{R_y} \end{bmatrix} \tag{109}$$

and

$$R_a = E\left(\underline{v}_a \underline{v}_a^T\right) \qquad \underline{v}_a = \begin{bmatrix} v_{\phi_x} \\ v_{\phi_y} \\ v_{\phi_z} \end{bmatrix} \tag{110}$$

The measurement error covariance can be a diagonal matrix (only zero elements off the diagonal). This indicates no cross-correlation between measurement errors. However, the measurements must frequently be taken in coordinates other than those used for navigation, and cross-correlation between measurement errors is common. The measurement instruments and geometry dictate measurement error correlations. If several error quantities are measured at the same time, the error covariance matrix R is constructed from the appropriate matrices defined above. In terms of the earlier example involving stacking measurement matrices,

$$R_{p,v} = \left[\begin{array}{c|c} R_p & O \\ \hline O & R_v \end{array}\right] \tag{111}$$

The zero submatrices in the off-diagonal position of Eq. 111 indicate a lack of correlation between position and velocity measurement errors. If measurement errors are time-correlated, the state vector must be augmented as described in Section 4 and under System Disturbances (p. 64).

AN ILLUSTRATION: NORTH-VERTICAL NAVIGATION IN A TACTICAL AIRCRAFT

The example chosen to demonstrate Kalman Filter operation comes directly from Ref. 3, in which a north-vertical inertial navigation system is aided by intermittent position fixes occuring either two or four times an hour. The Kalman Filter is employed to provide optimum use of these measurements. Altitude indications are assumed to come from an altimeter or some other noninertial device whose errors are very small and therefore not estimated. The gyro and accelerometer errors are modeled as random constants, and longitude and latitude fix errors are assumed to have exponential autocorrelation properties. The fourteen-element augmented state vector is given by

$$\underline{x}^T = \left[R\delta L \;\; R\cos L\delta\lambda \;\; \dot{R}\delta L \;\; \dot{R}\cos L\delta\dot{\lambda} \;\; \varphi_x \;\; \varphi_y \;\; \varphi_z \;\; \nabla_x \;\; \nabla_y \;\; \epsilon_x \;\; \epsilon_y \;\; \epsilon_z \;\; e_L \;\; e_\lambda \right] \tag{112}$$

where e_L and e_λ are the latitude and longitude measurement errors. The F matrix is given by

$$F = \left[\begin{array}{c|c|c} F_x & \begin{matrix} O \\ \hline I_5 \end{matrix} & O \\ \hline O & O & O \\ \hline O & O & \begin{matrix} -\beta_{e_L} & O \\ O & -\beta_{e_\lambda} \end{matrix} \end{array}\right] \qquad (14\times14) \tag{113}$$

where F_x is as prescribed in Fig. 27. The G matrix has 14 rows and 2 columns

$$G = \left[\begin{array}{c} O \\ \hline I_2 \end{array}\right] \tag{114}$$

The measurement matrix has 2 rows and 14 columns

$$H = \left| I_2 \;\middle|\; 0 \;\middle|\; I_2 \right| \tag{115}$$

Q_n (or $G\,Q\,G^T$) is at 14 x 14 matrix

$$Q_n = \left[\begin{array}{c|c} C & 0 \\ \hline 0 & A \end{array}\right] \tag{116}$$

where A is the 2 x 2 covariance matrix of white noise driving the linear model for position error generation.

The following parameters were used in calculating the Kalman Filter estimation errors:

RMS initial position errors, north and east, ft	50
Initial velocity error	None
RMS initial vertical tilt, sec	10
RMS initial azimuth error, sec	10
RMS constant gyro drift rate, deg/hr	0.1
RMS accelerometer bias error, μg	50
RMS uncorrelated position fix errors, north and east, n.mi	1
Latitude, deg	30
Aircraft heading	East

Any variation of these parameters is noted in the following discussion.

Figure 28 shows RMS vehicle position error time histories. The improvement in position accuracy resulting from taking fixes at 15-minute intervals as opposed to every half hour is demonstrated. Notice that the estimation errors (and therefore filter gain) exhibit an approximate steady-state behavior after about 2 hours.

A figure-of-merit is defined for this Kalman Filter-aided cruise inertial navigation system. It is the square root of the time average of mean square position error after 2 hours of filtering. This figure-of-merit is plotted in Fig. 29 as a function of RMS position measurement error for the case where position is determined every 15 minutes. Because latitude error grows faster between fixes, the figure-of-merit for δL is consistently larger. Of course, the other variables were

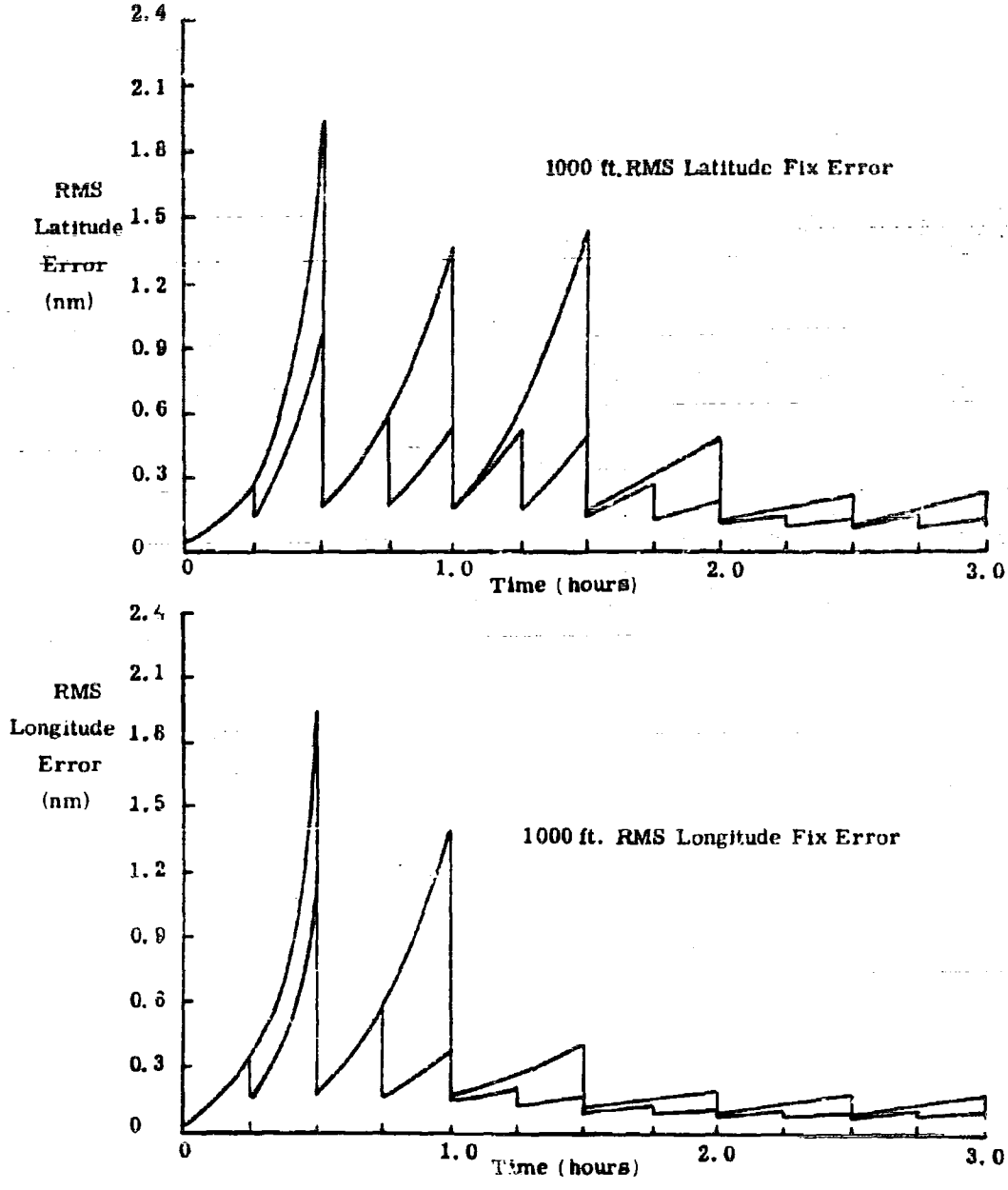

FIG. 28. RMS Position Error Histories.

held constant while measurement error was varied. Figure 30 displays variation of the figure-of-merit as a function of vehicle velocity. The essential insensitivity of position estimate errors to airspeed is demonstrated. The figure-of-merit was also found to be affected little by sizable variations of vehicle direction, operating latitude, inertial sensor errors, and platform azimuth alignment error about the parameters presented above.

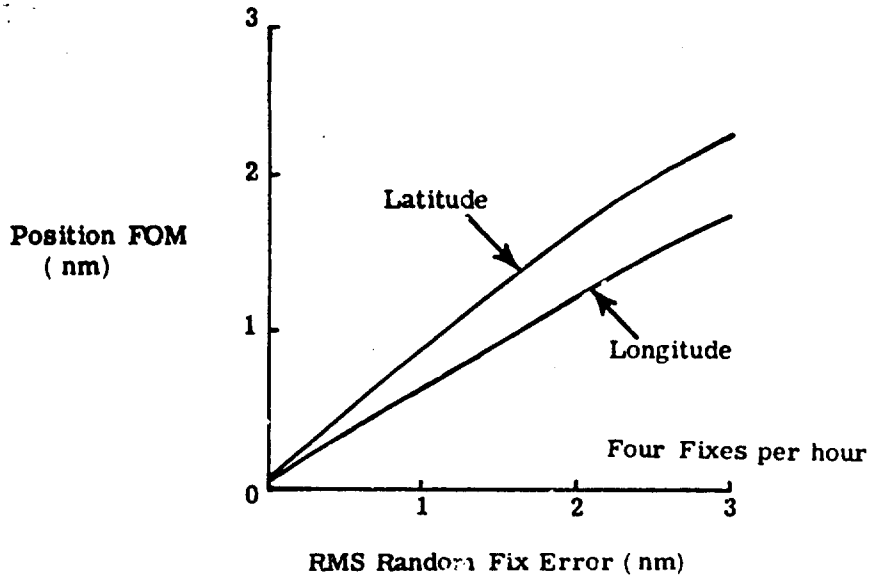

FIG. 29. Position FOM Versus RMS Random Fix Error.

Initial estimation accuracy is shown to have no effect on the RMS filter errors after 2 hours, assuming of course that the size of the initial errors is properly reflected in $P(t_o)$. This is illustrated in Fig. 31. The initial RMS tilt and azimuth alignment errors are six times as large in case 1 as in case 2. Figure 32 demonstrates the ability of the Kalman Filter to estimate gyro drift rate, thereby providing in-flight calibration. The accuracies shown are somewhat optimistic because the drift rate was assumed constant. A more realistic model for gyro drift rate is an exponentially-correlated error. In that case the drift rate will be time-varying and the filter estimation errors will approach a non-zero lower limit.

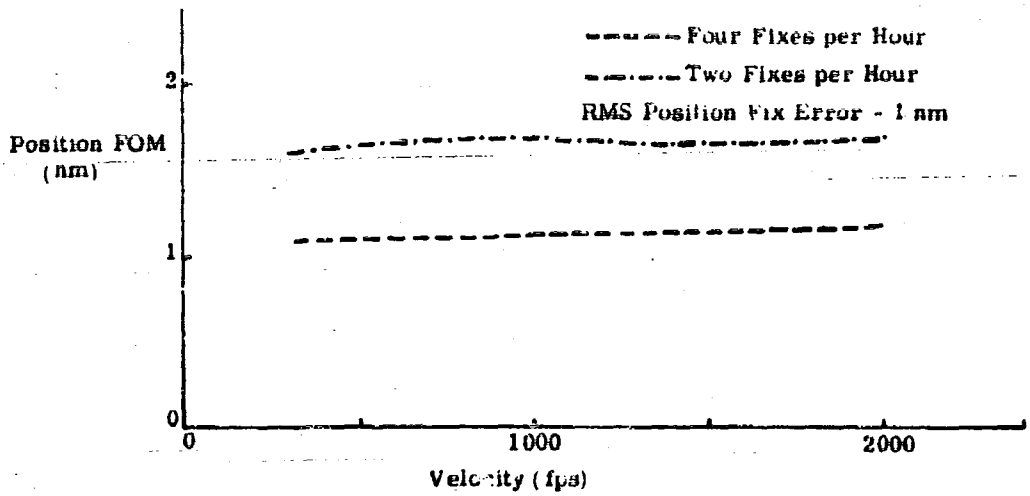

FIG. 30. Position FOM Versus Aircraft Velocity.

The example discussed is a practical one and the figures serve to illustrate an important point: the error covariance equations not only serve to prescribe the Kalman Filter gain matrix, but are also useful in performing consistent analyses of systems containing the optimum linear filter. They can be used to determine the accuracy changes that will result if inertial sensors or measurement devices are altered. The resulting trade-offs are specified in terms useful to the system designer.

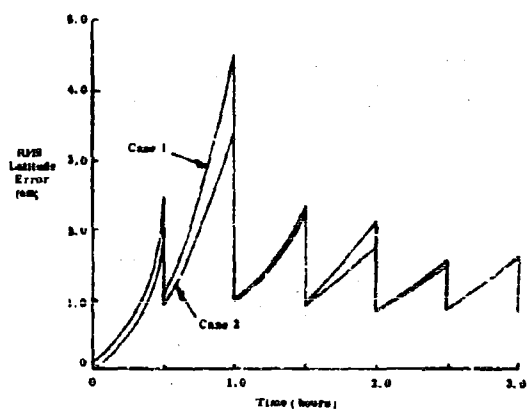

FIG. 31. Effect of Initial Conditions.

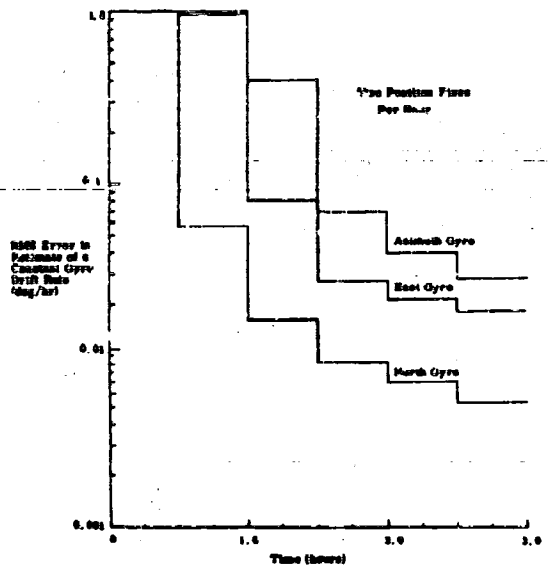

FIG. 32. Time History of RMS Errors in the Estimate of Constant Drift Rate.

Section 6. CORRECTIONS OF INERTIAL NAVIGATION SYSTEM ERRORS

At this point all the operations necessary to provide Kalman Filter estimates of the errors in inertial navigation systems have been presented. This chapter discusses two general schemes using these estimates to improve system accuracy. Emphasis will be placed on the technique which corrects errors within the system directly.

CORRECTION OF NAVIGATION SYSTEM OUTPUT

Because navigation system outputs such as position, velocity, and heading are the principal quantities of interest, the most apparent use of error estimates is to apply them as corrections to the system output (feedforward technique). Figure 33 illustrates this scheme. The feedforward approach has minimum complexity because only the quantities of interest are corrected. However, the linear error dynamics of inertial guidance systems actually result from a linearization of error behavior. It is conceivable that, if corrections were only applied to the system output and internal system errors were allowed to grow, the linearization would no longer be valid. In addition, some inertial navigation systems are so constructed that their outputs are directly connnected to other, dependent systems, precluding the use of feedforward correction. These considerations have led to the frequent use of a different scheme for employing system error estimates.

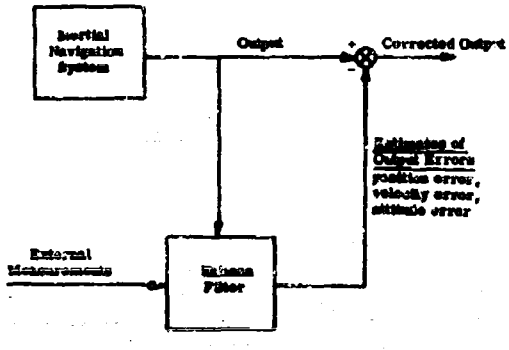

FIG. 33. Illustration of Feedforward Correction of System Output.

DIRECT REMOVAL OF NAVIGATION SYSTEM ERRORS

An alternate technique for the application of the system error estimates is to use them to change the state variables within the inertial navigator (feedback configuration). Figure 34 illustrates this approach. The quantities to be changed can all be represented as outputs of different integrators (or summing processes in a digital computer). This is a consequence of writing the state variable behavior in the form of a first-order differential equation. If all the system errors are corrected, the quantities of interest (position, velocity, etc.) will always have their "best" values. The use of this technique usually involves three distinct forms of control or error removal which differ because the integrators mentioned above may be of different types and may or may not be accessible. In the following discussion the assumption is made that discrete measurements are being used. Extension to the use of continuous error estimates is straightforward.

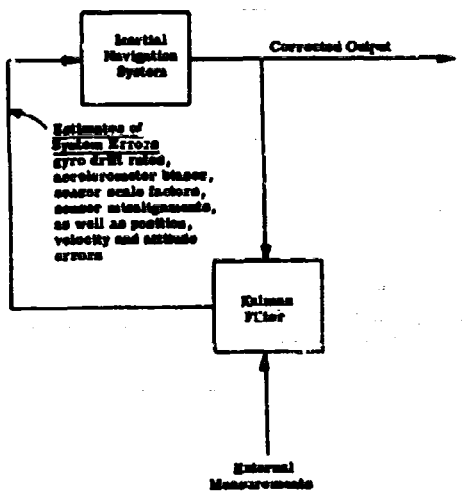

FIG. 34. Illustration of Feedback Correction of Navigation System Errors.

Reset or Impulsive Control

When the quantity whose error is to be corrected is an electrical signal at the output of an integrator (or in the memory of a digital computer), it can be changed immediately. The resetting of this value can be viewed as the application of an impulse of proper size to the integrator input, hence the expression "impulsive control." Impulsive correction minimizes the system errors for all times between measurements (Ref. 27). Typical of the variables subject to this control are position and velocity, as well as attitude when it is represented by a direction cosine matrix.

Rapid Torquing

When a gimballed platform is found to have an incorrect attitude, this error can be removed by rotating the platform. The integrators in this case are the integrating gyros which control platform angular rates. While an impulsive input to the gyros is not possible, the platform is rotated at its maximum rate until the error is corrected. This is a good approximation to impulsive control.

Continuous Correction

Not all of the system state errors estimated by the Kalman Filter can be rapidly corrected. It will be recalled that it is usually necessary to estimate correlated system disturbances and measurement errors. In so doing, the new state variables are often represented as outputs of fictitious linear systems. However, the integrator inputs of these systems cannot be reached. Thus, the Kalman Filter output cannot be applied as an impulsive correction. For example, consider the sum of a constant and an exponentially-correlated gyro drift rate. The system error estimates (estimates of gyro drift rate components) can only be applied as corrections at the gyro output, or equivalently as a torque with known effect on the output. Figure 35 illustrates this case.

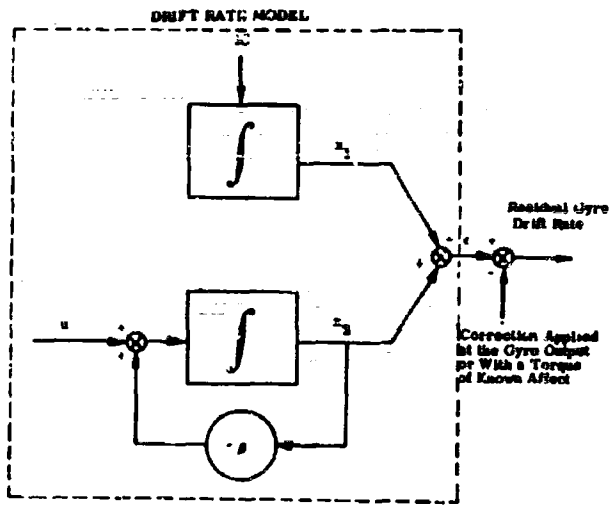

FIG. 35. Illustration of the Feedback Correction of a Typical Gyro Drift Rate Model.

The correction for the constant drift rate is an obvious one--effectively subtract the estimate of this quantity from the gyro output. The correction for the exponentially-correlated error is not as apparent; it follows from the difference in gyro error which would occur if the integrator were accessible. The correction for all time after t_n is then given in terms of the estimate of this error at t_n by

$$x_{corr_2} = \hat{x}_{2_n} e^{-\beta(t-t_n)} \tag{117}$$

Notice that x_{corr_2} is the Kalman Filter estimate of $x_2(t)$ when no correction is applied. Therefore, by subtracting this value the estimate of x_2 is made zero.

The gyro errors in this example and the corrections applied based on Kalman Filter estimates are illustrated in Fig. 36. Similar arguments can be used to prescribe the continuous corrections necessary for other forms of correlated system errors and disturbances. It should be emphasized that, when subsequent measurements produce additional error estimates, the corrections based on these new errors are added to those already being applied.

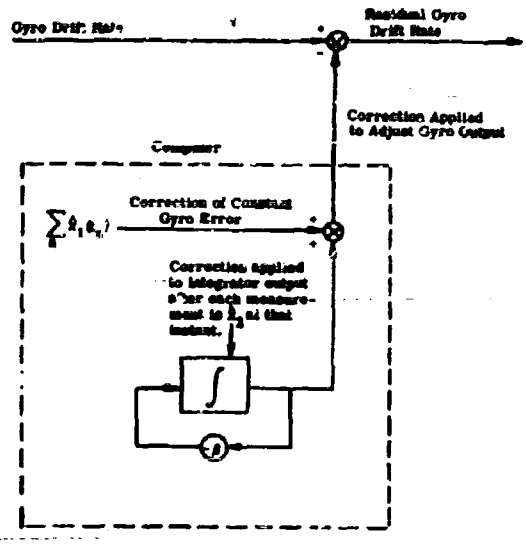

FIG. 36. Illustration of the Feedback Correction of Constant and Exponentially-Correlated Gyro Drift Rate.

FILTER EQUATION SIMPLIFICATION

One important result of applying error estimates directly to remove system errors is that this provides a simplification of the Kalman Filter equations. Equation 20 can be written as

$$\underline{x}_{n+1} = \Phi_n \underline{\hat{x}}_n + K_{n+1} \left(\underline{z}_{n+1} - H_{n+1} \Phi_n \underline{\hat{x}}_n \right) \qquad (118)$$

Since the feedback scheme causes

$$\underline{\hat{x}}_n = 0 \qquad (119)$$

immediately after the measurements are made, the next estimate of the system errors is given from Eq. 118 by

$$\underline{\hat{x}}_{n+1} = K_{n+1} \underline{z}_{n+1} \qquad (120)$$

It should be remembered that the quantity $\underline{z}_{n+1}$ in Eq. 120 is composed from the difference between the actual measurements and those indicated by the inertial system output variables. This simplification eliminates the need to compute $\Phi_n \underline{\hat{x}}_n$ and $H_{n+1} \Phi_n \underline{\hat{x}}_n$. The matrices Φ_n and H_{n+1} are, however, still required for the calculation of K_{n+1}.

Section 7. APPLICATION TO GYROCOMPASSING

Prior to the use of Kalman Filters in inertial navigation systems, platform alignment and the removal of cruise system errors were usually considered separately. In order to self-align the inertial navigator, certain additional electrical connections were made within the system which provided additional platform rotation commands. These techniques suffered some of the shortcomings discussed in Section 1 for cruise error reduction--they used stationary filters and did not account for time-varying inertial sensor and measurement errors. If the Kalman Filter is provided for estimating cruise system errors, it is easily employed to aid platform alignment as well. The term gyrocompassing, originally used to describe the tracking of both gravity and the horizontal component of earth rate by self-aligning inertial systems, is frequently applied to all schemes for self-alignment, including use of the Kalman Filter.

The filtering approach permits estimation of the system errors until they are determined to within a prescribed accuracy, followed by a rapid error-correction process. Consequently, the Schuler loop characteristic of locally-level systems is not destroyed during the alignment procedure and the inertial platform errors are not affected by vehicular motion. (The conventional gyrocompassing ground alignment approach is demonstrated in Ref. 28.) The alignment of strapdown systems is analogous to that of platform systems even though corrections are applied to the direction cosine matrix instead of rotating the instrument cluster.

FIXED-POSITION GYROCOMPASSING ALIGNMENT

When the carrying vehicle is not moving relative to the earth, position information is usually known with such accuracy that it can be considered error-free. In addition, any velocity indications in the inertial system can be taken as errors and used for direct inputs to the Kalman Filter. If attitude references are available, they can also be employed to aid in system alignment. If vehicle position is well known, measurement errors in position and velocity can only be generated by vibrations in the carrying vehicle. The desire to align rapidly, combined with a situation where only small measurement errors with short-period correlations exist, provides three basic alternatives for fixed-position alignment with the Kalman Filter.

One approach is to effect continuous filtering (Ref. 29). In this case, as a result of the continuous approach, velocity and position measurement error time correlations become significant and the state vector must be augmented to account for them. This necessitates using

a considerably modified and more complex version of the Kalman Filter than is necessary for cruise error estimation. An alternate scheme, which is more compatible with the equipment necessary for cruise inertial system augmentation, is to use the discrete version of the Kalman Filter, employing measurements at intervals larger than the short correlation time of the measurement errors. As a result, the errors in measurements can be assumed uncorrelated and the Kalman Filter equations of Section 2 can be used. A third approach, used in the following section, is to consider the measurement noise as uncorrelated because its correlation period is small relative to system characteristics. This permits continuous filtering with fewer state variables, but may not be as accurate as the first technique. The second approach is discussed below because it follows closely the ideas already presented.

Briefly, when north-vertical navigation coordinates are considered for a vehicle which is essentially motionless relative to the earth, the state vector can be defined by Eq. 82 and the F_x matrix of Eq. 84 specializes to

$$F_x = \begin{bmatrix} 0 & 0 & 1 & 0 & 0 & 0 & 0 \\ 0 & 0 & 0 & 1 & 0 & 0 & 0 \\ 0 & 0 & 0 & -2\Omega\sin L_o & 0 & g & 0 \\ 0 & 0 & 2\Omega\sin L_o & 0 & -g & 0 & 0 \\ \frac{-\Omega\sin L_o}{R} & 0 & 0 & \frac{1}{R} & 0 & -\Omega\sin L_o & 0 \\ 0 & 0 & \frac{-1}{R} & 0 & \Omega\sin L_o & 0 & \Omega\cos L_o \\ \frac{-\Omega\cos L_o}{R} & 0 & 0 & \frac{-\tan L_o}{R} & 0 & -\Omega\cos L_o & 0 \end{bmatrix} \qquad (121)$$

If the measurement errors are assumed uncorrelated, state vector augmentation is entirely due to inertial sensor errors. In addition, over the short estimation period of alignment these can be approximated as the sums of constants and random walk quantities. If the estimation period is very short, representation by random constants may suffice. In either case F_u is zero. The F matrix for the augmented state, Eq. 92, is given by

$$F = \left[\begin{array}{c|c} F_x & O \\ \hline & I_5 \\ \hline O & O \end{array}\right] \qquad (12\times12) \qquad (122)$$

If random walk behavior is included in the models of all inertial sensor errors, the matrix G Q G^T is

$$GQG^T = \left[\begin{array}{c|c} 0 & 0 \\ \hline 0 & Q_u \end{array}\right] \quad (12\times12) \tag{123}$$

where Q_u is the covariance matrix for the vector of uncorrelated inputs to the random-walk-generating integrators. Φ_n can be approximated for the short intervals between measurements by

$$\Phi_n \cong I_{12} + (t_{n+1} - t_n) F \tag{124}$$

The matrix Q_n in the error covariance equation is given in terms of a 5 x 5 matrix L_n as

$$Q_n = \left[\begin{array}{c|c} 0 & 0 \\ \hline 0 & L_n \end{array}\right] \tag{125}$$

where

$$L_n = E\left(\underline{\ell}_n \underline{\ell}_n^T\right) \quad \text{and} \quad \underline{\ell}_n = \int_{t_n}^{t_{n+1}} \underline{u}(\tau)\,d\tau \tag{126}$$

If only constant inertial sensor errors are considered, GQG^T and Q_n are zero. In any case, the mean square values of the random constants appear in the diagonal elements of the lower right 5 x 5 submatrix of the initial error covariance, $P(t_o)$.

If velocity and position measurements are used and position difference is assumed to contain no errors, the matrix R is

$$R = \begin{bmatrix} 0 & 0 & 0 & 0 \\ 0 & 0 & 0 & 0 \\ 0 & 0 & \sigma^2_{\dot{R}_x} & 0 \\ 0 & 0 & 0 & \sigma^2_{\dot{R}_y} \end{bmatrix} \qquad (127)$$

where $\sigma^2_{\dot{R}_x}$ is the mean square indicated vehicle velocity caused by vibration. Velocity errors are assumed uncorrelated in Eq. 127. The measurement matrix, $H_{p,v}$ is given in Eq. 106.

All of the matrices necessary for calculating the error covariance and filter gain as functions of time have been prescribed. If the disturbances and measurement noise are stationary or their time behavior is known beforehand, the filter gain matrix can be precomputed and stored. If they are stationary, the gain will reach a unique steady state. Some suboptimal filter possibilities are discussed in Section 9 for similar cases.

MOVING VEHICLE GYROCOMPASSING ALIGNMENT

The self-alignment of inertial navigation systems in moving vehicles is computationally similar to fixed-position gyrocompassing. Velocity and position differences again provide the Kalman Filter inputs. However, sizable measurement errors are common in the case of moving vehicle alignment. Position measurements are typically provided by Tacan, Loran, or Omega radio navigation aids. Velocity can be measured by Doppler radar in an aircraft or by a ship's speed log. Because velocity indications are usually given in vehicle coordinates, an independent heading reference is needed to resolve them into navigation coordinates. Any azimuth errors in this device will be transferred to the inertial system. In addition, position and velocity must be estimated in the moving vehicle case.

For example, consider the airborne alignment of an inertial navigation system with the aid of Doppler velocity indication and intermittent position fixes. It can be shown that the correlated measurement errors appearing in Doppler indications of velocity can be removed by prefiltering for a period of 30 to 60 seconds (Ref. 2). The prefilter output (input to the Kalman Filter) contains uncorrelated errors and a small bias error which is ignored in the following discussion. The system

matrix, F_x, is no longer constant. It is prescribed by Eq. 84 (or 85) with ω_x, ω_y, ω_z computed according to Eq. 78, 79, or 80, depending on the navigation coordinate frame. If no augmentation of the state vector results from correlated position or velocity measurements, the F and GQG^T matrices follow the form prescribed in Eq. 122 and 123. The matrices Φ_n and Q_n also are similar to those outlined in the preceeding section.

The measurement noise matrix is nonsingular. If the position fix errors are not cross-correlated, the R matrix will be

$$R = \left[\begin{array}{cc|c} \sigma^2_{\delta R_x} & 0 & \\ 0 & \sigma^2_{\delta R_y} & 0 \\ \hline & 0 & R_v \end{array}\right] \qquad (4\times 4) \qquad (128)$$

where $\sigma^2_{\delta R_x}$ is the mean square error in position fix along the x axis, etc. The matrix R_v describes the velocity measurement error covariance. Because Doppler velocity errors along and across the aircraft track differ and usually appear in both north and east velocity measurements, R_v is not commonly a diagonal matrix. If along- and cross-track Doppler errors are assumed not correlated with each other and given by the vector

$$\underline{v}_v = \begin{bmatrix} v_a \\ v_c \end{bmatrix} \qquad (129)$$

the velocity errors resolved into north and east components are given by $\underline{v}'_v$

$$\underline{v}'_v = \begin{bmatrix} \cos\alpha & -\sin\alpha \\ \sin\alpha & \cos\alpha \end{bmatrix} \underline{v}_v \qquad (130)$$

The R_v matrix is then dependent on the heading angle α

$$R_v = \mathrm{cov}\left[\underline{v}'_v, \underline{v}'_v\right]$$

$$= \left[\begin{array}{c|c} \sigma^2_{v_a}\cos^2\alpha + \sigma^2_{v_c}\sin^2\alpha & (\sigma^2_{v_a} - \sigma^2_{v_c})\sin\alpha\cos\alpha \\ \hline (\sigma^2_{v_a} - \sigma^2_{v_c})\sin\alpha\cos\alpha & \sigma^2_{v_a}\sin^2\alpha + \sigma^2_{v_c}\cos^2\alpha \end{array}\right] \qquad (131)$$

The fact that R is a function of vehicle heading imposes a restriction on the vehicle flight path when precomputation of the filter gain matrix is desired. The measurement matrix $H_{p,v}$ is similar to the one described in the previous section.

A comparison of Kalman Filter accuracy and the RMS errors that result from a fixed-gain alignment technique is shown in Fig. 37, 38, and 39 for this example. The important parameters used in arriving at these figures are:

RMS initial tilt angles, mrad	2
RMS initial azimuth error, mrad	10
RMS constant accelerometer errors, g	10^{-4}
RMS constant gyro drift rates, deg/hr	0.01
RMS Doppler bias error, ft/sec	
Cross-track	3.0
Along-track	2.0
RMS Doppler errors with 1-sec correlation time (along- and across-track), ft/sec	3
RMS uncorrelated Doppler errors at the end of a 30-sec prefiltering, ft/sec	
Cross-track	1.0
Along-track	0.75
RMS uncorrelated position fix error, ft	
North-south	600
East-west	600
Vehicle velocity (due east), ft/sec	800

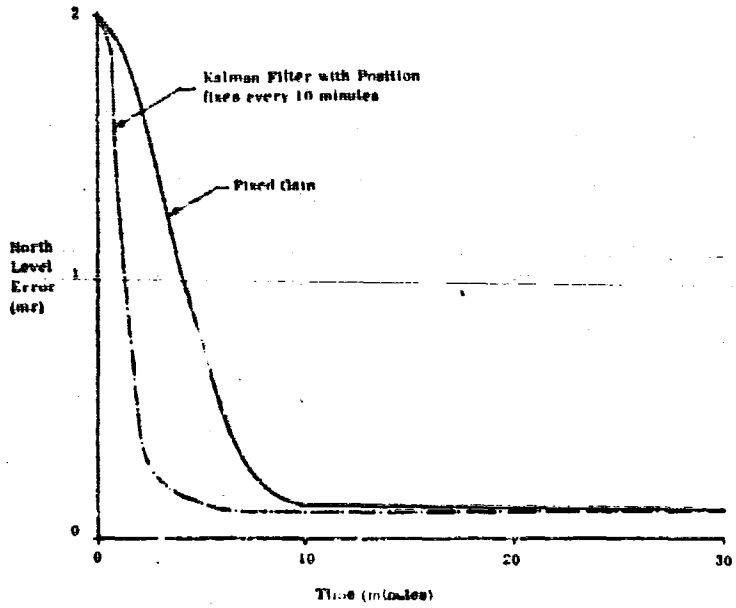

FIG. 37. Optimal Versus Conventional Airborne Erection Accuracy.

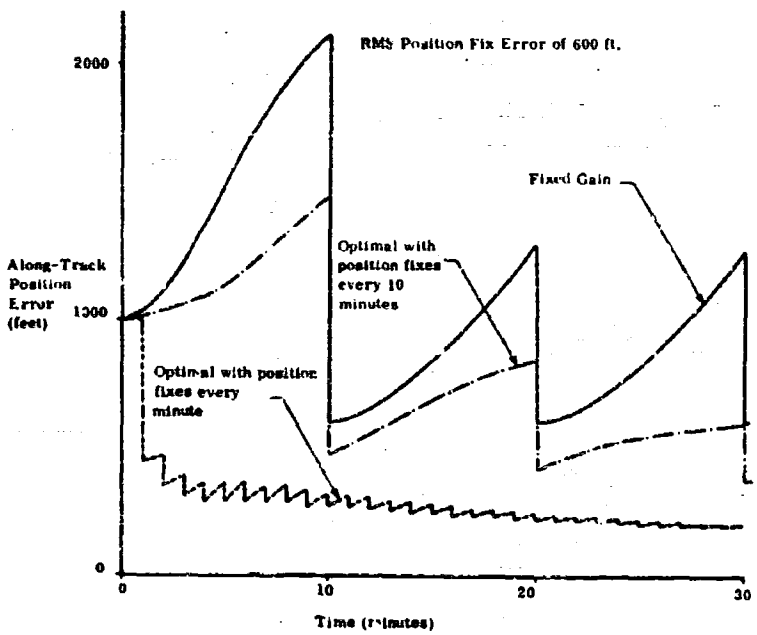

FIG. 38. Optimal Versus Conventional Airborne Alignment Accuracy.

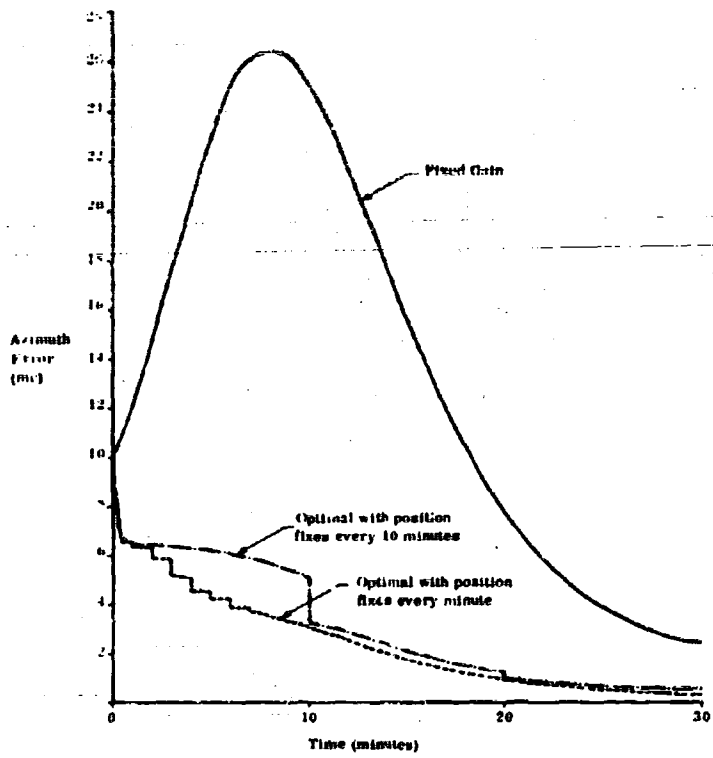

FIG. 39. Optimal Versus Conventional Airborne Alignment Accuracy.

The Kalman Filter exhibts a distinct accuracy advantage in estimating attitude errors (Fig. 37 and 39) regardless of the time interval between position fixes. This follows from the fact that velocity errors contain considerable information about system misorientation while position errors, though contributing some additional accuracy, are less useful. The similarity of Fig. 39 to Fig. 5 results from the fact that they describe situations which are almost identical. The Kalman Filter also provides more exact estimates of position than the fixed-gain filter (see Fig. 38). The better accuracy of the Kalman Filter in estimating all three quantities results from its time-varying nature and the fact that it considers time-varying inertial sensor errors. The fixed-gain filter errors approach those of the Kalman Filter in the steady state but the ability of the latter to provide faster alignment is well documented in the figures.

When the gyros and accelerometers have not been running for a considerable time before the start of filtering, their internal temperatures will not have been stabilized. To the extent that they can be determined, the temperature-caused errors can be subtracted from the sensor error models. If these effects can be accurately established, the Kalman Filter airborne alignment can be performed with an inertial system as it is being warmed up.

Section 8. APPLICATION TO ALIGNMENT TRANSFER

The Kalman Filter is a useful tool for the transfer alignment of one inertial system to another. The problem is essentially one of accurately estimating misalignment. Once the misorientation is detected, removing the errors is not difficult. While transfer alignment of a weapon inertial reference system from a "master" system imposes all the errors of the master on the "slave", this situation may often be preferred to that of aligning the slave to an "ideal" coordinate frame. Before filtering, the two systems are first brought into near alignment by some knowledge of their relative orientation. This is usually accomplished without difficulty because they are connected by a physical structure at the time of alignment. The residual misorientation caused by uncertainties in mounting and structural flexure is small and permits linearization of the equations describing alignment errors.

The alignment transfer technique employing the Kalman Filter is basically an extension of vector matching. The vectors employed are motions which can be measured by inertial sensors, such as linear acceleration and velocity or angular rate and displacement. Matching of vectors which are measured by inertial components already available eliminates the necessity for elaborate additional equipment to perform alignment, although a computer is required to process the measurements.

Transfer alignment using the Kalman Filter is accomplished by measuring the same vector in the two nearly-aligned coordinate systems and using the difference as the filter input. A good discussion of the principles involved in determining the relative alignment of orthogonal coordinate frames by vector matching can be found in Ref. 30. It is well known that the relative orientation of two axis systems cannot be determined uniquely by measuring a single vector. Two noncolinear vectors are needed, and for fixed measurement accuracies, two vectors at right angles are preferred. An example of alignment using two noncolinear vectors is the conventional gyrocompassing of an inertial system; the two vectors, with known orientation in the reference coordinate frame, are gravity and earth rate. The useful portion of earth rate is that part normal to gravity. At the poles, where the two vectors are parallel this technique becomes useless. Away from the poles the gyrocompassing system detects the two vectors and their misalignment with the platform axes, reorienting the platform until it is properly aligned. The gyrocompassing example also serves to illustrate the fact that transfer alignment is not restricted to the use of a reference inertial system. Any set of axes in which the necessary vectors can be measured will serve as the master coordinate frame.

GIMBALLED SYSTEM TRANSFER ALIGNMENT

Transfer alignment between two gimballed platforms consists of accurate estimation of the misalignment and subsequent rotation of the slave platform to bring its axes into coincidence with the master frame. This rotation can be accomplished with great precision. Therefore, though the correction of slave attitude could be accomplished during estimation, it would serve to increase the filter computations without increasing accuracy. Attitude correction is not required to preserve the linearity of the differential equations for alignment errors.

Coarse alignment to within a degree or two is accomplished by matching corresponding gimbal angles of the two systems. Consider the north-vertical coordinates described in Section 3; because no disturbance of the normal operation of both systems occurs during estimation, the Schuler tuning characteristic of these systems is unaltered. Previously proposed leveling schemes based on vector matching destroyed the Schuler characteristic, creating new alignment errors (see Ref. 31). Because both platforms are isolated from vehicle angular motion during the estimation process, structural flexure only provides an initial condition on the error statistics of the misalignment. Initial conditions for longitude and latitude are provided to the slave from the master system after completion of alignment. The ideas outlined in the balance of this section are a summary of work reported in Ref. 12.

After the slave system is given initial values of east velocity and north velocity from the master system, both platforms are operated in their normal modes while filtering is conducted. Earth rate commands to the gyros are identical and originate from the master system. Two or three of the velocity indications of the systems are compared and the differences are used as inputs to the Kalman Filter. Velocity differences due to the physical separation of the two systems are removed from these signals prior to their entrance into the filter. The differential equations for the velocity differences, δR, and small misalignment angles, ϕ, between the two nearly aligned gimballed systems can be written in the form of Eq. 2 where

$$\underline{x} \triangleq \begin{bmatrix} \dot{\delta R}_x \\ \dot{\delta R}_y \\ \dot{\delta R}_z \\ \varphi_x \\ \varphi_y \\ \varphi_z \end{bmatrix}, \quad F = \begin{bmatrix} 0 & 2\Omega_z & 0 & 0 & (g-a_z) & a_y \\ -2\Omega_z & 0 & 2\Omega_x & -(g-a_z) & 0 & -a_x \\ 0 & -2\Omega_x & 0 & -a_y & a_x & 0 \\ 0 & \frac{1}{R} & 0 & 0 & \omega_z & -\omega_y \\ -\frac{1}{R} & 0 & 0 & -\omega_z & 0 & \omega_x \\ 0 & \frac{-\tan L}{R} & 0 & \omega_y & -\omega_x & 0 \end{bmatrix} \tag{132}$$

G is the identity matrix and $\underline{u}$ is the vector of differences between accelerometer errors ∇ and gyro errors ϵ

$$\underline{u}^T = \left[(\nabla_{x_m} - \nabla_{x_s})(\nabla_{y_m} - \nabla_{y_s})(\epsilon_{x_m} - \epsilon_{x_s})(\epsilon_{y_m} - \epsilon_{y_s})(\epsilon_{z_m} - \epsilon_{z_s})\right] \tag{133}$$

The measurement matrix H is given by

$$H = \begin{bmatrix} 1 & 0 & 0 & 0 & 0 & 0 \\ 0 & 1 & 0 & 0 & 0 & 0 \\ 0 & 0 & 1 & 0 & 0 & 0 \end{bmatrix} \tag{134}$$

If only north and east velocities are being compared, the third rows and columns of F_x and H are deleted and ∇_z is dropped from $\underline{u}$. The noncolinear vector is provided by maneuvering the vehicle, thereby creating an acceleration vector with time-varying orientation relative to the master coordinates. The continuous version of the Kalman Filter is used and an infinity of noncolinear vector pairs results from the vehicle maneuvers.

Accelerometer errors, ∇, and gyro drift rates, ϵ, are represented by the sum of a random constant and a random walk. This description of inertial sensor errors augments the state vector with one additional variable for each sensor considered, thereby doubling the dimension of the problem. However, through familiarity with the importance of various effects, the state vector can be reduced (Ref. 12). In particular, the Schuler period and gyro drift rate are observed to have no significance for the problem considered there, due to the short time of observation.

Inspection of the F matrix for this problem and knowledge of its appearance in the differential equation for the error covariance matrix (Eq. 29) indicates that the accuracy of the Kalman Filter can be influenced by vehicle maneuvers through the accelerations a_x, a_y, and a_z. When vertical velocity is not available for comparison and the vehicle is restricted to horizontal maneuvers, the sum of the mean square errors in the estimates of ϕ_x, ϕ_y, and ϕ_z is minimized by rotating the acceleration vector at its maximum rate (Ref. 12). For an aircraft, this implies a maximum rate turn at constant speed. In addition, because in the absence of vertical acceleration the measurements $\delta\dot{R}_x$ and $\delta\dot{R}_y$ cannot distinguish between constant accelerometer error and platform tilt, the accuracy of the filter in estimating ϕ_x and ϕ_y is

directly limited by the size of the x and y axis accelerometer biases. This serves to demonstrate one aspect of the observability problem discussed in Section 3.

If all three velocity differences are available as inputs to the filter, the aircraft optimum horizontal maneuver is still the tightest turn permissible. In this case, the constraint between tilt angle estimation accuracy and constant accelerometer errors is removed because the additional measurement, $\delta\dot{R}_z$, also contains indications of ϕ_x and ϕ_y which are distinguishable from the constant portions of ∇_x and ∇_y. Consequently, estimates of the constant errors in the x and y accelerometers have greater accuracy. Similar improvements result when only horizontal velocities are compared but vertical maneuvers are performed. Inspection of the F matrix reveals that vertical maneuvers, by creating a time-varying a_z, provide a means of distinguishing between level misalignment (time-varying coefficient) and constant accelerometer errors.

Measurement noise, as mentioned earlier, can be generated by relative velocities between systems caused by structural flexure. In addition, some quantization and signal transmission noise may be significant. While the noise present in the velocity signals of either inertial reference system is typically a very small fraction of the true signal, errors in the velocity difference can have significant relative magnitude.

The use of the continuous version of the Kalman Filter and the size of the state vector generate a considerable computer load if all calculations are performed on-line. Precomputed gains, stored as functions of time and vehicle heading, can reduce this problem considerably. However, the vehicle carrying the two gimballed inertial systems would have to perform preplanned maneuvers. This can be a tactical problem, but typical alignment times are on the order of a minute or less.

The ability of the continuous Kalman Filter to provide quick, accurate estimates of the misalignment between two gimballed inertial systems is illustrated by Fig. 40 and 41. They show time histories of the RMS errors in Kalman Filter estimates of level and azimuth misalignment when only horizontal velocities are compared. The errors were found by solving the error covariance differential equation (Eq. 29) with following inputs:

Vehicle maneuver	3-g horizontal turn
Vehicle velocity, ft/sec	10^3
Measurement noise	1.5 ft/sec RMS from each system; flat power spectral density to 1,000 cps (see Appendix A)
RMS gyro drift rate, deg/hr	0.25
RMS constant accelerometer error, g	10^{-3}

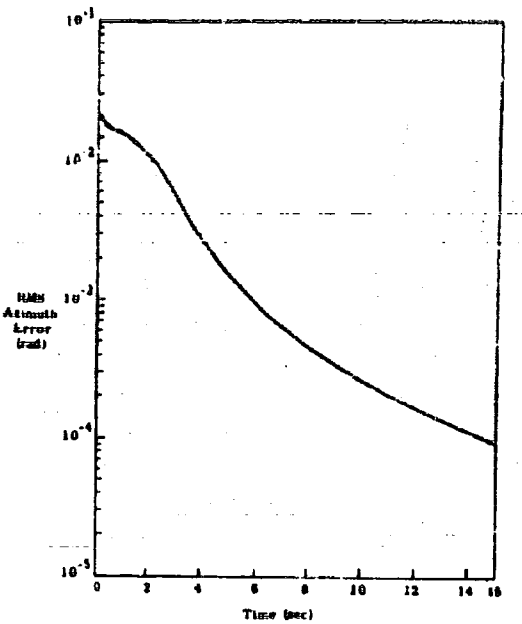

FIG. 40. RMS Azimuth Misalignment Estimation Error (Ref. 12).

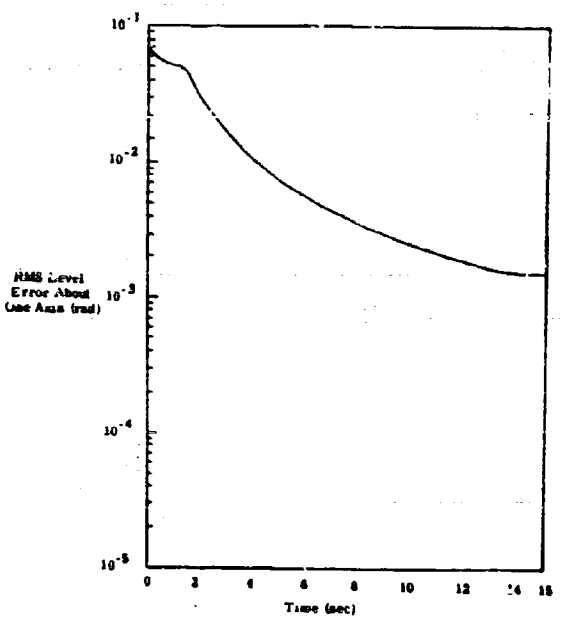

FIG. 41. Comparison of RMS Level Misalignment Estimation Errors.

The two figures indicate that at the end of a 15-second estimation period the azimuth misalignment is known much more accurately than level misalignment. It can be seen that the estimation errors for the level angle have reached a steady-state value of $\sqrt{2}$ milliradians. This corresponds to the lower limit imposed by the constant accelerometer errors. The factor of $\sqrt{2}$ results from adding the mean square accelerometer errors from corresponding sensors in the two systems. Of course, comparison of vertical velocities or performing a vertical maneuver will remove this constraint. It can be seen that the Kalman Filter holds considerable promise as a means of measuring the misalignment between two gimballed inertial guidance systems.

STRAPDOWN TO GIMBALLED SYSTEM TRANSFER ALIGNMENT

Alignment between a stabilized gimballed inertial reference system and a strapdown inertial system involves accurate determination of the transformation matrix relating the two coordinate frames. The initial coarse alignment is determined by calculating the transformation matrix from gimbal angles. For reasons similar to those discussed in the previous section, more accurate determination of the relative orientation is necessary.

Three variables are needed to describe the relative orientation between two sets of three orthogonal axes. However, in the strapdown application it is necessary to compute changes in orientation based on angular rates measured by the system gyros. In this case the differential equations for the Euler Angles contain a singularity corresponding to gimbal lock in a stabilized platform. For general angular motion, at least four parameters (analogous to four gimbals) are needed. It also is possible to compute all nine elements or direction cosines of the transformation matrix directly.

Though more variables are involved, the direction cosine calculations are linear. The differential equations for three- or four-parameter representations of rotation are highly nonlinear. Reference 32 provides a more complete discussion of transformation matrices. When the Kalman Filter is to be used, linearity of the original equations avoids potential errors that can result from linearization about a nominal trajectory. If the linearization is performed perfectly, no one set of parameters offers an estimation accuracy advantage over the others (Ref. 12). However, only calculation of the nine direction cosines will be considered below.

The true direction cosine matrix, C, relates an acceleration vector measured in platform coordinates, $\bar{a}_p$, to the same vector resolved in vehicle or strapdown coordinates, $\bar{a}_v$, according to

$$\bar{a}_p = C\bar{a}_v \tag{135}$$

The othogonality of the transformation dicates that the inverse of C is also its transpose, simplifying calculation of the relation C^{-1} considerably. The linear differential equation for C, in terms of the angular rate of the strapdown system expressed in vehicle coordinates, is given by

$$\dot{C} = C\Omega \tag{136}$$

where the matrix Ω is constructed from the vehicle angular rates ω_x, ω_y, and ω_z according to

$$\Omega = \begin{bmatrix} 0 & \omega_z & -\omega_y \\ -\omega_z & 0 & \omega_x \\ \omega_y & -\omega_x & 0 \end{bmatrix} \tag{137}$$

An initial error exists in knowledge of the C matrix. The matrix in the computer

$$C_c = C + \delta C \tag{138}$$

is the sum of the true matrix and a small difference which obeys a differential equation analogous to Eq. 136

$$\dot{\delta C} = \delta C\, \Omega \tag{139}$$

The platform accelerometer triad indicates the true acceleration vector $\bar{a}_p$ plus accelerometer errors $\bar{\nabla}_p$. The strapdown sensors provide the sum of $C^T\bar{a}_p$ and an error vector $\bar{\nabla}_v$. The difference between the strapdown measurement transformed by C_c and the platform indication is

$$\bar{\Delta} = (\delta C)\ C^T\bar{a}_p + C\bar{\nabla}_v - \bar{\nabla}_p \tag{140}$$

where the term $\delta C\bar{\nabla}_v$ has been considered a higher-order effect and ignored. Defining a new 3-element vector, $\bar{d}$, by

$$\begin{aligned} \dot{\bar{d}} &= \bar{\Delta} \\ \bar{d}\ (t_o) &= 0 \end{aligned} \tag{141}$$

an 18-element state vector can be composed from $\bar{d}$, $\bar{\nabla}_p$, $\bar{\nabla}_v$, and the elements of δC. This state vector, $\underline{x}$, obeys a linear differential equation

$$\dot{\underline{x}} = F\ \underline{x}$$

where the elements of F are composed from the elements of C, the accelerations measured by the platform accelerometers and the angular rates measured by the strapdown system gyros. Many of the elements of F are zero. The filter input is the vector $\bar{d}$, provided by integrating the acceleration difference $\bar{\Delta}$. The elements of $\bar{d}$ are velocity differences in the direction of the platform axes. The 18 state variables indicate that there are 324 elements in the error covariance matrix. Since rapid alignment or estimation of δC is desired using continuous measurements, a precomputed filter gain matrix may be necessary. Because any prescription of the K matrix requires knowledge of F, preplanned maneuvers must be executed precisely in order to obtain the accuracies promised by the error covariance analysis.

If angular maneuvers are restricted during alignment in order to avoid the singularity in the differential equations, the three Euler Angles can be estimated using the Extended Kalman Filter. The size of the state vector is then reduced to 12 elements. However, the elements of the F matrix for this case are more difficult to calculate, involving sines and cosines of time-varying Euler Angles. Again the filter gain matrix may be too complex for anything but precomputation. It should be noted that alignment using Euler Angle estimates does not restrict the

relative orientation of the two systems after estimation is completed. The Euler Angle estimates are converted into direction cosines at the end of filtering in order to correct the transformation matrix.

It is not clear what meaning can be attached to the sum of error variances in the estimates of the Euler Angles or the elements of C. An indication of filter accuracy with some physical meaning is required. If the error in C_c, δC, results from a small misalignment, the product of the transpose of the true transformation matrix and the computed matrix is a third transformation which can be approximated by

$$C^T C_c \approx \begin{bmatrix} 1 & \varphi_z & -\varphi_y \\ -\varphi_z & 1 & \varphi_x \\ \varphi_y & -\varphi_x & 1 \end{bmatrix} \tag{142}$$

The small angles ϕ_x, ϕ_y, and ϕ_z are the angular orientation errors about three orthogonal axes (x, y, and z) that are described by δC. Remembering that

$$\begin{aligned} C_c &= C + \delta C \\ C^T C &= I \end{aligned} \tag{143}$$

it is observed that

$$C^T \delta C \approx \begin{bmatrix} 0 & \varphi_z & -\varphi_y \\ -\varphi_z & 0 & \varphi_x \\ \varphi_y & -\varphi_x & 0 \end{bmatrix} \tag{144}$$

A reasonable figure-of-merit is the sum of the mean square errors in the estimates of ϕ_x, ϕ_y, and ϕ_z. In terms of errors in the estimate of δC, $\delta\hat{C}$, this can be expressed as the mean value of

$$\left(C_1^T \delta\hat{C}_2\right)^2 + \left(C_2^T \delta\hat{C}_1\right)^2 + \left(C_1^T \delta\hat{C}_1\right)^2$$

The vectors $\underline{C}_i$ and $\delta\tilde{\underline{C}}_i$ are the ith column vectors of the C and $\delta\tilde{C}$ matrices. The averaging process involves only the elements of the $\delta\tilde{C}$ matrix because C is deterministic. When the Kalman Filter is estimating $\delta\tilde{C}$ directly, the figure-of-merit can be expressed in terms of the true direction cosines and elements of the error covariance matrix which lie both on and off the diagonal. When the filter estimates Euler Angles, the error covariance matrix elements enter the figure-of-merit in a more complex fashion. Of course, this evaluation of filter accuracy is only conducted during preliminary analysis of the Kalman Filter alignment technique.

Section 9. KALMAN FILTER IMPLEMENTATION CONSIDERATIONS

In this section some of the practical details of implementing the Kalman Filter are discussed. The purpose here is to introduce the reader to a few problems and to demonstrate common approaches to reducing them. Of course, practical considerations generate subjective solutions. Consequently, no attempt is made to discuss all of the problems encountered and the approaches presented are not the only ones possible.

COMPUTER COMPLEXITY

The compact vector-matrix notation in which the Kalman Filter equations are written is deceptive. Literally thousands of multiplications can be described by a few strokes of the pen and equations can easily be written that cannot be solved quickly enough by even the largest and fastest modern computers. Many reports are available, and many more will be written, describing in detail, for one system or another, the memory requirements and number of computer operations needed to incorporate a single external measurement using the Kalman Filter. Among these are Ref. 2, describing airborne alignment and cruise error removal using position fixes and Doppler velocity information, and Ref. 33 which compares Kalman Filter computer requirements to those for a growing-memory digital filter.

A few general comments can be made to illustrate how demands on the computer are related to the formulation used in the Kalman Filter. Basically, the computer requirements are related to the number of elements in the state vector and the number and repetition rate of external measurements. The computer time requirement is directly related to the frequency at which measurements reach the discrete filter, because the covariance and estimation difference equations are solved with each new input. Also, to be useful, the filter equation (Eq. 20) must be solved in a small fraction of the time between measurements. The continuous filter requires solution of differential equations and, if a digital computer is being used, the time step size required determines whether any computer time is available for other calculations.

The number of digital computer operations necessary to incorporate each new measurement (or the number of integrators, multipliers, and resolvers in an analog computer implementation of the continuous filter) is largely determined by the state vector size. One of the basic differences between conventional filters and the Kalman Filter is that the latter attempts to measure random errors if they are time-correlated. This feature is also the major cause of large state vectors in the filter equations. Unfortunately, state vector size and computational complexity are not linearly related. The matrix difference (or differential)

equations describing error covariance behavior, Eq. 21, 25, and 29, represent n^2 scalar equations where n is the number of state variables. Furthermore, the multiplication of two n x n matrices, often required in the solution of these equations, represents n^3 separate scalar multiplications that must be carried out by the computer. The seriousness of this situation is often relieved in particular applications through efficient programming. This is possible when many of the matrix elements are zero.

Computer requirements are reduced if the matrices which appear in the system and error covariance differential equations are constant. Analytic solutions exist for the error covariance matrices for the discrete and continuous filters when F, H, G, Q, and R are constant (Ref. 7 and 34). Implementation of these solutions is usually less demanding of computer time if the measurement schedule is periodic and the interval between measurements is much longer than the time step required for accurate solution of the differential equations.

A problem sometimes arises when an error covariance matrix is reduced from an initially large value to a very small quantity. In this case, significant digits are frequently lost and the positive definiteness of the covariance matrix can be destroyed. A square root formulation of the Kalman Filter has been developed which is helpful in this situation (Ref. 35). It avoids the necessity of using double precision in this case or permits the use of shorter word lengths than might otherwise be required for problems of this sort. On the other hand, the square root formulation requres more calculations than the single precision conventional formulas. Also, if measurements provide knowledge of some state variables that is much more accurate than the estimates immediately prior to observation, Eq. 22 is a more precise equation for updating the error covariance matrix than Eq. 25 (see Ref. 36).

Frequently, a reduction in computer requirements can be achieved by prefiltering the external measurements. Consider the case where Doppler velocity measurements are used to aid an inertial navigation system (Ref. 2). The velocity indications are available several times a second but velocity errors are essentially constant over a much longer period. By averaging the differences between Doppler measurements and inertial system indications over several seconds the correlation between measurement errors at the input to the Kalman Filter may be reduced to a negligible amount. A double reduction of computer requirements can result; the state vector size may be reduced because it is no longer necessary to consider correlated measurement errors, and the measurements reach the filter less frequently, permitting slower calculation rates. The averaging process causes a significant reduction in the mean square measurement noise, providing fewer measurements of higher quality. However, an additional measurement error does occur because

the average is biased when the inertial system velocity error is changing during the prefiltering process. In general, this technique is useful because the Doppler velocity measurements are provided much more frequently than necessary.

It frequently happens that the system model, painstakingly constructed during the initial analysis to include every possible detail, is later sharply reduced because of computer limitations. If this reduction is to be accomplished without making the Kalman Filter useless, a means for analyzing its effect on accuracy is necessary. Such a procedure is outlined under "The Effects of Imperfect Models" (p.115). As usual, practical considerations dictate an engineering approach to implementation of the Kalman Filter. It is necessary to determine trade-offs between accuracy and computer complexity. The final choice is at least partly subjective. Typical state vector size for Kalman Filter applications to inertial navigation systems ranges from 6 to 21 elements. Computer memory requirements range from approximately 1,200 to approximately 4,000 words, reflecting the fact that efficient programming can partially relieve the "curse of dimensionality." Unfortunately, the larger state vectors usually appear in aircraft applications where measurements are taken more frequently and computer size is more critical.

OBSERVABILITY

In any situation where many variables are to be measured or estimated by observing a small number of output quantities, the question of observability arises. For example, in the state and measurement equations

$$\begin{bmatrix} \dot{x}_1 \\ \dot{x}_2 \\ \dot{x}_3 \end{bmatrix} = \begin{bmatrix} f_{11} & f_{12} & 0 \\ f_{21} & f_{22} & 0 \\ 0 & 0 & f_{33} \end{bmatrix} \begin{bmatrix} x_1 \\ x_2 \\ x_3 \end{bmatrix} + G\underline{u} \qquad (145)$$

$$\underline{z} = \begin{bmatrix} 1 & 0 & 0 \\ 0 & 1 & 0 \end{bmatrix} \underline{x} + \underline{v} \qquad (146)$$

the variable x_3 is not observable. No amount of filtering of the measurements will improve the accuracy in knowledge of x_3. The literature contains many statements of the strict mathematical definition for observability (see Ref. 7 and 8). More common in the application of the Kalman Filter to inertial navigation systems is the observability problem demonstrated by

$$\begin{bmatrix} \dot{x}_1 \\ \dot{x}_2 \\ \dot{x}_3 \end{bmatrix} = \begin{bmatrix} f_{11} & c_1 & c_2 \\ 0 & 0 & 0 \\ 0 & 0 & 0 \end{bmatrix} \begin{bmatrix} x_1 \\ x_2 \\ x_3 \end{bmatrix} + G\underline{u} \qquad (147)$$

$$z = x_1 + v \qquad (148)$$

where the f elements are time-varying but c_1 and c_2 are constant. Equations 147 and 148 illustrate the case where two variables (x_2 and x_3) can be recovered from the measurement only as a linear combination. This is the situation discussed in Section 8 where the velocity difference between two nearly coincident inertial systems is influenced in the same way by platform level misalignment and constant level-accelerometer errors. The two effects are not separable. A similar situation arises in estimating constant east gyro drift rate and azimuth error in a north-vertical system when only position measurements are available. The Kalman Filter corrects the estimates of the two inseparable variables according to the variances of their estimation errors. If one variable is known much more accurately than the other, almost all of the difference $(z-\hat{x}_1)$ is used to correct the least precise estimate. For the problem discussed under "Gimballed System Transfer Alignment" (p. 94), when the initial uncertainty in $g\phi_y$ is much greater than the standard deviation of x-axis accelerometer error, the Kalman Filter will attribute the entire effect to the tilt angle, ϕ_y. As a result, the RMS steady-state estimation errors in $g\phi_y$ and ∇_x are identical and essentially equal to the RMS accelerometer error. There is no accuracy improvement in the estimate of constant accelerometer error. If the two initial error variances were approximately equal, both estimates would be improved by the Kalman Filter. Only when the two errors are made separately observable by providing an additional measurement or a time-varying element in the system matrix can both estimates be improved by the filter regardless of the initial error variances.

SUBOPTIMAL FILTERS

Several forms of suboptimal filters have already been suggested. Generally, a suboptimal filter is a modification or simplification of the optimal or Kalman Filter. In a sense, any Kalman Filter is suboptimal because all the effects on system state behavior can never be determined. The important consideration in going from the Kalman Filter to a suboptimal formulation is an ability to analyze the effect on accuracy that is produced by the change.

Simplified Model

In order to reduce computational complexity, certain known dynamics that exist in the system, its disturbances, or in the measurement errors are often intentionally ignored. Of course, this neglected behavior is understood by the designer to have a minor effect on the state variables of interest. The new, simplified dynamics are described by a state differential (or difference) equation and a measurement equation similar in form to those for the original, complete system. The same error covariance equations can be applied to the simplified system, though reduction in state vector size will reduce the computer capability required for their solution. In a like manner, the same equations are used to find the Kalman Filter gain matrix. Unfortunately, the error covariance matrix found using the simplified forms of system, measurement, or random vector covariance matrices does not provide correct values for the estimation errors in the complete system. It is only correct when the true system is accurately described by the simplified equations. To analyze the effect of using the simplified filter, a sensitivity analysis must be conducted. A discussion of sensitivity analyses is provided on p. 114. These computations generate the error covariance matrix for the complete state vector estimate when the filter incorporates the simplified gain matrix and the simplified descriptions of state dynamics and the measurement process. The errors described can be compared to those calculated for the complete Kalman Filter, and trade-offs are determined.

As an example of simplifying state dynamics, consider the use of stellar measurements to correct inertial navigation system errors. Star sightings usually measure the error angles between computed and platform axes, described by the vector $\bar{\psi}$. The differential equation for $\bar{\psi}$ is given in Appendix C as

$$\dot{\bar{\psi}} = \bar{\psi} \times \bar{\omega} + \bar{\varepsilon} \qquad (149)$$

If stellar measurements are taken frequently and $\bar{\psi}$ is therefore kept small, the predominant effect in the differential equation is the drift rate vector, $\bar{\varepsilon}$. The entire system state vector differential equation can then be approximated by the 3-element form

$$\dot{\bar{\psi}} = \bar{\varepsilon} \tag{150}$$

Augmentation is made to account for the correlation properties of the gyro errors, but the resulting state contains 4 elements less than that using the system state description provided in Eq. 82. In reducing the state vector size, it was observed that certain elements were being measured directly, and the usual state vector formulation was changed (from $\bar{\phi}$ to $\bar{\psi}$) to accommodate that fact. In addition, certain terms ($\bar{\psi} \times \bar{\omega}$) were dropped because they were expected to have little effect on the state vector differential equation. The consequence of these changes is a reduced state vector and simpler state differential equations, both of which provide smaller computer requirements. Reference 37 presents results of computer simulations indicating that the simplified filter gives good accuracy despite these approximations.

As a practical matter it is often wise to increase the magnitude of the disturbance covariance matrix, Q, when system model simplifications are made. Frequently, fictitious system disturbances are assumed where none exist. These adjustments account for the errors in state extrapolation caused by approximations in the model. The effect is to make the filter gains higher, thereby making the filter more dependent on measurements and less dependent on inaccurate state vector extrapolation.

Simplifications of the system model, the measurement model, or the error correlation properties can be made in many cases. Based on the knowledge that certain effects or terms are relatively minor, they are made with the intent of reducing computer requirements for the filter or for filter-gain matrix calculations. Eventually, a sensitivity analysis as outlined in "Effects of Imperfect Models" (p. 115) is necessary to establish the accuracy trade-offs involved.

Precomputed Gains

A great deal of the Kalman Filter computer burden can be relieved if the error covariance equations can be solved beforehand and the filter gain matrix computed and stored for use during subsequent filter operation. As mentioned earlier, this is only possible when the measurement schedule and system dynamics are known in advance. If no new information about system and measurement behavior (including the statistics of disturbances and measurement errors) arises during filter operation, a Kalman Filter employing correct precomputed gains remains optimum. When

the Kalman Filter is applied to inertial navigation systems, vehicle course and speed during filtering must be assumed to permit precomputed gains. If any deviation from this trajectory can occur, a sensitivity analysis will reveal what changes will take place in the estimation error statistics.

When precomputed filter gains are used, further simplification can be made by modifying their time behavior. Often, only the steady-state filter gains (when they exist, see p. 17) are used. This is equivalent to using the Wiener filter. It permits the storage of a number of constant quantities equal to the product of state vector dimension with measurement vector size. Less drastic simplifications of the filter gain time behavior are often produced by approximating the behavior of gain matrix elements by analytic or discontinuous functions of time. Figure 42 illustrates the use of a declining exponential or a two level constant to replace a gain element with similar behavior. In both cases the computer memory requirement is reduced to storing a small number of constants and the gain element is easily computed when it is required.

If the system behavior is dependent on quantities other than time, filter gains can be precomputed for a range of these variables and an interpolation scheme applied after they are determined. In navigation systems the gain elements may depend on vehicle course and speed. More generally, the gains in the extended Kalman Filter may depend on the state variables themselves. An illustration of this case arises in using the Kalman Filter to estimate position and velocity of an unknown ballistic reentry vehicle. Nonlinear state equations result. Furthermore, the filter equations must be solved quickly and precomputed gains are very desirable. However, certain gain matrix elements can be specified by interpolation on the basis of estimated altitude (Ref. 32). Other precomputed gain elements were insensitive to all known physical parameters and their time-varying characteristics were approximated. A sensitivity analysis revealed little deterioration in accuracy resulted from the filter gain approximations. Figure 43 compares results for the optimum and suboptimum filters. Of course these are single simulation runs made with identical random disturbances and measurement noise. Similarity of ensemble error statistics was established by sensitivity analysis and Monte Carlo techniques.

When approximations to the optimal filter are produced by modifying the filter-gain matrix behavior only, analysis of the effect on error covariances is easily performed. For the discrete filter, Eq. 22 can be used to compute the error covariance matrix with any filter-gain matrix. A similar expression for the continuous filter is given by

$$\dot{P} = (F - KH)\,P + P(F - KH)^T + KRK^T + GQG^T \qquad (151)$$

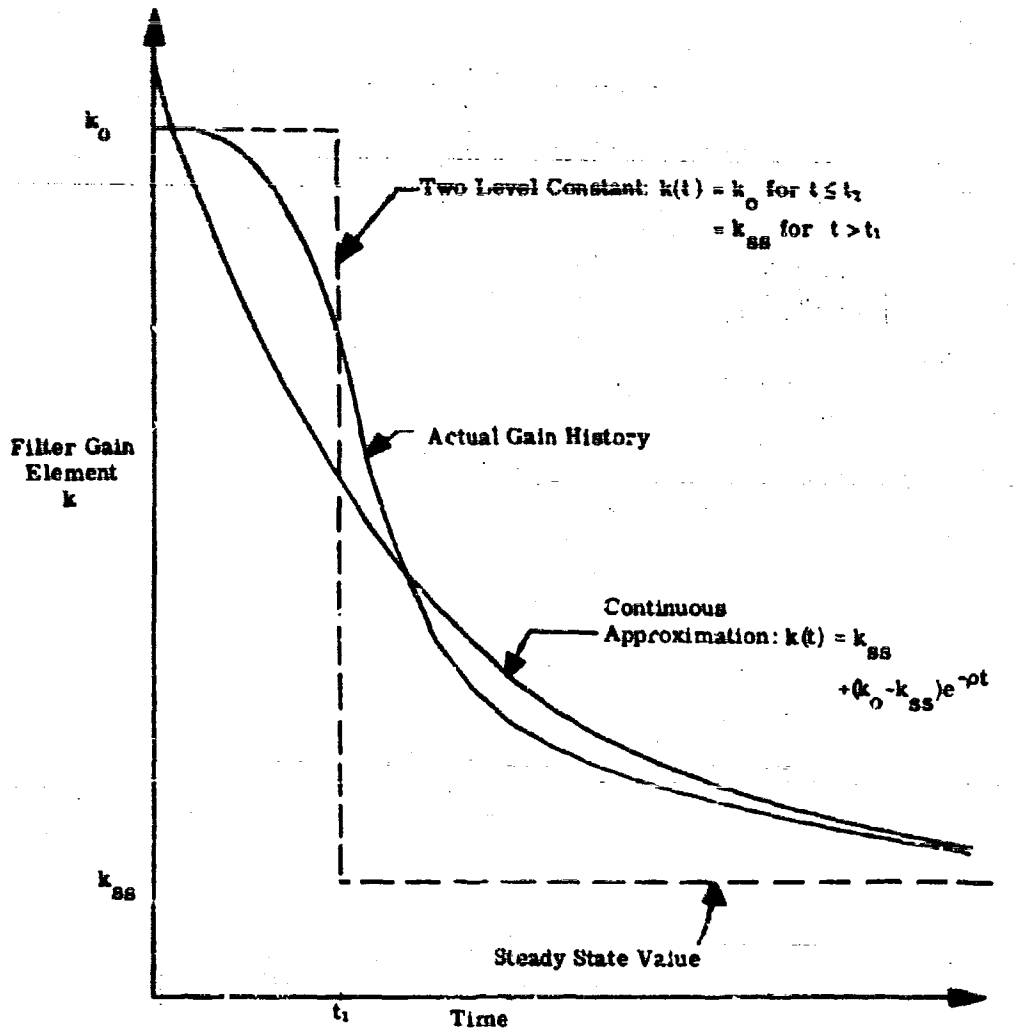

FIG. 42. Approximation of Kalman Filter Gain Element Time Behavior.

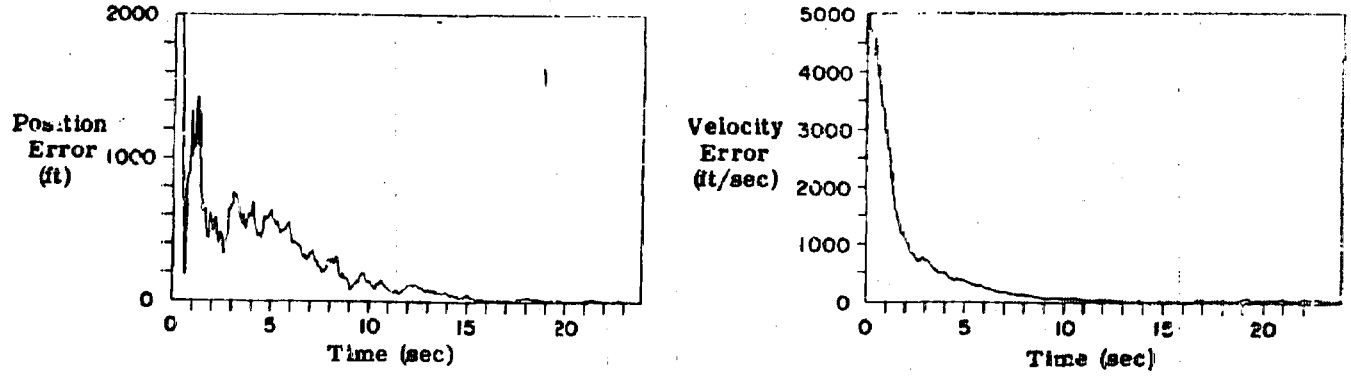

(a) Fully Implemented Extended Kalman Filter

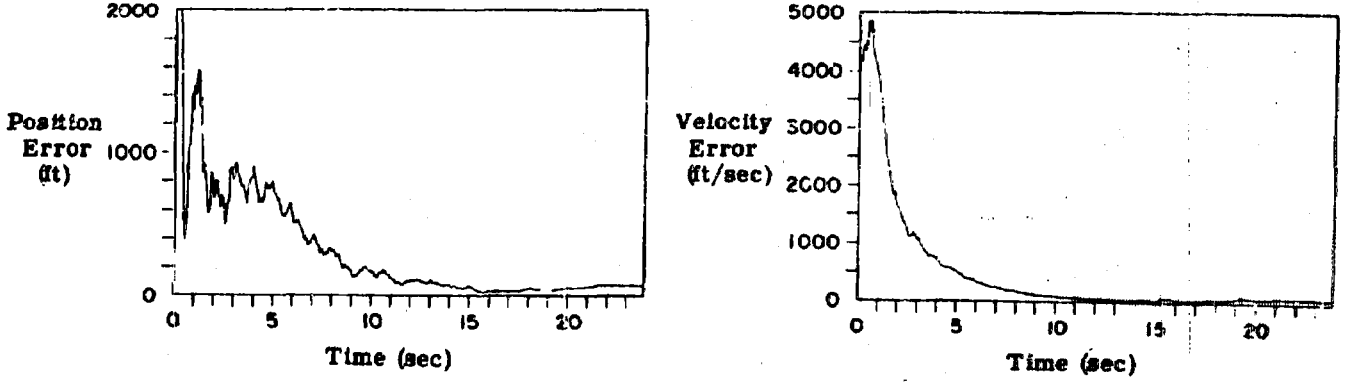

(b) Precomputed Gain Matrix

FIG. 43. Comparison of Errors In a Kalman Filter and an Associated Suboptimum Filter (Ref. 38).

By substituting the modified gains in one of these equations, filter accuracies can be obtained for comparison with those resulting when the optimum filter is used. If the system state dynamics and measurement process are also changed, a more elaborate scheme is required to determine the estimation errors. This is outlined in subsequent sections. As with all other attempts to simplify the filter, modified descriptions of filter gain are usually based on insight into the problem at hand.

Decoupling Equations

Many classical analyses of inertial navigation systems were simplified by separating portions of the problem. Small cross-coupling terms in the differential equations were ignored and one large set of equations was reduced to two or more smaller sets. A similar approach can be taken in order to simplify the Kalman Filter equations. Though the decoupling of system dynamics is usually based on good physical intuition, detailed mathematical approaches do exist (see Ref. 39).

Referring to the system described in Section 5, the terms in the matrix F_x of Eq. 84 involving vehicle accelerations or coordinate frame angular rates are typically much smaller than the others. They are the cross-coupling terms relating the two level loops and the azimuth drive of a north-vertical inertial system. If these quantities are ignored, F_x becomes

$$F_x = \begin{bmatrix} 0 & 0 & 1 & 0 & 0 & 0 & 0 \\ 0 & 0 & 0 & 1 & 0 & 0 & 0 \\ 0 & 0 & 0 & 0 & 0 & g & 0 \\ 0 & 0 & 0 & 0 & -g & 0 & 0 \\ 0 & 0 & 0 & \frac{1}{R} & 0 & 0 & 0 \\ 0 & 0 & -\frac{1}{R} & 0 & 0 & 0 & 0 \\ 0 & 0 & 0 & 0 & 0 & 0 & 0 \end{bmatrix} \qquad (152)$$

Now, by rearranging rows and columns of F_x (rearranging the order in which the state variables appear in $\underline{x}$),

$$F_x = \left[\begin{array}{ccc|ccc|c} 0 & 1 & 0 & 0 & 0 & 0 & 0 \\ 0 & 0 & g & 0 & 0 & 0 & 0 \\ 0 & -\frac{1}{R} & 0 & 0 & 0 & 0 & 0 \\ \hline 0 & 0 & 0 & 0 & 1 & 0 & 0 \\ 0 & 0 & 0 & 0 & 0 & -g & 0 \\ 0 & 0 & 0 & 0 & \frac{1}{R} & 0 & 0 \\ \hline 0 & 0 & 0 & 0 & 0 & 0 & 0 \end{array}\right] \tag{153}$$

for the state vector defined by:

$$\underline{x}^T = \left[\delta R_x \; \dot{\delta R}_x \; \varphi_y \; \delta R_y \; \dot{\delta R}_y \; \varphi_x \; \varphi_z\right] \tag{154}$$

The partitioning lines in the system matrix serve to illustrate the fact that F_x is composed from zeros except for the submatrices along the diagonal. The state vector-matrix equation can be decomposed into three independent sets of differential equations. A considerable reduction in computer time and memory requirements results. The added consideration of correlated sensor errors does not alter the situation. When gyro and accelerometer errors are constant, the three state equations are

$$\left[\begin{array}{c} \dot{\delta R}_x \\ \ddot{\delta R}_x \\ \dot{\varphi}_y \\ \dot{\nabla}_x \\ \dot{\epsilon}_y \end{array}\right] = \left[\begin{array}{ccc|cc} 0 & 1 & 0 & 0 & 0 \\ 0 & 0 & g & 1 & 0 \\ 0 & -\frac{1}{R} & 0 & 0 & 1 \\ \hline 0 & 0 & 0 & 0 & 0 \\ 0 & 0 & 0 & 0 & 0 \end{array}\right] \left[\begin{array}{c} \delta R_x \\ \dot{\delta R}_x \\ \varphi_y \\ \nabla_x \\ \epsilon_y \end{array}\right] \tag{155}$$

$$\begin{bmatrix} \dot{\delta R}_y \\ \ddot{\delta R}_y \\ \dot{\varphi}_x \\ \dot{\nabla}_y \\ \dot{\epsilon}_x \end{bmatrix} = \left[\begin{array}{ccc|cc} 0 & 1 & 0 & 0 & 0 \\ 0 & 0 & -g & 1 & 0 \\ 0 & \frac{1}{R} & 0 & 0 & 1 \\ \hline 0 & 0 & 0 & 0 & 0 \\ 0 & 0 & 0 & 0 & 0 \end{array}\right] \begin{bmatrix} \delta R_y \\ \dot{\delta R}_y \\ \varphi_x \\ \nabla_y \\ \epsilon_x \end{bmatrix} \tag{156}$$

and

$$\begin{bmatrix} \dot{\varphi}_z \\ \dot{\epsilon}_z \end{bmatrix} = \begin{bmatrix} 0 & 1 \\ 0 & 0 \end{bmatrix} \begin{bmatrix} \varphi_z \\ \epsilon_z \end{bmatrix} \tag{157}$$

No measurement equation is available for the state given by Eq. 157. It is unobservable. The error covariance equation for this state vector is given by Eq. 14 or 21. A marine inertial navigation system is treated in Ref. 39. By eliminating cross-coupling terms, the state is reduced from one vector of 16 elements to four vectors with 4 elements each. Analysis of the relative accuracy for this scheme compared to the full Kalman Filter indicates that estimation errors do not increase significantly as a result of the approximations involved in decoupling.

SENSITIVITY ANALYSES

The error covariance matrix computed for the Kalman Filter by Eq. 21 and 25 or Eq. 29 is based on the assumption that the description of system dynamics and the measurement process is exactly correct. In addition, the random disturbances and measurement errors are assumed to be correctly described by the covariance matrices provided. Because some uncertainty about the true system behavior or measurements may exist or because the random vector covariance matrices are usually calculated from incomplete empirical data, a technique for checking the effect of incorrect descriptions is desirable. Once established, the same relations can also be used to investigate the relative accuracy of suboptimal filtering schemes. This section provides a brief discussion of the steps necessary to perform sensitivity analyses and to check suboptimal filter formulations.

The Effects of Erroneous Statistics

Imperfect specification of the statistics for random disturbances and measurement errors is not uncommon. These quantities, as they appear in the R and Q matrices are usually computed from incomplete data. For example, gyro drift rate data may be available from tests performed on a limited number of similar gyros. Also, these tests may have been of an undesirably short duration and the laboratory environment probably differs significantly from that of the inertial navigator. Obviously, the statistical behavior of the drift rate for this particular model gyro is not thoroughly established by these tests. Broad confidence limits exist for the statistical drift rate descriptions. However, the Kalman Filter formulation requires that, for the error covariance analysis to be accurate, the exact statistical behavior of random quantities be described in the R or Q matrices and in the initial error covariance, $P(t_0)$. In order to determine the effect incorrect error statistics will have on the filter estimation errors, a range of values for these matrices may be investigated. The sensitivity curve that can result is illustrated in Fig. 44.

When an incorrect description of error statistics is used to find the filter gain matrix, the true error covariance matrix which results can be determined using Eq. 22 for the discrete filter. The filter gain matrix is computed in the usual manner, based on the best guess of error statistics. To check the effect of an incorrect choice, a different value of Q, R, or $P(t_0)$ is substituted in Eq. 21 and 22 with the same values for K. A new history of estimation errors results. Comparison with the original error covariances indicates the sensitivity of the Kalman Filter to incorrect statistics. A similar procedure can be carried out for the continuous filter using Eq. 151. (See also Ref. 40.)

The Effects of Imperfect Models

A more complex analysis is required to determine the sensitivity of a Kalman filter to changes or errors in the system equations or the measurement process. Consider the problem of analyzing simplifications in the filter. The designer knows the true state and its behavior--this represents his best understanding of the system operation. A good description of the measurement is also available. The true state difference equation for the discrete formulation is written

$$\underline{x}_{n+1} = \Phi_n \underline{x}_n + \underline{w}_n \qquad (158)$$

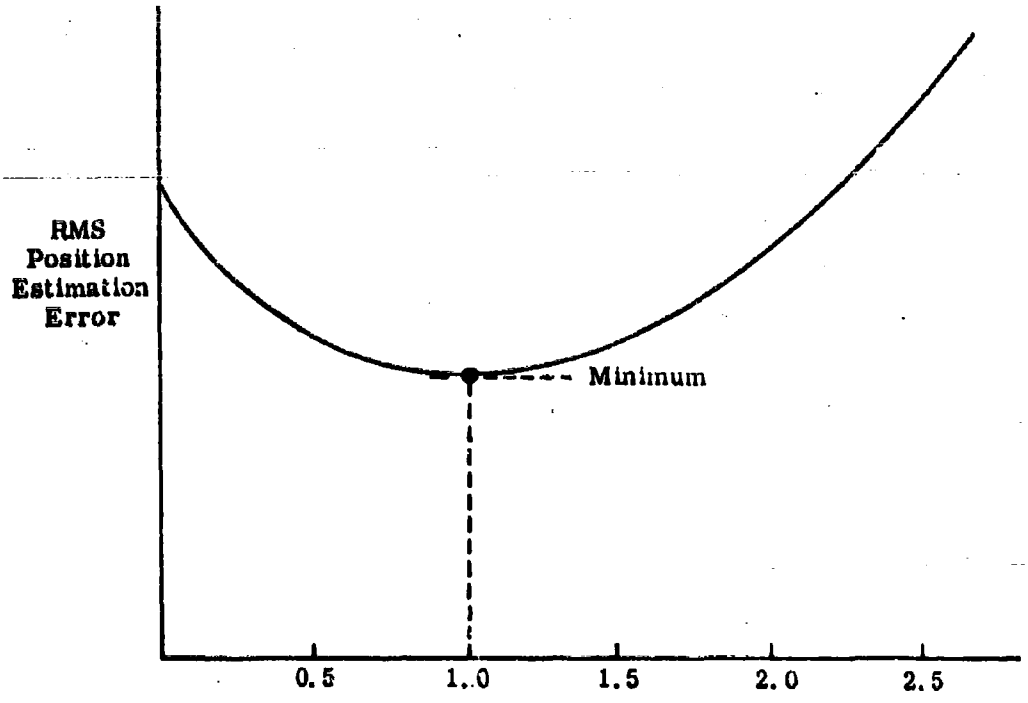

FIG. 44. Sensitivity of RMS Position Error to Error in Estimated Gyro Drift Rate.

But, for simplicity, the filter operates with a different set of transition and measurement matrices described by Φ_n^* and H_n^*. The estimate of the state immediately after each measurement, $\underline{\hat{x}}_n^*$, obeys

$$\underline{\hat{x}}_{n+1}^* = \Phi_n^* \, \underline{\hat{x}}_n^* + K_n^* \left[\underline{z}_n - H_n^* \, \Phi_n^* \, \underline{\hat{x}}_n^* \right] \tag{159}$$

which is similar to Eq. 20. It should be noted that frequently, as a result of simplifying the state vector, $\underline{\hat{x}}_n^*$ may not contain as many elements as the true state, $\underline{x}$. Consequently, the error of interest must be expressed as

$$\underline{\tilde{x}} = \underline{x} - W \, \underline{\hat{x}}^* \tag{160}$$

where the matrix W accounts for the difference in state vector dimension and for any linear transformation that may be used in defining the simplified state. As before, the quantity of interest is the error covariance

$$\begin{aligned} P &= \text{cov}\,(\tilde{\underline{x}}, \tilde{\underline{x}}) \\ &= E\,(\tilde{\underline{x}}, \tilde{\underline{x}})^T \\ &= \text{cov}\,(\underline{x}, \underline{x}) - [\text{cov}\,(\underline{x}, \hat{\underline{x}}^*)]\, W^T \\ &\quad - W\,\text{cov}\,(\hat{\underline{x}}^*, \underline{x}) + W[\text{cov}\,(\hat{\underline{x}}^*, \hat{\underline{x}}^*)]\, W^T \end{aligned} \tag{161}$$

The covariances required to solve for the estimation error covariance matrix using Eq. 161 can be calculated by defining a new vector, $\underline{r}$,

$$\underline{r} \triangleq \begin{bmatrix} \underline{x} \\ \hline \hat{\underline{x}}^* \end{bmatrix} \tag{162}$$

Remembering that

$$\underline{z}_n = H_n\, \underline{x}_n + \underline{v}_n \tag{163}$$

a difference equation for $\underline{r}$ is found using Eq. 156 and 159

$$\left[\begin{array}{c} \underline{x}_{n+1} \\ \hline \hat{\underline{x}}^*_{n+1} \end{array}\right] = \left[\begin{array}{c|c} \Phi_n & 0 \\ \hline K^*_n H_n & (I - K^*_n H^*_n)\, \Phi^*_n \end{array}\right] \left[\begin{array}{c} \underline{x}_n \\ \hline \hat{\underline{x}}^*_n \end{array}\right] + \left[\begin{array}{c} \underline{w}_n \\ \hline K^*_n \underline{v}_n \end{array}\right] \tag{164}$$

In Eq. 164, starred matrices refer to those used in the simplified model of the Kalman Filter. The new state variable difference equation is in the form of Eq. 8. Given initial conditions for the covariance of $\underline{r}$, that matrix can be calculated for all future measurement times using Eq. 12. The covariance of $\underline{r}$ can be expressed by

$$\text{cov}(\underline{r}, \underline{r}) = \left[\begin{array}{c|c} \text{cov}(\underline{x}, \underline{x}) & \text{cov}(\underline{x}, \hat{\underline{x}}^*) \\ \hline \text{cov}(\hat{\underline{x}}^*, \underline{x}) & \text{cov}(\hat{\underline{x}}^*, \hat{\underline{x}}^*) \end{array}\right] \tag{165}$$

The quantities needed to solve Eq. 161 are contained as submatrices of the covariance for the new vector, as shown in Eq. 165. Notice that, unless the true state and the simplified state have the same dimension,

$$\text{cov}(\hat{\underline{x}}^*, \underline{x}) \text{ and } \text{cov}(\underline{x}, \hat{\underline{x}}^*)$$

are not square. Several computer programs solving matrix difference equations of the form given by Eq. 12 are in widespread use.

More efficient calculation of the matrices on the right side of Eq. 161 result from the observation that

$$\text{cov}(\hat{\underline{x}}^*, \underline{x}) = [\text{cov}(\underline{x}, \hat{\underline{x}}^*)]^T \tag{166}$$

Defining

$$\begin{aligned} P_1 &\triangleq \text{cov}(\underline{x}, \underline{x}) \\ P_2 &\triangleq \text{cov}(\hat{\underline{x}}^*, \hat{\underline{x}}^*) \\ P_3 &\triangleq \text{cov}(\underline{x}, \hat{\underline{x}}^*) \end{aligned} \tag{167}$$

smaller matrix difference equations can be written for P_1, P_2, and P_3:

$$\begin{aligned} P_{1_{n+1}} &= \Phi_n P_{1_n} \Phi_n^T + Q_n \\ P_{2_{n+1}} &= K_n^* H_n P_{1_n} H_n^T K_n^{*T} + K_n^* H_n P_{3_n} \Phi_n^{*T} (I - K_n^* H_n^*)^T \\ &\quad + (I - K_n^* H_n^*) \Phi_n^* P_{3_n}^T H_n^T K_n^{*T} + (I - K_n^* H_n^*) \Phi_n^* P_{2_n} \Phi_n^{*T} (I - K_n^* H_n^*)^T \\ P_{3_{n+1}} &= \Phi_n P_{1_n} H_n^T K_n^{*T} + \Phi_n P_{3_n} \Phi_n^{*T} (I - K_n^* H_n^*)^T \end{aligned} \tag{168}$$

Once the error covariance has been computed using Eq. 161, it can be compared to that resulting from the true system as calculated by Eq. 21 and 25. Of course, a similar procedure is available for the continuous case.

When the sensitivity of a Kalman Filter design to correct specification of the true system is to be investigated, the same procedure is followed. However, the Φ^* and H^* matrices are now those used in designing the filter and K^* is the resulting filter-gain matrix. The altered Φ and H matrices are substituted for the unstarred quantities in the above equations.

All of the calculations in this section are carried out off-line, before actual use of the filter. They provide a complete approach for analyzing the sensitivity of the Kalman Filter to erroneous specification of system and measurement behavior or to incorrect statistics for random quantities.

Appendix A
COVARIANCE MATRICES

The covariance matrix for two random vector processes is defined in terms of the ensemble average values of the vectors and the ensemble average value of their outer product. The covariance matrix for $\underline{a}(t)$ and $\underline{b}(t)$ is given by (E denotes ensemble expectation)

$$\text{cov}[\underline{a}(t), \underline{b}(t)] = E\,[\underline{a}(t)\,\underline{b}^T(t)] - E\,[\underline{a}(t)]\,E\,[\underline{b}^T(t)] \qquad (169)$$

Since only zero mean quantities are dealt with in Kalman Filter work, the simplification

$$\text{cov}[\underline{a}(t), \underline{b}(t)] = E\,[\underline{a}(t)\,\underline{b}^T(t)] \qquad (170)$$

can be made. The covariance of the errors in the Kalman Filter estimate of the state $\underline{x}$ is described by the matrix P

$$P(t) = \text{cov}[\tilde{\underline{x}}(t), \tilde{\underline{x}}(t)] \qquad (171)$$

The covariance matrix for system disturbances is given by

$$Q_n = \text{cov}(\underline{w}_n, \underline{w}_n)$$

in the discrete filter, and

$$Q = \text{cov}(\underline{u}, \underline{u}) \qquad (172)$$

in the continuous filter. For measurement noises, the covariance is the same in both cases:

$$R = \text{cov}(\underline{v}, \underline{v}) \qquad (173)$$

The requirement that the measurement noise and system disturbances be uncorrelated in time gives the restrictions

$$\begin{aligned} \text{cov}[\underline{u}(t), \underline{u}(\tau)] &= Q(t)\ \delta(t-\tau) \\ \text{cov}[\underline{v}(t), \underline{v}(\tau)] &= R(t)\ \delta(t-\tau) \end{aligned} \tag{174}$$

in the continuous estimation case. The operator δ is the Dirac delta function. When the discrete version of the Kalman Filter is used, the corresponding requirement is that disturbances and noises must be essentially uncorrelated over the smallest measurement interval.

$$\begin{aligned} \text{cov}(\underline{w}_m, \underline{w}_n) &= 0 \qquad \text{for } m \neq n \\ &= Q_n \qquad \text{for } m = n \\ \text{cov}(\underline{v}_m, \underline{v}_n) &= 0 \qquad \text{for } m \neq n \\ &= R_n \qquad \text{for } m = n \end{aligned} \tag{175}$$

Though it seldom arises, the case when measurement noises and system disturbances are cross-correlated can be treated (Ref. 7).

NOISE AND DISTURBANCE COVARIANCES FOR THE CONTINUOUS FILTER

In the discrete version, the diagonal elements of R_n and Q_n are readily identified as the mean square values of particular elements from the random noise and disturbance vectors. Computing the elements of Q(t) and R(t) matrices used in Eq. 29 for the continuous filter in the same manner would be incorrect. Inspection of Eq. 29 reveals that these covariance matrices have the units of Q_n and R_n, respectively, multiplied by the unit of time. The necessity for this can be observed from Eq. 174 because the Dirac delta function carries with it units of time. A different explanation follows from the fact that truly uncorrelated signals do not exist in nature. This presents no problem in the discrete case because disturbances and measurement errors whose correlation time is insignificant compared to the smallest observation interval can always be defined. However, when the interval is caused to vanish, what are considered as uncorrelated random signals are

frequently quantities whose autocorrelation periods are much shorter than the characteristic times of the system and the measurements. Reference 10 shows that, under these circumstances, the derivative of the error covariance matrix for a continuous process excited by a random disturbance depends on the time integral of the correlation

$$E\,[\underline{u}(t)\,\underline{u}^T(\tau)]$$

Assuming that u(t) is exponentially correlated with correlation period $1/\beta$, the driving term becomes

$$Q(t) \cong \frac{2}{\beta} E\,[\underline{u}(t)\,\underline{u}^T(t)] \tag{176}$$

If one element of $\underline{u}$ has a mean squared value of σ^2 and a flat, one-sided power spectral density, S_{uu}, out to a bandwidth β, the power spectral density is related to σ^2 and β by:

$$S_{uu} = \frac{\sigma^2}{\beta} \tag{177}$$

and the corresponding diagonal element of the Q matrix is given by

$$q = 2S_{uu}^{*} \tag{178}$$

THE COVARIANCE MATRIX DIFFERENTIAL EQUATION

Given the state vector differential equation,

$$\dot{\underline{x}}(t) = F(t)\,\underline{x}(t) + G(t)\,\underline{u}(t) \tag{179}$$

*Combining Eq. 177 and 178, we get $q = 2\sigma^2/\beta$. This result differs from that in the footnote on p. 50 because here we desire to approximate a correlated random variable by an equivalent uncorrelated signal. In Section 4 we found the strength of an uncorrelated signal which produces a certain size output when passed through a first-order linear filter.

we wish to study the dynamics of the error covariance matrix P(t), defined as

$$P(t) = E\,[\tilde{\underline{x}}(t)\,\tilde{\underline{x}}^T(t)] \tag{180}$$

Consider the function P(t, t-ε), where ε is a small position number.

$$P(t,t-\varepsilon) = E\,[\tilde{\underline{x}}(t)\,\tilde{\underline{x}}^T(t-\varepsilon)] \tag{181}$$

Differentiation with respect to time yields

$$\begin{aligned}\dot{P}(t,t-\epsilon) &= E[\dot{\tilde{\underline{x}}}(t)\,\tilde{\underline{x}}^T(t-\epsilon) + \tilde{\underline{x}}(t)\,\dot{\tilde{\underline{x}}}^T(t-\epsilon)] \\ &= F(t)E[\tilde{\underline{x}}(t)\,\tilde{\underline{x}}^T(t-\epsilon)] + G(t)E[\underline{u}(t)\,\tilde{\underline{x}}^T(t-\epsilon)] \\ &\quad + E[\tilde{\underline{x}}(t)\,\tilde{\underline{x}}^T(t-\epsilon)]\,F^T(t-\epsilon) + E[\tilde{\underline{x}}(t)\,\underline{u}^T(t-\epsilon)]\,G^T(t-\epsilon)\end{aligned} \tag{182}$$

The second term on the right-hand side of Eq. 182 must be zero, as there can be no correlation between the state of the system at a given time and a driving noise which exists in the future. To evaluate the last term in this equation, we use the solution to Eq. 179 given by Eq. 7 when t_n is zero.

$$\tilde{\underline{x}}(t) = \Phi(t,0)\,\tilde{\underline{x}}(0) + \int_0^t \Phi(t,\tau)G(\tau)\underline{u}(\tau)\,d\tau \tag{183}$$

Postmultiplying Eq. 183 by $\underline{u}^T(t-\varepsilon)$ and taking the ensemble average of both sides results in

$$\begin{aligned}E\,[\tilde{\underline{x}}(t)\,\underline{u}^T(t-\epsilon)] &= \Phi(t,0)\,E[\tilde{\underline{x}}(0)\,\underline{u}^T(t-\epsilon)] \\ &\quad + \int_0^t \Phi(t,\tau)\,G(\tau)\,E[\underline{u}(\tau)\,\underline{u}^T(t-\epsilon)]\,d\tau \\ &= \Phi(t,t-\epsilon)\,G(t-\epsilon)\,Q(t-\epsilon)\end{aligned} \tag{184}$$

The first term goes to zero for reasons already described, and the second (integral) term is readily evaluated due to the delta function in the integrand.

Substituting Eq. 184 into Eq. 182 and using the fact that $\Phi(t,t) = I$, the limit as $\varepsilon \to 0$ yields

$$\dot{P}(t) = F(t)\, P(t) + P(t)\, F^T(t) + G(t)\, Q(t)\, G^T(t) \qquad (185)$$

Appendix B

A KALMAN FILTER DERIVATION

It is possible to derive the Kalman Filter by optimizing an assumed form of linear estimator. Based on the desire to avoid a growing memory filter, a recursive estimator is sought in the form (see Section 2):

$$\underline{\hat{x}}_n(+) = \underline{\hat{x}}_n(-) + K_n\left|\underline{z}_n - H_n\,\underline{\hat{x}}_n(-)\right| \tag{186}$$

where $\underline{\hat{x}}_n(-)$ and $\underline{\hat{x}}_n(+)$ are the estimates of state vector $\underline{x}_n$ immediately before and immediately after the measurement $\underline{z}_n$, at time t_n. That is, the state estimate is corrected at the time of each measurement according to a weighted difference between the actual and anticipated measurement vectors. The optimum weighting matrix K_n is to be specified.

An equation for the estimation error after incorporation of the nth measurement, denoted $\underline{\tilde{x}}_n(+)$, can be obtained from Eq. 186 through substitution of the measurement equation

$$\underline{z}_n = H_n\,\underline{x}_n + \underline{v}_n \tag{187}$$

and the relations

$$\begin{aligned}\underline{\hat{x}}_n(+) &= \underline{x}_n + \underline{\tilde{x}}_n(+)\\ \underline{\hat{x}}_n(-) &= \underline{x}_n + \underline{\tilde{x}}_n(-)\end{aligned} \tag{188}$$

The result is

$$\underline{\tilde{x}}_n(+) = \left(I - K_n\,H_n\right)\underline{\tilde{x}}_n(-) + K_n\,\underline{v}_n \tag{189}$$

Using Eq. 189, the expression for the change in the error covariance matrix when a measurement is employed (Eq. 22) can be derived. From the definition

$$P_n(+) = \mathrm{cov}\left[\tilde{x}_n(+), \tilde{x}_n(+)\right] = E\left[\tilde{x}_n(+)\,\tilde{x}_n^T(+)\right]$$

Eq. 189 gives

$$P_n(+) = E\left\{\begin{matrix}(I - K_n H_n)\,\tilde{x}_n(-)\,\tilde{x}_n^T(-)\,(I - K_n H_n)^T + v_n^T K_n^T) \\ + K_n v_n\,\tilde{x}_n^T(-)\,(I - K_n H_n)^T + v_n^T K_n^T)\end{matrix}\right\}$$

However

$$E\left[\tilde{x}_n(-)\,\tilde{x}_n^T(-)\right] = P_n(-)$$

$$E\left[v_n v_n^T\right] = R_n$$

and, as a result of uncorrelated measurement errors,

$$E\,\tilde{x}_n(-)\,v_n^T = E\,v_n\,\tilde{x}_n^T(-) = 0$$

Thus

$$P_n(+) = (I - K_n H_n)\,P_n(-)\,(I - K_n H_n)^T + K_n R_n K_n^T \qquad (190)$$

It is desired to choose K_n to minimize the sum of the diagonal elements (trace) of the error covariance matrix $P_n(+)$.

$$\text{trace}\,[P_n(+)] = E\left[\sum_i \tilde{x}_{i_n}(+))^2\right] = E\left[\tilde{x}_n^T(+)\,\tilde{x}_n(+)\right] \qquad (191)$$

This is equivalent to minimizing the length of the estimation error vector. To find the value of K_n which provides the minimum, it is necessary to take the partial derivative of the trace of $P_n(+)$ with respect to K_n and equate it to zero. Use is made of the relation for the partial derivative for the trace of the product of two matrices A and B

$$\frac{\partial}{\partial A}\left[\text{trace}\,(ABA^T)\right] = 2AB$$

if B is symmetric. From Eq. 190, the result is

$$-2\left(1 - K_n H_n\right) P_n(-) H_n^T + 2K_n R_n = 0 \qquad (192)$$

Solving for K_n,

$$K_n = P_n(-) H_n^T \left[H_n P_n(-) H_n^T + R_n\right]^{-1} \qquad (193)$$

which is the Kalman Filter gain matrix as expressed in Eq. 24. Substitution of Eq. 193 into Eq. 190 gives

$$P_n(+) = P_n(-) - P_n(-) H_n^T \left[H_n P_n(-) H_n^T + R_n\right]^{-1} H_n P_n(-) \qquad (194)$$

which is Eq. 25 in the text.

A Simpler Form for K_n: There is a matrix inversion relationship which states that, for P_n as given in Eq. 194, P_n^{-1} is expressible as (Ref. 10)

$$P_n^{-1}(+) = P_n^{-1}(-) + H_n^T R_n^{-1} H_n \qquad (195)$$

We use this result to manipulate K_n as follows

$$\begin{aligned} K_n &= P_n(-) H_n^T \left[H_n P_n(-) H_n^T + R_n\right]^{-1} \\ &= P_n(+) P_n^{-1}(+) P_n(-) H_n^T \left[H_n P_n(-) H_n^T + R_n\right]^{-1} \\ &= P_n(+)\left[P_n^{-1}(-) + H_n^T R_n^{-1} H_n\right] P_n(-) H_n^T \left[H_n P_n(-) H_n^T + R_n\right]^{-1} \end{aligned}$$

Expanding and collecting terms yields:

$$
\begin{aligned}
K_n &= P_n(+)\, H_n^T \left[I + R_n^{-1} H_n P_n(-) H_n^T \right] \left[H_n P_n(-) H_n^T + R_n \right]^{-1} \\
&= P_n(+)\, H_n^T R_n^{-1} \left[R_n + H_n P_n(-) H_n^T \right] \left[H_n P_n(-) H_n^T + R_n \right]^{-1} \qquad (196) \\
&= P_n(+)\, H_n^T R_n^{-1}
\end{aligned}
$$

which is the simpler form sought. The equations for the continuous Kalman Filter can be derived in a similar manner or will result from the above equations by taking the limit as the measurement interval vanishes. Although the derivation here was for an assumed recursive, single-stage filter, the result has been shown to be the solution for a much more general problem.

Appendix C

DERIVATION OF NAVIGATION SYSTEM ERROR DYNAMICS

Three nearly coincident orthogonal coordinate frames must be defined in order to study the propagation of errors in an inertial navigation system. The three axis systems are different only to the extent that errors exist in the navigator. The most familiar coordinate frame considered is the "ideal or true navigation frame." Its definition follows one of those presented under Inertial Navigation Systems (p. 34). The remaining two frames are described only by thier relative orientation with respect to the true navigation axes.

The "computer axes" are defined by the orientation the computer believes the navigation axes have. In the absence of initial condition errors, the computer for a gimballed north-vertical system will calculate latitude and longitude changes by twice integrating the properly scaled outputs of the north and east accelerometers. If the accelerometer outputs provide incorrect indications of the true north and east acceleration, the computer and true axis systems will no longer coincide. For small angle misalignments the relative orientation can be described by a vector. The vector $\underline{\delta\theta}$ represents the rotation necessary to bring the true axes into coincidence with the computer axes.

The third coordinate system of interest will be called the "platform axes." This description is proper when gimballed inertial systems are being considered. A more general definition--one which includes the possibility of strapdown systems--is that the platform axes describe the coordinate frame into which accelerometer outputs have been resolved when they leave the inertial measurement unit. The platform axes can differ from the computer axes because the inertial angular rate demanded of the platform by the computer is not accurately implemented (gyro drift rates) and because the commands are given in computer axes but executed in platform axes. The small angle rotation necessary to bring the computer axes into coincidence with the platform axes is represented by $\underline{\psi}$. A similar angle relating true axes to platform axes is written as $\underline{\phi}$ and expressed by

$$\overline{\phi} = \overline{\psi} + \overline{\delta\theta} \tag{197}$$

Several other important quantities can be defined:

$\overline{\omega}$ = inertial angular rate of true axes

$\overline{\omega_C}$ = inertial angular rate of computer axes

$\overline{\omega_P}$ = inertial angular rate of platform axes.

The vectors $\bar{\Omega}$, $\bar{V}$ and $\bar{\epsilon}$ are defined in previous sections of this report. However, the use of subscripts in this appendix will differ from the section on inertial navigation systems. Here the subscripts C and P are used to indicate relation to the computer axes and platform axes, respectively, while the absence of subscript indicates relation to the true axes. The subscript I is again used to designate inertially-fixed coordinates.

To begin, the expression relating the acceleration of a point relative to inertial space is written in terms of accelerations and velocities relative to the computer axes and the inertial angular rate, $\bar{\omega}_C$.

$$\left(\frac{d^2\bar{R}}{dt^2}\right)_I = \left(\frac{d^2\bar{R}}{dt^2}\right)_C + 2\bar{\omega}_C \times \left(\frac{d\bar{R}}{dt}\right)_C + \left(\frac{d}{dt}\ \bar{\omega}_C\right)_C \times \bar{R}$$

$$+ \bar{\omega}_C \times (\bar{\omega}_C \times \bar{R}) \qquad (198)$$

Equation 198 results from a theorem by Coriolis. It describes the ideal behavior of the computed value of $\bar{R}$ when a perfect indication of $(d^2\bar{R}/dt^2)_I$ is provided. The subscripts C and I indicate the coordinate frames in which the differentiation takes place or, in the case of the vector $\bar{\omega}_C$, designate the coordinate frame under consideration. The vector quantities in Eq. 198 can be resolved into any coordinate frame desired. The computer, in the absence of information about system errors, assumes that all three axis systems are parallel. It will solve the equation in C coordinates and the solution will be in error if specific force is not properly indicated and resolved. Improper indication results from accelerometer errors, and improper resolution results from misalignment between the computer and platform axis systems. The indicated specific force is related to the actual value in the computer coordinate frame by

$$\bar{f}_i = \bar{f} - \bar{\psi} \times \bar{f} + m\bar{V} \qquad (199)$$

In addition, in order to obtain $(d^2\bar{R}/dt^2)_I$, the mass attraction acceleration must be added to the accelerometer outputs according to Eq. 42. Because the near-earth navigation coordinate systems outlined previously all indicate local vertical, it will be more convenient to work in terms of the gravity vector, $\bar{g}$,

$$\bar{g} = \bar{G} - \bar{\Omega} \times (\bar{\Omega} \times \bar{R}) \qquad (200)$$

However, for the purpose of investigating the effects of small errors in the computed value of R on the navigation error propagation, $\overline{g}$ can be assumed parallel to R and obeying

$$\overline{g} \simeq -\omega_s^2 \, \overline{R} \tag{201}$$

where

$$\omega_s \simeq \sqrt{\frac{|\overline{g}|}{|\overline{R}|}} \tag{202}$$

When $|\overline{R}|$ is the radius of the earth, ω_s is the Schuler frequency. Then

$$\overline{\delta g} = -\omega_s^2 \, \overline{\delta R} - 2\omega_s \, (\delta\omega_s) \, \overline{R} \tag{203}$$

and the perturbations in the left side of Eq. 198 caused by misalignment between platform and computer axes and small errors in the computed value of $\overline{R}$ are, to the first order,

$$-\overline{\psi} \times \frac{\overline{f}}{m} + \overline{V} + \overline{\Omega} \times (\overline{\Omega} \times \overline{\delta R}) - \omega_s^2 \, \overline{\delta R} - 2\omega_s \, (\delta\omega_s) \, \overline{R}$$

Equating these to the first-order perturbations of the right side of Eq. 198 provides an expression for the propagation of navigation system errors

$$\left\{ \begin{array}{l} \left(\dfrac{d^2 \delta \overline{R}}{dt^2}\right)_C + 2\overline{\omega}_C \times \left(\dfrac{d\delta \overline{R}}{dt}\right)_C + \left(\dfrac{d}{dt}\,\overline{\omega}_C\right)_C \times \delta \overline{R} \\ + \overline{\omega}_C \times (\overline{\omega}_C \times \delta \overline{R}) - \overline{\Omega} \times (\overline{\Omega} \times \delta \overline{R}) + \omega_s^2 \, \delta \overline{R} \end{array} \right\} = \left\{ \begin{array}{l} -\overline{\psi} \times \dfrac{\overline{f}}{m} + \overline{\nabla} \\ -2\omega_s (\delta\omega_s) \, \overline{R} \end{array} \right\} \tag{204}$$

The notation of Eq. 204 can be simplified by noting that the first four terms on the left can be related through the theorem of Coriolis (Eq. 198) to similar products and derivatives as viewed from the true (unsubscripted) axes

$$\begin{Bmatrix} \ddot{\delta R} + 2\dot{\bar{\omega}} \times \dot{\delta R} + \dot{\bar{\omega}} \times \delta\bar{R} + \bar{\omega} \times (\bar{\omega} \times \delta\bar{R}) \\ -\bar{\Omega} \times (\bar{\Omega} \times \delta\bar{R}) + \omega_s^2 \delta\bar{R} \end{Bmatrix} = \begin{Bmatrix} -\dot{\bar{\psi}} \times \dfrac{\bar{f}}{m} + \bar{\nabla} \\ -2\omega_s (\delta\omega_s) R \end{Bmatrix} \tag{205}$$

Replacing the absolute value notations for $|\bar{\psi}|$ and $|\bar{g}|$ by R and g, the quantity $\delta\omega_s$ can be further refined by noting that, from its definition,

$$\omega_s = \sqrt{\frac{g}{R}} = \sqrt{\frac{g_0 R_0^2}{R^3}} \tag{206}$$

Then

$$\delta\omega_s = -\frac{3}{2} |\delta\bar{R}| \sqrt{\frac{g_0 R_0^2}{R^5}}$$

$$-\frac{3}{2} \frac{|\delta\bar{R}|}{R} \omega_s \tag{207}$$

Equation 205 becomes

$$\begin{Bmatrix} \ddot{\delta R} + 2\dot{\bar{\omega}} \times \dot{\delta R} + \dot{\bar{\omega}} \times \delta R + \bar{\omega} \times (\bar{\omega} \times \delta\bar{R}) \\ -\bar{\Omega} \times (\bar{\Omega} \times \delta\bar{R}) + \omega_s^2 \left(\delta\bar{R} - 3 |\delta\bar{R}| \frac{\bar{R}}{R}\right) \end{Bmatrix} = -\bar{\psi} \times \frac{\bar{f}}{m} + \bar{\nabla} \tag{208}$$

Equation 208 can be used to demonstrate the fact that, if the navigation equations are solved along a coordinate axis which is not orthogonal to $\bar{R}$, the navigation error along this axis is described by an unstable differential equation. Of course, not all navigation system axes can be orthogonal to $\bar{R}$ and, in fact, near-earth navigation coordinate systems usually have one axis parallel to the position vector. Many of the terms in Eq. 208 which are dependent on ω and Ω can be neglected when considering vehicles traveling near the earth's surface at reasonable speeds. Rearranging and simplifying, Eq. 208 can be written

$$\ddot{\delta R} + \omega_s^2 \left(\delta\bar{R} - 3 |\delta\bar{R}| \frac{\bar{R}}{R}\right) = -\dot{\bar{\psi}} \times \frac{\bar{f}}{m} + \bar{\nabla} - 2(\bar{\omega} \times \dot{\delta R}) \tag{209}$$

In the north-vertical coordinates the vector R is essentially parallel to the z axis. In that case the term

$$3\omega_s^2 |\delta\bar{R}| \frac{\bar{R}}{R}$$

provides no component in the north and east directions. The x and y components of Eq. 209 are

$$\delta\ddot{R}_x + \omega_s^2 \delta R_x = \left\{ \begin{array}{l} 2(\omega_z \delta\dot{R}_y - \omega_y \delta\dot{R}_z) \\ + \frac{1}{m} (\psi_z f_y - \psi_y f_z) + \nabla_x \end{array} \right\} \tag{210}$$

$$\delta\ddot{R}_y + \omega_s^2 \delta R_y = \left\{ \begin{array}{l} 2(\omega_x \delta\dot{R}_z - \omega_z \delta\dot{R}_x) \\ + \frac{1}{m} (\psi_x f_z - \psi_z f_x) + \nabla_y \end{array} \right\} \tag{211}$$

The unforced portions of these equations exhibit a pure oscillatory characteristic at the Schuler frequency. However, along the axis which is is not essentially orthogonal to $\bar{R}$, the quantity $-3 |\delta\bar{R}| \bar{R}/R$ provides a component of mangitude

$$-3\sqrt{\delta R_x^2 + \delta R_y^2 + \delta R_z^2}$$

or

$$-3\lambda \delta R_z$$

where

$$\lambda = \sqrt{1 + \left(\frac{\delta R_x}{\delta R_z}\right)^2 + \left(\frac{\delta R_y}{\delta R_z}\right)^2} \geq 1$$

The z component of Eq. 209 is

$$\delta\ddot{R}_z + \omega_s^2 (1 - 3\lambda)\, \delta R_z = \left\{ \begin{array}{l} 2(\omega_y \delta\dot{R}_x - \omega_x \delta\dot{R}_y) \\ + \frac{1}{m} (\psi_y f_x - \psi_x f_y) + \nabla_z \end{array} \right\} \qquad (212)$$

Ignoring the time-varying nature of $[(\delta R_x)^2 + (\delta R_y)^2]$, the unforced portion of Eq. 212 is unstable; the error in indicating the z component of R will grow unbounded. Similar behavior would result for errors in the x and y directions if they were defined with components parallel to $\bar{R}$. Of course, this behavior does not result from a peculiar characteristic $\bar{R}$, but rather from the need to compensate accelerometer outputs for mass attraction forces and the fact that $\bar{R}$ and gravity are approximately parallel. Because the mass attraction forces obey an inverse-square distance law and must be calculated according to the indicated distance from the earth's center, the instability results. This can be seen more simply by considering a scheme to navigate in the vertical direction only. Figure 45 illustrates the calculations necessary. The quantity

$$g_{comp} = - \frac{g_o R_o^2}{R^2}$$

is added to the accelerometer output to give the upward acceleration with respect to inertial space. Double integration gives the computed value of distance to the center of the earth, R. A small error in the indicated value of R, δR, causing it to be too large, will reduce the size of g_{comp}, making the indicated value of acceleration too large. The integrations cause the indicated value of R to grow even larger, etc. The fact that the error, δR, grows unbounded is evident.

The implication of this instability for practical navigation is that, at least for long periods, inertial navigation along axes not perpendicular to the mass attraction force is not feasible. Over short periods of time such as that encountered for a missile launch the error growth may not be significant. However, cruise navigators usually instrument only horizontal

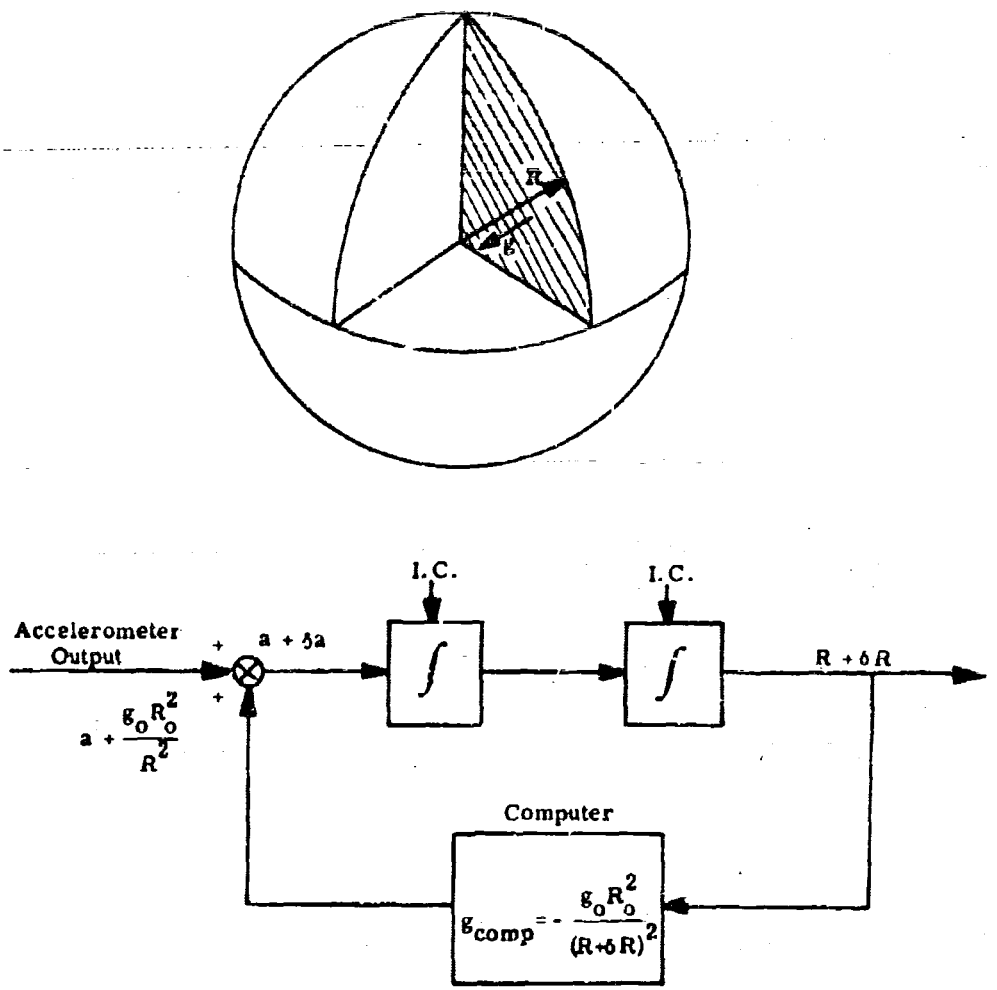

FIG. 45. Navigation in the Vertical Direction.

axes and use altimeters or depth gages to indicate vertical distance. When vertical motion has high-frequency characteristics or must be indicated very accurately, a vertical accelerometer may be used, but mass attraction forces are computed from height indications given by other instruments.

Returning to Eq. 210 and 211, for near-earth navigation in north-vertical or free azimuth coordinates the x and y components of $\overline{\delta\theta}$ are given by

$$\delta\theta_x = \frac{\delta R_y}{R} \tag{213}$$

$$\delta\theta_y = -\frac{\delta R_x}{R} \tag{214}$$

In addition, for the north-vertical system

$$\delta\theta_z = -\frac{\delta R_y}{R} \tan L \tag{215}$$

because the platform axes are rotated about the z axis according to y velocity. The tangent plane navigation coordinate system does not exhibit a misalignment $\overline{\delta\theta}$ based on position errors, because no axis system rotation results from position changes. The same is true of $\delta\theta_z$ in the free azimuth system. For the two locally level navigation frames, Eq. 213 and 214 are useful. Since, from Eq. 197,

$$\overline{\phi} = \overline{\psi} + \overline{\delta\theta} \tag{216}$$

then

$$\omega_s^2\, \delta R_x = \frac{g}{R}\, \delta R_x = -g\, \delta\theta_y$$

$$= g\,(\psi_y - \phi_y) \tag{217}$$

and

$$\omega_s^2\, \delta R_y = g\,(\phi_x - \psi_x) \tag{218}$$

Furthermore, for near-earth cruise vehicles

$$\begin{aligned} f_y/m &\triangleq a_y \\ f_x/m &\triangleq a_x \\ f_z/m &\cong -g \end{aligned} \tag{219}$$

From Eq. 210, 211, 217, 218, and 219, the differential equations for x and y position errors in near-earth, locally level cruise inertial navigators can be written

$$\delta\ddot{R}_x = g\varphi_y + \psi_z a_y + \nabla_x + 2\omega_z \delta\dot{R}_y \tag{220}$$

$$\delta\ddot{R}_y = -g\varphi_x - \psi_z a_x + \nabla_y - 2\omega_z \delta\dot{R}_x \tag{221}$$

To completely describe the error dynamics of inertial navigation systems the attitude error behavior must also be specified analytically. To begin, two relations between the inertial angular rates of the platform and computer coordinates and $\bar{\psi}$ are stated

$$\bar{\omega}_p = \bar{\omega}_c + \bar{\psi} \times \bar{\omega}_c + \bar{\epsilon} \tag{222}$$

and

$$\dot{\bar{\psi}} = \bar{\omega}_p - \bar{\omega}_c \tag{223}$$

Combining Eq. 222 and 223 and approximating $\bar{\omega}_c$ by $\bar{\omega}$,

$$\dot{\bar{\psi}} = \bar{\psi} \times \bar{\omega} + \bar{\epsilon} \tag{224}$$

This is the basic equation describing the error angle dynamics. Expressions result for the components of $\dot{\psi}$

$$\dot{\psi}_x = \epsilon_x + \omega_z \psi_y - \omega_y \psi_z \tag{225}$$

$$\dot{\psi}_y = \epsilon_y + \omega_x \psi_z - \omega_z \psi_x \tag{226}$$

$$\dot{\psi}_z = \epsilon_z + \omega_y \psi_x - \omega_x \psi_y \tag{227}$$

Using the x component of Eq. 197, 213, and 225

$$\begin{aligned} \dot{\varphi}_x &= \dot{\psi}_x + \delta\dot{\theta}_x \\ &= \epsilon_x - \omega_y \psi_z + \omega_z (\varphi_y - \delta\theta_y) + \frac{\delta\dot{R}_y}{R} \\ &= \epsilon_x - \omega_y \psi_z + \omega_z \varphi_y + \omega_z \frac{\delta R_x}{R} + \frac{\delta\dot{R}_y}{R} \end{aligned} \tag{228}$$

In a like manner,

$$\dot{\varphi}_y = \epsilon_y + \omega_x \psi_z - \omega_z \varphi_x + \omega_z \frac{\delta R_y}{R} - \frac{\delta\dot{R}_x}{R} \tag{229}$$

and

$$\dot{\varphi}_z = \epsilon_z - \omega_x \varphi_y + \omega_y \varphi_x - \omega_y \frac{\delta R_y}{R} - \omega_x \frac{\delta R_x}{R} + \delta\dot{\theta}_z \tag{230}$$

Equations 220, 221, 228, 229, and 230 are the primary error dynamic equations for near-earth inertial systems of the locally level type or for a tangent plane system that is near its initial point. The term $\delta\theta_z$ on the right side of Eq. 230 is

$$-\tan L \frac{\delta\dot{R}_y}{R} + \omega_y \frac{\delta R_y}{R} \sec^2 L$$

when a north-vertical system is being considered and is zero for tangent plane and free azimuth coordinates. Usually, terms of the nature

$$\omega \frac{\delta R}{R}$$

and

$$2\omega\, \delta\dot{R}$$

are relatively small and can be dropped. The three near-earth systems described in the section on inertial navigation systems differ only in the way they provide $\bar{\omega}$. In terms of latitude, L, and longitude, λ, they are

1. North-Vertical System

$$\begin{aligned} \omega_x &= (\dot{\lambda} + \Omega) \cos L \\ \omega_y &= -\dot{L} \\ \omega_z &= -(\dot{\lambda} + \Omega) \sin i \end{aligned} \tag{231}$$

2. Free Azimuth System

$$\begin{aligned} \omega_x &= (\dot{\lambda} + \Omega) \cos L \cos \alpha - \dot{L} \sin \alpha \\ \omega_y &= -(\lambda + \Omega) \cos L \sin \alpha - \dot{L} \cos \alpha \\ \omega_z &= 0 \end{aligned} \tag{232}$$

3. Tangent Plane System

$$\begin{aligned} \omega_x &= \Omega \cos L_o \\ \omega_y &= 0 \\ \omega_z &= -\Omega \sin L_o \end{aligned} \tag{233}$$

where α is the angle between north horizontal and the free azimuth x axis, and L_o is the initial point latitude.

SHORT-TERM ERROR PROPAGATION

The behavior of inertial navigation system errors over a short period (2 or 3 hours) can be exhibited by considering Eq. 220, 221, 228, 229 and 230. It will be recalled that they describe the behavior of locally-level near-earth systems. The major terms in these equations are used to produce the block diagrams for the x and y loops shown in Fig. 46. While the two information loops generated are interconnected through the quantity ω_z, the principal short-period dynamics result from the feedback paths shown. The unforced short-period behavior can be obtained in Laplace Transform notation by inspection of Fig. 46.

$$(s^2 + g/R)\ \phi_x = 0 \tag{234}$$

$$(s^2 + g/R)\ \phi_y = 0 \tag{235}$$

The unforced dynamics consist of undamped oscillations at the Schuler frequency (84-min period). The effects of sensor errors on position, velocity, and attitude errors follow from the equations

$$\delta R_i\ (s) = \frac{\nabla_i\ (s)}{s^2 + g/R} \tag{236}$$

$$\delta \dot{R}_i\ (s) = \frac{s\nabla_i\ (s)}{s^2 + g/R} \tag{237}$$

$$\phi_i\ (s) = \frac{s\varepsilon_i\ (s)}{s^2 + g/R} \tag{238}$$

Constant bias terms described by

$$\nabla_i\ (s) = \frac{\nabla_i}{s} \tag{239}$$

provide growing position errors and oscillating velocity errors. Constant gyro drift rate generates an oscillating attitude error.

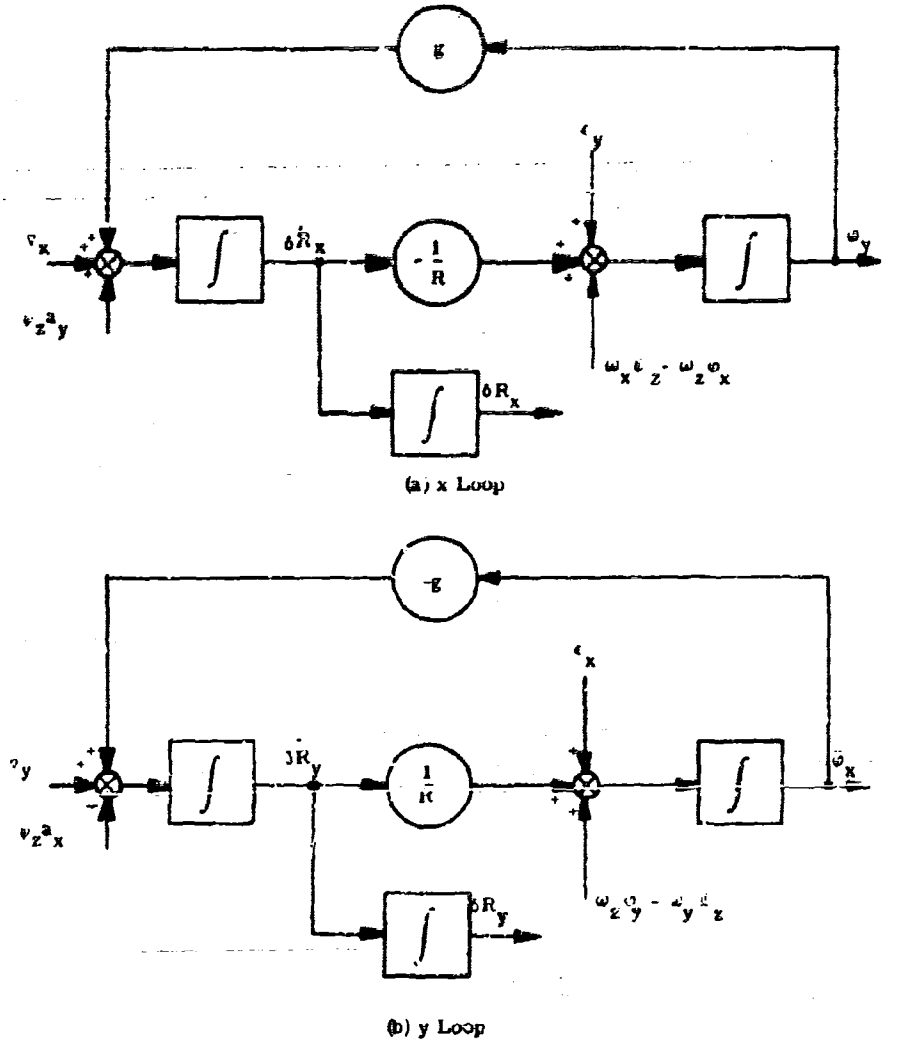

(a) x Loop

(b) y Loop

FIG. 46. Block Diagram of Short-Period Error Behavior in Locally Level Systems.

LONG-TERM ERROR PROPAGATION

In north-vertical inertial navigation systems, error dynamics of a frequency considerably lower than those described above occur. Essentially, these additional dynamics result from uncertainty in the computer's knowledge of the orientation of the earth rotation vector, $\bar{\Omega}$.

If it is assumed that the navigator is not moving with respect to the earth,

$$\dot{\delta L} = \frac{\dot{\delta R}_x}{R} \tag{240}$$

$$\dot{\delta\lambda} = \frac{\dot{\delta R}_y}{R \cos L} \tag{241}$$

$$\dot{\delta\theta}_x = \dot{\delta\lambda} \cos L \tag{242}$$

$$\dot{\delta\varepsilon}_y = -\dot{\delta L} \tag{243}$$

$$\dot{\delta\theta}_z = -\dot{\delta\lambda} \sin L \tag{244}$$

From Eq. 197, 225, 226, 227, and 241 and the above expressions, differential equations result for the components of $\bar{\phi}$.

$$\dot{\phi}_x = \frac{\dot{\delta R}_y}{R} - \Omega \sin L\, \delta L - \Omega \sin L\, \phi_y \tag{245}$$

$$\dot{\phi}_y = -\frac{\dot{\delta R}_x}{R} + \phi_z\, \Omega \cos L + \phi_x\, \Omega \sin L \tag{246}$$

$$\dot{\phi}_z = -\frac{\dot{\delta R}_y}{R} \tan L - \delta L\, \Omega \cos L - \phi_y\, \Omega \cos L \tag{247}$$

Terms which do not provide closed information loops have been omitted from these equations. Notice that the use of Eq. 241 has eliminated $\delta\lambda$ from consideration. Finally, Eq. 220 and 221 provide

$$\frac{\ddot{\delta R}_x}{R} = \frac{g}{R}\,\phi_y \qquad (248)$$

and

$$\frac{\ddot{\delta R}_y}{R} = -\frac{g}{R}\,\phi_x \qquad (249)$$

Equations 240 and 245 through 249 can be written in terms of Laplace Transforms and arranged in the vector-matrix form

$$\begin{bmatrix} 1 & 0 & 0 & 0 & 0 & -s \\ 0 & -1 & s & \Omega \sin L & 0 & \Omega \sin L \\ 1 & 0 & -\Omega \sin L & s & -\Omega \cos L & 0 \\ 0 & \tan L & 0 & \Omega \cos L & s & \Omega \cos L \\ s & 0 & 0 & -\frac{g}{R} & 0 & 0 \\ 0 & s & \frac{g}{R} & 0 & 0 & 0 \end{bmatrix} \begin{bmatrix} \frac{\dot{\delta R}_x}{R} \\ \frac{\dot{\delta R}_y}{R} \\ \phi_x \\ \phi_y \\ \phi_z \\ \delta\lambda \end{bmatrix} = 0 \qquad (250)$$

By setting the determinant of the coefficient matrix in Eq. 250 to zero, the behavior of the variables can be seen

$$\left(S^2 + \frac{g}{R}\right)^2 \left(S^2 + \Omega^2\right) = 0 \qquad (251)$$

The two Schuler frequency characteristics result from the x and y loop short-period error behavior. The additional oscillation is a 24-hour or long-period mode which is not important when durations of 2 or 3 hours are considered, but is significant in long-term cruise navigators.

Many cross-coupling terms have been ignored both in this discussion and the one preceding. Their effects are usually secondary compared to those displayed here. Consideration of a vehicle moving over the earth's surface would have modified the 24-hour mode, but for most applications the size of $\vec{\lambda}$ is much less than Ω. When the acceleration compensation error terms (of the nature $2\omega\,\delta R$) are retained in Eq. 220 and 221, the short-term oscillation frequencies are modified slightly. A more detailed analysis is presented in Ref. 41. Figure 47 shows the result of a simulation in which the errors in a stationary north-vertical system were excited by a constant x-axis gyro drift rate. The 84-minute mode is clearly visible. In addition, the first quarter of a 24-hour mode is evident.

The error equations developed in this Appendix are further specialized to provide system behavior matrices, F, for the several navigation schemes considered in Section 5.

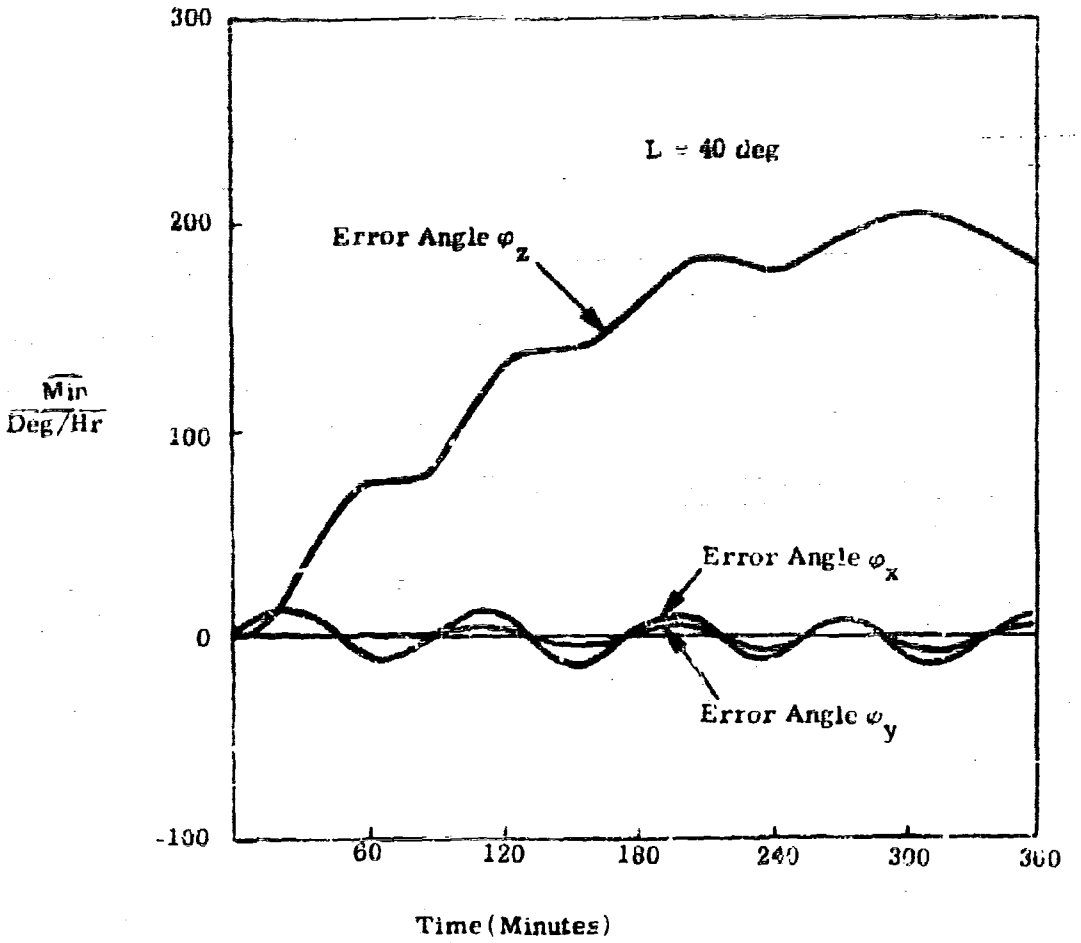

FIG. 47. Platform Tilt Errors Resulting From Constant North Axis Gyro Drift Rate.

REFERENCES

1. Derusso, Paul M., Rob J. Ray, and Charles M. Close. State Variables for Engineers. John Wiley & Sons, Inc., New York, 1965.

2. IBM Corporation. Synergistic Navigation System Study, by Kenneth A. Klementis, et al. Owego, N. Y., October 1966. Report No 67-928-7.

3. The Analytic Sciences Corporation. Error Analysis of a Strapdown Aided Aircraft Inertial Navigation System, by Arthur Gelb and Stephen A. Levine. Winchester, Mass., October 1966, Technical Report 110-2.

4. Wiener, Norbert. The Extrapolation, Interpolation and Smoothing of Stationary Times Series. John Wiley & Sons, Inc., New York, 1949.

5. Kalman, R. E., and R. S. Bucy. New Results in Linear Filtering and Prediction Theory. ASME, TRANS (Journal of Basic Engineering), Vol. 83D, March 1961, pp. 95-108.

6. Bryson, A. E., and [illegible]. Johansen. Linear Filtering for Time-Varying Systems Using Measurements Containing Colored Noise. IEEE TRANS on Automatic Control, Vol. AC-10, January 1965, pp. 4-10.

7. Research Institute for Advanced Studies. New Methods and Results in Linear Prediction and Filtering Theory, by R. E. Kalman. Baltimore, Maryland, 1961. (Technical Report 61-1.)

8. Athans, M., and P. L. Falb. Optimal Control. McGraw-Hill Book Co., New York, 1966.

9. Kalman, R. E. A New Approach to Linear Filtering and Prediction Problems. ASME, TRANS (Journal of Basic Engineering), Vol. 82D, March 1960, pp. 35-45.

10. Bryson, Arthur E., Jr., and Yu-Chi Ho. Optimum Programming, Estimation and Control (in process).

11. Denham, Walter F., and Jason L. Speyer. Optimal Measurement and Velocity Correction Programs for Midcourse Guidance. AIAA J, Vol. 2, No. 5, May 1964, pp. 896-907.

12. Sutherland, Arthur A., Jr. Application of Optimal Linear Estimation to the Alignment of Inertial Guidance Systems. Sc.D. Thesis, M.I.T. Department of Aeronautics and Astronautics, September 1966.

13. Raytheon Company. Smoothing for Linear and Non-Linear Dynamic Systems, by Malcolm Frazier and Arthur E. Bryson, Jr. Lexington, Mass., October 1962. (BR-2033).

14. Harvard University, Cruft Laboratory. Identification of Linear Dynamic Systems, by Yu-Chi Ho and Robert C. K. Lee. Cambridge, Mass., May 1964. (Technical Report No. 446).

15. Stanford Research Institute. Research on the Design of Adaptive Control Systems, by J. Peschon, et al. Menlo Park, Calif., September 1966. (NASA CR 81731).

16. Denham, W. F., and Samuel Pines. Sequential Estimation When Measurement Function Non-Linearity is Comparable to Measurement Error. AIAA/ION, PROC Guidance and Control Conference, August 1965, pp. 174-180.

17. Harder, D. and J. E. Connor. Study of Filter Techniques in Distant Planet Satellite Orbit Parameter Estimation. AIAA/JACC, PROC, Guidance and Control Conference, August 1966, pp. 534-543.

18. Neal, S. R. Non-Linear Estimation Techniques. July 1967 (in process).

19. Grumman Aircraft Engineering Corporation, Research Department. The Effect of Linearity Assumptions and Unknown Noise Sources on Kalman Filtering in Orbit Determination, by W. O'Dwyer, J. Mendelsohn, and A. Kaercher. Bethpage, N. Y., GAEC-RD, May 1967. (Report RE-2851.)

20. Draper, Charles S., Walter Wrigley, and John Hovorka. Inertial Guidance. Pergamon Press, New York, 1960.

21. Gelb, A. Synthesis of a Very Accurate Inertial Navigation System. IEEE TRANS. Aerospace and Navigational Electronics, Vol. 12, June 1965, pp. 119-128.

22. Bryson, A. E., Jr., and L. J. Henrikson. Estimation Using Sampled-Data Sequentially Correlated Noise. AIAA, PROC, Guidance, Control and Flight Dynamics Conference (Astrodynamics), August 1967, Paper No. 67-541.

23. Fitzgerald, Robert J. Filtering Horizon--Sensor Measurements for Orbital Navigation. AIAA/JACC, PROC, Guidance and Control Conference, August 1966, pp. 500-509.

24. Wilcox, James C. Self-Contained Orbital Navigation Systems with Correlated Measurement Errors. AIAA/ION, PROC, Guidance and Control Conference, August 1965, pp. 231-247.

25. Dushman, Alan. On Gyro Drift Models and Their Evaluation. IRE, TRANS, Aerospace and Navigational Electronics, Vol. ANE-9, No. 4, December 1962.

26. Collins Radio Company. An Accuracy Study of a Doppler Navigation System Assuming Time Stationary Random Input Errors, by James C. Styers. Cedar Rapids, Iowa, May 1961. Report No. CER-1396.

27. Bona, B. E., and Robert J. Smay. Optimum Reset of Ships Inertial Navigation System. IEEE, TRANS, Aerospace and Electronic Systems, Vol. AES-2, No. 4, July 1966, pp. 409-414.

28. Sandberg, Herbert J., Arthur Gelb, and Alan, L. Friedman. Alignment of Inertial Navigators in Low-Speed Vehicles. AIAA J, Vol. 1, No. 9, Sept. 1963, pp. 2030-2034.

29. Fagin, S. L., E. Grinoch, and A. Graefe. Continuous Time Varying Optimal Feedback Applied to the Augmentation and Rapid Alignment of Inertial Systems. Supplement to the IEEE, TRANS, Aerospace and Electronic Systems, Vol. AES-2, No. 4, July 1966, pp. 661-670.

30. Lipton, Arthur H. Alignment of Inertial Systems on a Moving Base. Sc.D. Thesis, M.I.T. Department of Aeronautics and Astronautics, August 1966.

31. Pitman, George R., Jr., Editor. Inertial Guidance. John Wiley and Sons, Inc., New York. 1962.

32. Auburn Research Foundation, Auburn University. An Introduction to Analytic Platforms for Inertial Guidance, by J. T. Lowry. Auburn, Ala., ARF(A), April 1966. (NASA-CR-75074.)

33. Massachusetts Institute of Technology, Electronic Systems Laboratory. Augmented Inertial Navigation Systems, by Donald R. Knudson. Cambridge, Mass., April 1966. (Report ESL-R-264.)

34. Martin-Marietta Corporation. A User's Manual for the Automatic Synthesis Program (Program C), by R. E. Kalman and T. S. Englar. Baltimore, Md., June 1966. (NASA CR-475.)

35. Bellantoni, J. J., and K. W. Dodge. A Square Root Formulation of the Kalman-Schmidt Filter, AIAA Paper No. 67-90, AIAA 5th Aerospace Sciences Meeting, New York, January 1967.

36. Joseph, P. D. Automatic Rendevous, Part II: On Board Navigation for Rendevous Missions, Course Notes for Space Control Systems - Attitude, Rendevous, and Docking, UCLA Engineering Extension, 1964.

37. Bona, B. E., and C. E. Hutchinson. An Optimum Stellar-Inertial Navigation System, Journal of the Institute of Navigation, Vol. 12, No. 2, Summer 1965, pp. 171-178.

38. Larson, R. E., R. M. Dressler, and R. S. Ratner. Precomputation of the Weighing Matrix in an Extended Kalman Filter. Joint Automatic Control Conference, University of Pennsylvania, June 1967.

39. Pentecost, Eugene E., and Allen R. Stubberud. Synthesis of Computationally Efficient Sequential Linear Estimators. IEEE, TRANS, Aerospace and Electronic Systems, Vol. AES-3, No. 2, March 1967, pp. 242-249.

40. Nishimura, T. Error Bounds of Continuous Kalman Filters and the Application to Orbit Determination Problems, IEEE, TRANS, Automatic Control, Vol. AC-12, June 1967, pp. 268-275.

41. Broxmeyer, Charles. Inertial Navigation Systems. McGraw-Hill Book Co., New York, 1964.

BIBLIOGRAPHY

1. Brock, Larry D. Application of Statistical Estimation of Navigation Systems. Ph.D. Thesis, M.I.T. Department of Aeronautics and Astronautics, June 1965.

2. Carson, R. C. Investigation of the Suitability of Kalman Optimal Filter Theory for Improving the Performance of Aircraft Type Self-Contained Navigation Systems. U.S. Naval Air Development Center, Johnsville, Pa., November 1966. (Report No. NADC-AM-6644.)

3. Fagin, Samuel L. Feedback Realization of a Continuous Time Optimal Filter. IEEE, TRANS, Aerospace and Electronic Systems, Vol. AES-3, May 1967, pp. 494-509.

4. Fang, Bernard T. Kalman-Bucy Filter for Optimum Radio-Inertial Navigation. IEEE, TRANS, Automatic Control, Vol. AC-12, August 1967, pp. 430-431.

5. Greensite, Arthur L. Analysis and Design of Space Vehicle Flight Control Systems, Vol. VI--Stochastic Effects. General Dynamics Corp., San Diego, Calif., July 1967. (NASA-CR-825).

6. Heffes, H. The Effect of Erroneous Models on the Kalman Filter Response, IEEE, TRANS, Automatic Control, Vol. AC-11, July 1966, pp. 541-543.

7. Huddle, J. R. On Suboptimal Linear Filter Design, correspondence in IEEE TRANS, Automatic Control, Vol. AC-12, June 1967, pp. 317-318.

8. Kwakernaak, H. Optimal Filtering in Linear Systems with Time Delays, IEEE, TRANS, Automatic Control, Vol. AC-12, April 1967, pp. 169-173.

9. Macomber, George R., and Manuel Fernandez. Inertial Guidance Engineering. Prentice-Hall, Inc., 1962.

10. Nishimura, T. On the A Priori Information in Sequential Estimation Problems. IEEE, TRANS, Automatic Control, Vol. AC-11, April 1966, pp. 197-204.

11. Pinson, John C. "Inertial Guidance for Cruise Vehicles," Chapter 4 of Guidance and Control of Aerospace Vehicles, ed. by C. J. Leondes. McGraw-Hill Book Co., Inc., New York, 1963.

12. Richman, Jack, and Bernard Friedland. Design of Optimum Mixer-Filter for Aircraft Navigation System. Proceedings of the 19th National Aerospace Electronics Conference, May 1967, pp. 429-438.

13. Schlee, F. H., C. J. Standish, and N. F. Toda. Divergence in the Kalman Filter. AIAA J, Vol. 5, June 1967, pp. 1114-1120.

UNCLASSIFIED

Security Classification

DOCUMENT CONTROL DATA - R & D

Security classification of title, body of abstract and indexing annotation must be entered when the overall report is classified)

1. ORIGINATING ACTIVITY (Corporate author)
The Analytic Sciences Corporation
6 Jacob Way
Reading, Mass.

2a. REPORT SECURITY CLASSIFICATION
Unclassifed

2b. GROUP
---

3. REPORT TITLE
APPLICATION OF THE KALMAN FILTER TO AIDED INERTIAL SYSTEMS

4. DESCRIPTIVE NOTES (Type of report and inclusive dates)
Final Report

5. AUTHOR(S) (First name, middle initial, last name)
Sutherland, Arthur A., Jr.
Gelb, Arthur

6. REPORT DATE	7a. TOTAL NO. OF PAGES	7b. NO. OF REFS
August 1968	152	54

8a. CONTRACT OR GRANT NO.	9a. ORIGINATOR'S REPORT NUMBER(S)
N60530-67-C-1052	NWC TP 4652
b. PROJECT NO.	
c.	9b. OTHER REPORT NO(S) (Any other numbers that may be assigned this report)
d.	

10. DISTRIBUTION STATEMENT
THIS DOCUMENT IS SUBJECT TO SPECIAL EXPORT CONTROLS AND EACH TRANSMITTAL TO FOREIGN GOVERNMENTS OR FOREIGN NATIONALS MAY BE MADE ONLY WITH PRIOR APPROVAL OF THE NAVAL WEAPONS CENTER.

11. SUPPLEMENTARY NOTES	12. SPONSORING MILITARY ACTIVITY
	Naval Weapons Center China Lake, California 93555

13. ABSTRACT

The purpose of this tutorial report is to allow the reader with a limited background in optimum estimation techniques and/or inertial system theory to achieve a level of competence which will permit his participation in the design and evaluation of aided inertial guidance systems. To this end, the Kalman Filter is described in some detail, with full use made of intuitive concepts. Next, the theory of inertial navigation is presented. Based on an understanding of inertial systems and the Kalman Filter, the reader is then shown how the two are combined to provide accurate, aided inertial systems. Problems arising in the application of the Kalman Filter to practical situations are discussed and common methods for solving them are illustrated. Examples in inertial navigation, gyrocompassing, and alignment transfer are provided in support of the theoretical development.

DD FORM 1473 (PAGE 1)

UNCLASSIFIED

Security Classification

14 KEY WORDS	LINK A		LINK B		LINK C	
	ROLE	WT	ROLE	WT	ROLE	WT
Aided inertial navigation Kalman Filter						

DEPARTMENT OF THE NAVY
NAVAL WEAPONS CENTER
CHINA LAKE AND CORONA LABORATORIES

CHINA LAKE, CALIFORNIA
93555
IN REPLY REFER TO
751/GCA:ga
6 June 1969

From: Commander, Naval Weapons Center
To: Distribution List of NWC TP 4652

Subj: NWC TP 4652, Application of the Kalman Filter to Aided Inertial Systems, dated August 1968; errata for

Encl: Replacements for Equations 159, 164, and 168

1. It is requested that the corrections shown below be incorporated in NWC TP 4652. The corrections have been printed on gummed stock so that they may be pasted in place.

Page 116: Replace Equation 159 with new equation
Page 117: Replace Equation 164 with new equation
Page 118: Replace Equation 168 with new equation

C. E. VAN HAGAN
By direction

AD-851 052L

ERRATA

Page 116, Eq. 159 should read:

$$\underline{\hat{x}}^*_{n+1} = \Phi^*_n \underline{\hat{x}}^*_{n-n} + K^*_{n+1} \left[\underline{z}_{n+1} \; -H^*_{n+1} \; \Phi^*_n \underline{\hat{x}}^*_{n-n} \right] \tag{159}$$

Page 117, Eq. 164 should read:

$$\left[\begin{array}{c} \underline{x}_{n+1} \\ \hline \underline{\xi}^*_{n+1} \end{array}\right] = \left[\begin{array}{c|c} \Phi_n & 0 \\ \hline K^*_{n+1} H_{n+1} \Phi_n & (I - K^*_{n+1} H^*_{n+1}) \Phi^*_n \end{array}\right] \left[\begin{array}{c} \underline{x}_n \\ \hline \underline{\xi}^*_n \end{array}\right] + \left[\begin{array}{c} \underline{w}_n \\ \hline K^*_{n+1} (\underline{v}_{n+1} + H_{n+1} \underline{w}_n) \end{array}\right] \tag{164}$$

Page 118, Eq. 168 should read:

$$\begin{aligned} P_{1_{n+1}} &= \Phi_n P_{1_n} \Phi_n^T + Q_n \\ P_{2_{n+1}} &= \tilde{\Phi}^*_{n+1} H_{n+1} P_{1_n} H^T_{n+1} K^{*T}_{n+1} + K^*_{n+1} H_{n+1} P_{3_n} \Phi^{*T}_n \left(I - K^*_{n+1} H^*_{n+1}\right)^T \\ &\quad + K^*_{n+1} R_{n+1} K^{*T}_{n+1} + K^*_{n+1} H_{n+1} Q_n H^T_{n+1} K^{*T}_{n+1} + \left(I - K^*_{n+1} H^*_{n+1}\right) \Phi^*_n P^T_{3_n} H^T_{n+1} K^{*T}_{n+1} \\ &\quad + \left(I - K^*_{n+1} H^*_{n+1}\right) \Phi^*_n P_{2_n} \Phi^{*T}_n \left(I - K^*_{n+1} H^*_{n+1}\right)^T \\ P_{3_{n+1}} &= \Phi_n P_{1_n} H^T_{n+1} K^{*T}_{n+1} + \Phi_n P_{3_n} \Phi^{*T}_n \left(I - K^*_{n+1} H^*_{n+1}\right)^T + Q_n H^T_{n+1} K^{*T}_{n+1} \end{aligned} \tag{168}$$

19 May 1969